

Characterizing the RanGAP1-RanBP2 complex in mitosis

Dissertation
zur Erlangung des mathematisch-naturwissenschaftlichen Doktorgrades
"Doctor rerum naturalium"
der Georg-August-Universität zu Göttingen

vorgelegt von
Annette Flotho
aus Aachen

Göttingen 2008

Referent: Prof. Dr. Frauke Melchior

Zentrum Biochemie und Molekulare Zellbiologie, Abteilung Biochemie I
der Georg-August-Universität zu Göttingen

Korreferent: Prof. Dr. Ralf Ficner

Institut für Mikrobiologie und Genetik, Abteilung Molekulare Strukturbiologie
der Georg-August-Universität zu Göttingen

Tag der mündlichen Prüfung: 30.10.2008

CONTENT

ABSTRACT	11
INTRODUCTION	12
1. The Ran GTPase system and its function in interphase	12
2. The Ran GTPase system in mitosis	15
3. RanGAP1 and RanBP2 in mitosis	17
4. RanGAP1 targeting to the nuclear envelope and to mitotic structures	19
5. Sumoylation	20
6. Sumo modification of RanGAP1	22
7. The Sumo E3 ligase RanBP2	23
8. Regulation of the RanGAP1-RanBP2 complex	24
9. Aim of this work	26
MATERIALS & METHODS	27
1. Materials	27
1.1. Technical equipment	27
1.2. Consumable supply	28
1.3. Chemicals, reagents and enzymes	29
1.4. Kits	30
1.5. Buffers and stock solutions	30
1.6. Media	32
1.7. Cell lines	33
1.8. Oligonucleotides, vectors and plasmids	33
1.9. Proteins	36
1.10. Antibodies	37
1.11. Software	40
2. Methods	41
2.1. Molecular biological techniques	41
2.1.1. Culturing and storage of bacteria	41
2.1.2. Plasmid preparation	41
2.1.3. Cloning	42
2.1.4. Sequencing	44

2.1.5. Vectors and plasmids constructed in this work	44
2.2. Cell biological techniques	46
2.2.1. Culturing and storage of mammalian cells	46
2.2.2. Cell cycle arrest and synchronization	47
2.2.3. Transfection	47
2.2.4. Selection of stable HeLa cell lines expressing HA-hRanGAP1	48
2.2.5. Immunofluorescence and fluorescence microscopy	48
2.2.6. In situ sumoylation	49
2.3. Biochemical techniques	50
2.3.1. SDS PAGE and analysis	50
2.3.2. Antibody purification	52
2.3.3. Protein expression and purification	53
2.3.4. Mammalian cell lysate and extract preparation	55
2.3.5. Immunoprecipitation	56
2.3.6. Cross-linking of proteins	56
2.3.7. Pull-down with peptide affinity matrices	57
2.3.8. In vitro interaction of recombinant Crm1 and sumoylated RanGAP1	58
2.3.9. In vitro sumoylation with recombinant proteins	58
2.3.10. In vitro sumoylation of recombinant proteins with endogenous RanBP2 E3 ligase	59
2.3.11. In vitro sumoylation and purification of endogenous RanGAP1-RanBP2 associated proteins	59
2.3.12. MS analysis	60
2.3.13. Double step affinity purification of Ubc9*Sumo	62
2.3.14. In vivo analysis of the Ubc9 sumoylation site	63
RESULTS	64
Chapter I: Characterizing the RanGAP1-RanBP2 complex in mitosis	64
1. Establishing stable cell lines expressing RanGAP1 phospho-variants	64
2. RanGAP1 localization to kinetochores in mitosis does not depend on RanGAP1 phosphorylation	67
3. Crm1 and Ran are stable components of the mitotic RanGAP1-RanBP2-Ubc9 complex	69

3.1. Searching for RanGAP1 interacting proteins	69
3.2. The export receptor Crm1 constitutes a major component of the RanGAP1-RanBP2 complex	73
3.3. The GTPase Ran stably interacts with the RanGAP1-RanBP2-Ubc9-Crm1 complex	78
4. Does the Crm1-Ran subcomplex act as a substrate recruitment machinery for the mitotic RanGAP1-RanBP2-Ubc9 complex?	81
4.1. Proteins of unknown identity associate with and can be sumoylated by the mitotic RanGAP1-RanBP2-Ubc9 complex	82
4.2. Unraveling the identity of RanGAP1-RanBP2-Ubc9-associated Sumo substrates	84
4.3. Testing selected candidate Sumo targets	92
4.3.1. Topoisomerase II α , the only known in vivo substrate of RanBP2, binds to and is modified by the mitotic RanGAP1-RanBP2-Ubc9 complex	95
4.3.2. The Sumo E3 ligase PIAS1 associates with mitotic RanGAP1 in a complex distinct to the RanBP2-containing complex	96
4.3.3. The spindle/centrosome-associated proteins CKAP-5 and TACC2 bind to the RanGAP1-RanBP2 complex	99
4.3.4. The mitotic kinase Plk1 is a Sumo target in vitro and the Polo box is important for PIAS1-mediated sumoylation	100
4.3.5. The de-ubiquitinating enzyme USP7 binds to and is sumoylated by the mitotic RanGAP1-RanBP2-Ubc9 complex	105
5. The mitotic RanGAP1-RanBP2-Ubc9 complex exhibits weak sumoylation activity towards Sp100	106
Chapter II: An alternative mechanism of substrate specificity in sumoylation	109
6. Ubc9 sumoylation regulates Sumo target discrimination	109
6.1. Conjugation of Sumo to lysine 14 in mammalian Ubc9 enhances its activity towards certain SIM-containing Sumo targets in vitro	109
6.2. Mammalian Ubc9 is sumoylated on lysine 14 in vivo	111
6.3. Overexpression of a Sumo-deficient Ubc9 K14R variant does not alter the overall Sumoylation pattern in cells	113
DISCUSSION	114
1. Crm1 and Ran are stable interaction partners of the RanGAP1-RanBP2 complex	114

2. Functional aspects of Crm1 binding	117
3. RanGAP1 associates with two E3 ligases	119
4. <i>In vivo</i> targets of the Sumo E3 ligase RanBP2 – evaluation and alternative approaches	120
5. Crm1 and Ran as a specificity module for the Sumo E3 ligase RanBP2?	122
6. Ubc9 sumoylation as means for Sumo substrate selection	123
7. The role of mitotic RanGAP1 phosphorylation	124
8. Plk1 as putative mitotic Sumo substrate	125
9. Outlook	126
REFERENCES	127
SUPPLEMENTARY INFORMATION	139
1. Sequence of TACC2 (“isoform 7”)	139
ABBREVIATIONS	141
CURRICULUM VITAE	148

ABSTRACT

The RanGAP1-RanBP2 complex represents a fascinating macromolecular assembly comprising at least two enzymatic activities. On one hand, it harbors the GTP hydrolysis activating function of RanGAP1 together with RanBP2, and on the other hand, RanBP2 in concert with Ubc9 contains Sumo conjugating activity. Together, these proteins are not only crucial regulators of nucleocytoplasmic transport in interphase cells but they also play an important yet ill-defined role in kinetochore function during mitosis. To gain insight into the RanGAP1-RanBP2 complex specifically in mitotic cells, I searched for mitosis-specific interaction partners. This led to the identification of the nuclear export receptor Crm1 and the GTPase Ran as stable components in complex with RanGAP1, RanBP2 and Ubc9 in mitotic cells. In addition, the complex seemed to contain many different proteins at substoichiometric levels. These could, for example, be NES containing Crm1 interactors and/or targets for RanBP2 dependent sumoylation. As RanBP2 dependent Sumo targets are largely unknown, I devised a strategy to enrich sumoylated proteins from immunoprecipitated RanGAP1-RanBP2 complexes. This allowed mass-spectrometric identification of 90 putative Sumo substrates specifically enriched in mitotic RanGAP1 complexes; 6 of these were selected for further validation. All candidates associated with mitotic RanGAP1 complexes (Topo II α , TACC2, CKAP-5, Plk1, USP7, PIAS1), and most of these could be sumoylated *in vitro* with recombinant factors (TACC2, Plk1) or as proteins associated with mitotic RanGAP1-RanBP2 complexes as source of Sumo E3 ligase activity (TopoII α , Plk1, USP7). Strikingly, the Sumo E3 ligase PIAS1 also co-purified with RanGAP1 from mitotic cells and was efficiently sumoylated in these experiments. Further analysis suggested that mitotic RanGAP1 is present in a complex with PIAS1 distinct from the RanGAP1-RanBP2 complex. In a side project, I could show that the Sumo conjugating enzyme Ubc9 is sumoylated on lysine 14 in cells. This finding was crucial to supplement a biochemical study by Knipscheer et al. that identified a novel mechanism for Sumo substrate selection and contributed to the publication Knipscheer, Flotho, Klug et al. (2008) Mol Cell.

INTRODUCTION

Compartmentalization of a cell into a cytoplasmic and a nuclear fraction emerged approximately 2 billion years ago as a major advance in the evolution of complex forms of life. The nuclear envelope as a hallmark of a eukaryotic cell constitutes a barrier that allows to control access to genes and to individually regulate their expression. This innovation offered however two major challenges. First, a system was needed that guaranteed for the regulated communication between these two compartments. Secondly, the genome now enclosed in a separate organelle, had to segregate before parental cell division could occur. Eukaryotic cells have acquired a system crucial to both aspects, this is the Ran GTPase system.

1. The Ran GTPase system and its function in interphase

Ran is a small GTPase belonging to the Ras superfamily (Gorlich and Kutay 1999; Kuersten et al. 2001; Fried and Kutay 2003). It is a unique member in its role to regulate the active transport of many proteins and macromolecules across the nuclear envelope. Like other GTPases, Ran cycles between a GDP and a GTP bound state resulting in a switch in protein conformation and concomitantly, a change in the functional output. Due to both Ran's low intrinsic GTPase activity and the low guanine nucleotide exchange rate the Ran GTPase cycle absolutely requires two unique auxiliary activities: the GTP hydrolysis-promoting function of RanGAP1 (Ran GTPase activating protein 1) together with the Ran binding domains of RanBP1 (Coutavas et al. 1993; Bischoff et al. 1995a) or RanBP2 (Wu et al. 1995; Yokoyama et al. 1995; Villa Braslavsky et al. 2000), also known as Nup358 (Ran binding protein 1 or 2), and the guanine nucleotide dissociating activity of RCC1 (regulator of chromosome condensation), to allow for the exchange of GDP for GTP.

A further class of proteins essential to nuclear protein transport is the superfamily of the Ran-binding importin β -related transport receptors (Strom and Weis 2001; Mosammaparast and Pemberton 2004). Transport receptors recognize and bind to specific transport signal sequences within cargo proteins and mediate their translocation through the nuclear pore complexes (NPCs), the translocation channels of the nuclear envelope. From a structural point of view, transport receptors of the importin β

superfamily have a superhelical design formed by an array of HEAT repeats; dependent on the Ran-binding state this structure wraps around its transport cargo or, conversely, opens up in a spring-like fashion to release a cargo or expose a binding site for new cargoes (Conti et al. 2006; Stewart 2006, 2007). The two best-studied karyopherins are importin β and chromosome-region maintenance factor-1 (CRM1). Importin β can bind directly to some import cargoes, however more frequently it interacts via the adaptor protein importin α with nuclear localization signal (NLS) containing proteins to allow for their translocation into the nucleus. CRM1 in contrast mediates nuclear export of proteins harboring a nuclear export signal (NES) of the leucine-rich type (consensus sequence L-x(2,3)-[LIVFM]-x(2,3)-L-x-[LI] (Bogerd et al. 1996)).

Two basic principles have been identified that account for Ran's regulatory function in vectorial protein transport across the nuclear membrane (illustrated in Fig. 1). One is the varying interaction pattern of Ran depending on its nucleotide bound state: in its GTP bound form Ran exhibits a high affinity for import complexes built by an import receptor and an import cargo; binding of RanGTP induces a conformational change in the receptor leading to the release of the import substrate. GTP hydrolysis on Ran lowers the affinity for the import receptor allowing for a new round of cargo binding. Conversely, export receptors bind to their cargoes only in complex with RanGTP; in this case GTP hydrolysis results in the disassembly of export complexes. The second underlying mechanism is the localized production of RanGTP and RanGDP in the nucleus and cytoplasm, respectively. This is achieved by restricting RCC1 to the nucleus (Ohtsubo et al. 1989) where it dynamically associates with the histones H2A/H2B (Nemergut et al. 2001) whereas RanGAP1, RanBP2 and the major pool of RanBP1 reside in the cytoplasm (Hopper et al. 1990; Bischoff et al. 1995a; Melchior et al. 1995; Richards et al. 1996). Together, these mechanisms provide a means to assemble import complexes and disassemble export complexes in the cytoplasm and to disassemble import complexes and assemble export complexes in the nucleus. This allows for vectorial transport in both directions across the nuclear membrane.

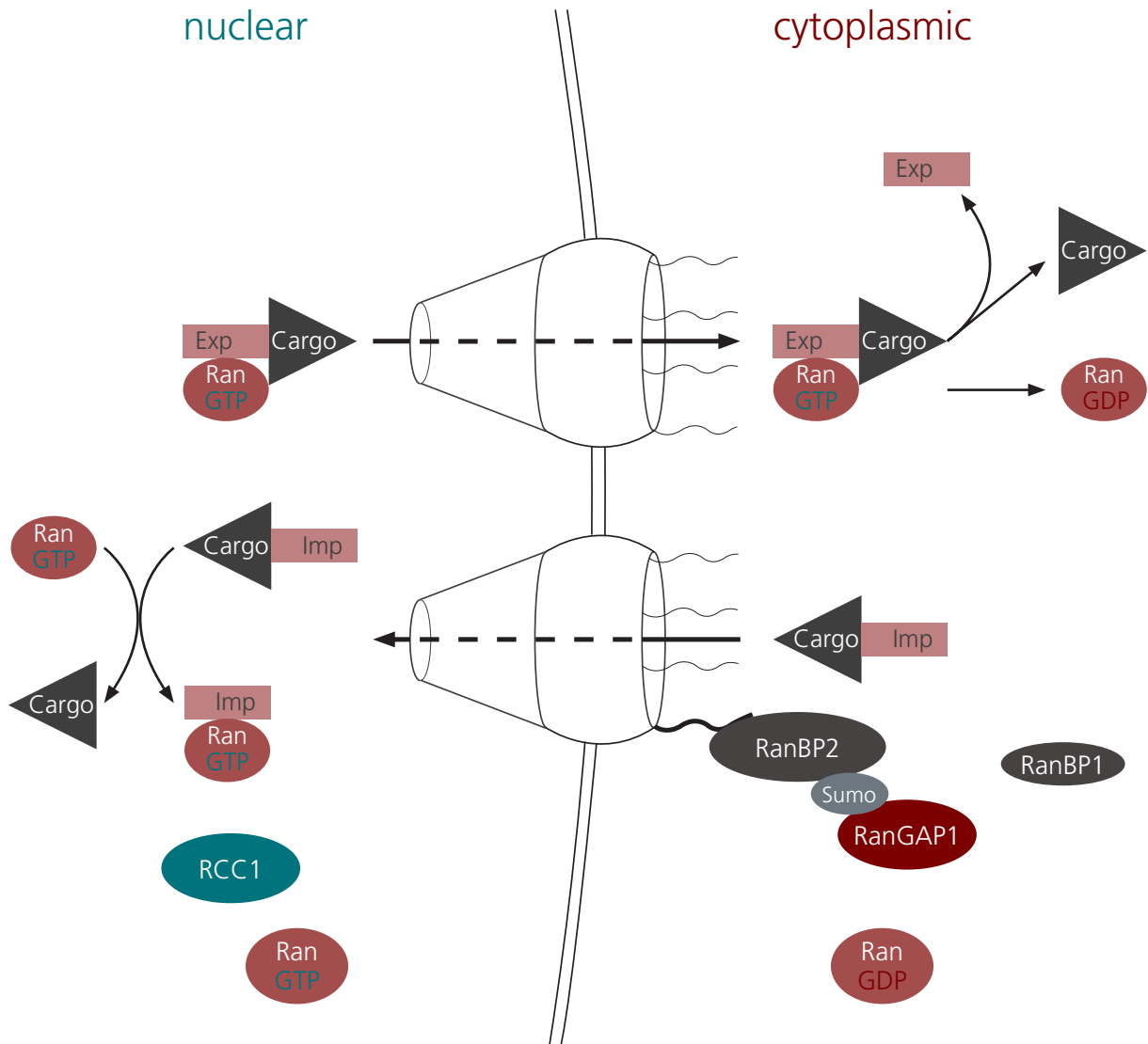


Fig. 1: Regulation of nuclear transport by the Ran GTPase system. The localization of RCC1 to the nucleus and RanGAP1, RanBP1 and RanBP2 to the cytoplasm determines the nucleotide-bound state of the Ran. Depending on the Ran status, import and export complexes are formed or being disassembled.

Special in this context is the localization of RanGAP1 and RanBP2. RanBP2 constitutes part of the cytoplasmic filaments of the NPCs (Wu et al. 1995; Yokoyama et al. 1995; Walther et al. 2002) and is thought to facilitate the passage of transport receptor complexes through the pore channel by transient interactions of RanBP2's phenylalanine-glycine (FG) repeats, a motif common to many nucleoporins (Weis 2007). While RanGAP1 by itself is a soluble cytoplasmic protein, a large pool of it associates with RanBP2 forming a stable complex at the NPCs of mammalian cells (Matunis et al. 1996; Mahajan et al. 1997; Weis 2007). This interaction absolutely depends on modification of RanGAP1 with the small ubiquitin-related modifier Sumo1. While the pore-associated RanGAP1-RanBP2 complex has been suggested to support nuclear

transport (Mahajan et al. 1997; Kehlenbach et al. 1999), the requirement for this specialized fraction has long been a matter of debate. Recent work however supports a model according to which the RanGAP1-RanBP2 complex serves as a docking station for efficient importin β recycling and for the reassembly of novel import complexes directly at the cytoplasmic face of the NPC (Hutten et al. 2008).

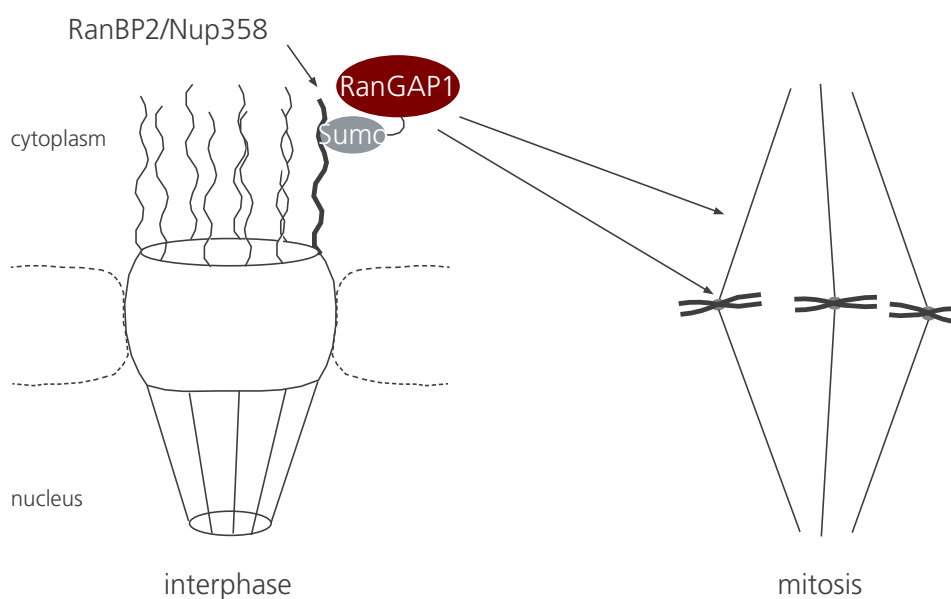


Fig. 2: RanGAP1-RanBP2 localization in interphase and mitosis. RanGAP1 together with RanBP2 localizes to the cytoplasmic filaments of nuclear pore complexes in interphase and to the spindle and kinetochores in mitosis. Essential to complex formation of the two proteins is the modification of RanGAP1 with Sumo1.

2. The Ran GTPase system in mitosis

While the nuclear envelope disassembles during cell division in mammalian cells and therefore nuclear transport ceases, the Ran system has been adopted in the orchestration of multiple events during mitosis, not only in mammals but also in vertebrates and yeast (Weis 2003; Clarke and Zhang 2008). Although defects in the Ran system were originally identified to result in mitotic perturbations (Ohtsubo et al. 1989; Coutavas et al. 1993; Ren et al. 1993) the significance of these observations was being veiled by the concomitant aberrations in nucleo-cytoplasmic transport. Major advances in this field were achieved by biochemical studies in meiotic *Xenopus laevis* egg extracts that allowed to investigate mitosis-relevant processes independent of the previous interphase cycle. Meanwhile Ran's functions in centrosome duplication (Wang et al. 2005), microtubule dynamics (Carazo-Salas et al. 2001; Wilde et al. 2001), mitotic

spindle assembly (Clarke and Zhang 2008; Kalab and Heald 2008), kinetochore function (Arnaoutov and Dasso 2003; Salina et al. 2003; Joseph et al. 2004), NPC (Zhang et al. 2002a; Harel et al. 2003; Ryan et al. 2003; Walther et al. 2003; Ryan et al. 2007) and nuclear envelope re-assembly (Clarke and Zhang 2008) have been established; however details as to how the cell engages the Ran system to regulate these different events still remain poorly defined. According to current working models it appears that local regulation of complex formation with transport receptors may be a common denominator to both Ran's function in interphase and in mitotic processes.

One of the most intensively investigated aspects is Ran's involvement in spindle assembly and organization. From numerous studies a picture has emerged according to which Ran mediates spindle formation by affecting multiple spindle assembly parameters: centrosome-dependent and chromatin-dependent microtubule nucleation (Kalab et al. 1999; Ohba et al. 1999; Wilde and Zheng 1999; Zhang et al. 1999; Carazo-Salas et al. 2001; Gruss et al. 2001), microtubule dynamics (stabilization and flux) and microtubule motor activity (Carazo-Salas et al. 2001; Wilde et al. 2001; Mitchison et al. 2004). One molecular mechanism contributing to spindle assembly is the localized release of spindle assembly factors in the vicinity of mitotic chromosomes (Fig. 3). Indeed a number of proteins required for spindle assembly such as TPX2 (Gruss et al. 2001), NuMA (Nachury et al. 2001; Wiese et al. 2001), Kid (Trieselmann et al. 2003) and others have been shown to bind to the importin α /importin β heterodimer via a NLS; importantly, this interaction suppresses their activity to promote spindle formation. Binding of RanGTP to importin β liberates these mitotic cargo molecules from the transport receptor thereby activating them. Since RCC1 associates with chromatin also in mitosis (Hutchins et al. 2004; Li and Zheng 2004) the resulting high concentration of RanGTP around mitotic chromosomes is thought to release spindle-promoting activities specifically in the vicinity of chromatin (Nachury et al. 2001; Moore et al. 2002; Trieselmann and Wilde 2002). Studies using fluorescence resonance energy transfer (FRET) based reporters were indeed able to visualize the existence of a RanGTP cloud produced around mitotic chromosomes in both *Xenopus* egg extracts (Kalab et al. 2002) and somatic mammalian cells (Kalab et al. 2006). Combined with mathematic modelling this led to the hypothesis that a concentration gradient of RanGTP in complex with importin β (or, correspondingly, of liberated mitotic cargo molecules), highest around the chromosomes and decreasing

towards the centrosomes, may provide a means to convey spatial information required for proper spindle formation (Caudron et al. 2005). In support of this hypothesis, variations in the concentration of RanGAP1/RanBP1 or RCC1 in *Xenopus* egg extracts resulted in misformed mitotic spindles.

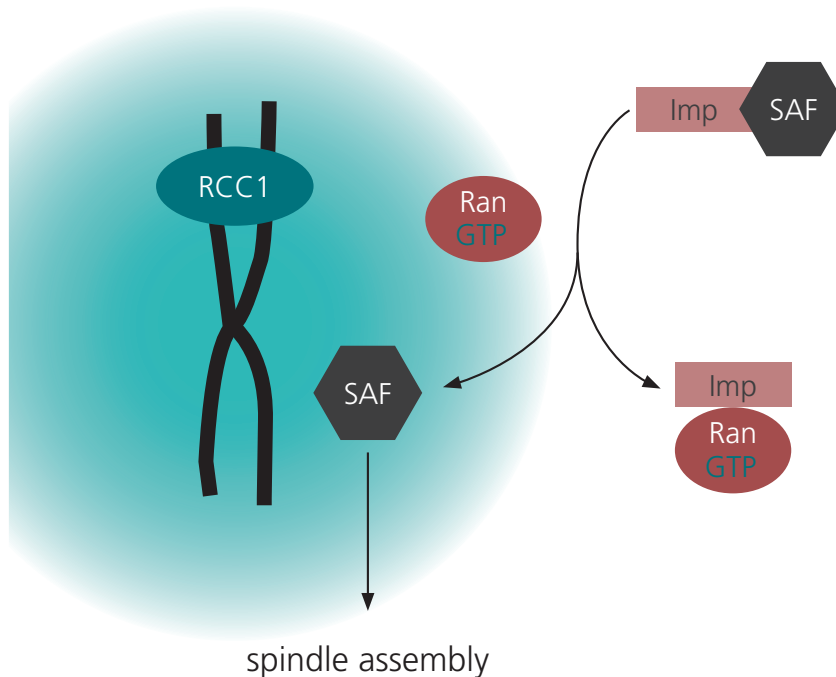


Fig. 3: Ran-dependent mechanism of mitotic spindle assembly. Chromosome-associated RCC1 produces high concentrations of RanGTP in the vicinity of chromosomes. This leads to localized release and thereby activation of importin β -associated spindle assembly factors (SAF) promoting spindle assembly around chromosomes.

3. RanGAP1 and RanBP2 in mitosis

A fact neglected by the gradient model is that a fraction of RanGAP1 in complex with RanBP2 relocates from the cytoplasmic side of the NPC in interphase to the spindle microtubules and kinetochores in mitosis (Joseph et al. 2002). Again, RanBP2 is likely to be the localizing determinant: RanGAP1 is lost from the spindle and kinetochores upon downregulation of RanBP2 by siRNA treatment as well as upon interference with the RanGAP1-RanBP2 interaction using a sumoylation-deficient RanGAP1 K524R variant. Kinetochores temporally correlates with spindle microtubule – kinetochores (kMT) attachment and RanGAP1 fails to localize to kinetochores in cells that are

defective in capturing spindle microtubules at kinetochores due to depletion of the kinetochore proteins Hec1 and Nuf2 or upon microtubule destabilization by nocodazole suggesting that RanGAP1-RanBP2 are loaded onto the kinetochores along spindle microtubules (Joseph et al. 2004).

Functionally, the RanGAP1-RanBP2 complex has been shown to be essential for kinetochore structure and function. Several kinetochore proteins including Cenp-E, Cenp-F and the checkpoint proteins Mad1 and Mad2 mislocalize upon depletion of RanBP2 (Salina et al. 2003; Joseph et al. 2004) concomitant with aberrant kinetochore structure (Salina et al. 2003). Additionally, the attachment of spindle microtubules to kinetochores is compromised; while the attachment can still form it is less stable and spindle microtubules disintegrate upon exposure to cold, a hallmark of defective kMT attachments (Joseph et al. 2004). Accordingly, mitotic spindles display an elongated phenotype (Joseph et al. 2004) and fail to properly align and segregate the chromosomes (Salina et al. 2003; Joseph et al. 2004). Ultimately, this leads to the formation of multinucleate cells.

Another factor essential for recruitment of RanGAP1 and RanBP2 to kinetochores is the nuclear export factor Crm1 (Arnaoutov et al. 2005). So far, Crm1 is the only transport receptor implicated in the regulation of mitotic events besides importin α and importin β . Similar to RanGAP1 and RanBP2, Crm1 also localizes to kinetochores throughout most of mitosis; ternary complex formation of Crm1 with RanGTP and a NES cargo is beneficial but not essential for this localization. Strikingly, however, interfering with ternary complex assembly by RCC1 depletion or by LMB treatment, a drug that modifies and thereby inactivates the NES binding site of Crm1, results in displacement of RanGAP1-RanBP2 from kinetochores. In addition to defects in mitotic progression and chromosome segregation LMB treated cells show signs of increased tension across the centromeres and display severe defects in kinetochore fiber (k-fiber) definition and attachment: a bundle of spindle microtubules usually forms a stable fiber that attaches end-on to one kinetochore thereby building a stable connection; upon LMB treatment in contrast, several centromeres are often found arrayed along one single k-fiber and kMT attachments are lost or only thin fibers connect to centromeres after cold treatment, a phenotype highly reminiscent of the one observed after RanGAP1-RanBP2 displacement from kinetochores after RCC1 depletion. Taken together, the mitotic

defects observed upon interfering with RanGAP1-RanBP2, Crm1 and RCC1 are partially overlapping suggesting that ternary complex formation indeed plays an important role in kinetochore integrity.

4. RanGAP1 targeting to the nuclear envelope and to mitotic structures

As already mentioned, mammalian RanGAP1 is targeted to NPCs and to the spindle and kinetochores by the same mechanism, that is the modification of RanGAP1 with Sumo1. Vertebrate RanGAP1 is built of two separate domains, a N-terminal catalytic domain and a C-terminal tail region, connected via a flexible acidic linker. The catalytic domain is constructed of an array of leucine rich repeat modules forming a crescent-like structure with the outer surface built out of α helices and the inner one out of β sheets (Hillig et al. 1999). The C-terminal tail composed almost exclusively of α helices (Bernier-Villamor et al. 2002) is sufficient for sumoylation and proper RanGAP1 localization. Lysine 524 in humans or the corresponding lysine 526 in mouse RanGAP1 (Mahajan et al. 1998; Matunis et al. 1998; Joseph et al. 2002) serves as the Sumo acceptor site.

Whereas the N-terminal catalytic domain is highly conserved throughout the eukaryotic kingdom the C-terminal tail region is much less conserved (illustrated in Fig. 4): it is still present and functional in a homologous manner in *Xenopus laevis* (Saitoh et al. 1997), however in *Drosophila melanogaster*, the primary sequence differs completely despite the presence of a presumptive modification site (Kusano et al. 2001). A mutant form also known as *segregation distorter* featuring both, a truncation of this site and a putative NES localizes to the nucleus; it is therefore conceivable that *Drosophila* also uses a comparable mechanism to situate dRanGAP at the nuclear envelope. In contrast, the C-terminal tail region is completely absent in yeast (Becker et al. 1995) and in plants (Pay et al. 2002). While RanGAP1 is an exclusively soluble cytoplasmic protein in yeast, plants have developed a plant-specific N-terminal extension, the so-called WPP domain (named after its highly conserved Trp-Pro-Pro motif), which is necessary and sufficient to localize *Arabidopsis thaliana* RanGAP1 to the nuclear envelope in interphase (Rose and Meier 2001). It appears that plant root tip cells require at least one protein of each, the WPP interacting WIP and WIT families, to localize RanGAP1 to the nuclear envelope (Zhao et al. 2008). Strikingly, the same mechanism involving the WPP domain of RanGAP1 also

mediates targeting of plant RanGAP1 to the growing cell plate, a structure separating the two dividing cells in mitosis (Jeong et al. 2005). Thus, higher eukaryotes have developed distinct mechanisms to target RanGAP1 to analogous structures in different species suggesting that there may be a functional link between the interphase and mitosis-specific localization of RanGAP1.



Fig. 4: RanGAP1 homologs. Vertebrate RanGAP1 consists of a N-terminal catalytic domain and a C-terminal tail domain joined by a flexible linker. The catalytic domain is highly conserved throughout the eukaryotic kingdom (given examples: *Homo sapiens*, *Xenopus laevis*, *Drosophila melanogaster*, *Arabidopsis thaliana*, *Saccharomyces cerevisiae*). The C-terminal tail harboring the sumoylation site is less conserved: it differs significantly in *D. melanogaster* and is completely missing in plants and yeast. In contrast, *A. thaliana* has developed an unrelated N-terminal extension, a so-called WPP domain, that is required to target plant RanGAP1 to the nuclear envelope and to mitotic structures.

5. Sumoylation

Sumo is the acronym for small ubiquitin-related modifier, a family of ~10 kD proteins that structurally resemble ubiquitin but differ in the surface-charge distribution and in a N-terminal flexible extension not present in ubiquitin (Bayer et al. 1998; Bernier-Villamor et al. 2002; Saitoh et al. 2002; Zhang et al. 2002b). Covalent attachment of Sumo molecules via an enzymatically mediated reaction alters inter- or intramolecular protein-protein or protein-DNA interactions, which can result in changes in localization, activity or stability of the modified substrate (Johnson 2004; Hay 2005; Kerscher et al. 2006; Geiss-Friedlander and Melchior 2007). At least three Sumo paralogs have been identified to be expressed ubiquitously in vertebrates, Sumo1 – Sumo3. While Sumo2 and Sumo3 are almost identical, they share only ~50 % identity with Sumo1. All Sumo proteins are expressed as immature precursor proteins that need to be processed in order to expose a glycine-glycine motif at their C termini for conjugation to a substrate.

Modification of proteins with Sumo requires the action of an enzymatic cascade (a schematic overview over sumoylation is given in Fig. 5). In the first step, Sumo is activated in an ATP-consuming reaction by the single Sumo E1 enzyme, the heterodimer

of Aos1 and Uba2. The resulting Sumo adenylate is competent to form a thioester linkage between the carboxyl group of the Sumo C terminus and the thiol group of the Uba2 catalytic cysteine. In the next step, the Sumo thioester is handed over to the catalytic cysteine of the single Sumo E2 enzyme Ubc9, a 17 kD protein with homology to other members of the Ubc (ubiquitin conjugating enzyme) family. Finally, Sumo is transferred from the E2 directly to the substrate to form a covalent isopeptide linkage to the ϵ amino group of the target. In most cases, this final step requires a third class of enzymes for efficient and selective modification, the so-called Sumo E3 ligases; these assist the final conjugation step by bridging the interaction between Ubc9 and the substrate.

In contrast to the single E1 and E2 enzymes, a relatively small but still growing number of E3 ligases have been identified. The largest group representing SP-RING type E3 ligases comprises the PIAS family (including PIAS1 – PIAS4 in mammals, the homologs of which are Siz1 and Siz2 in yeast), MMS21 and Zip3. SP-RING E3 ligases are thought to bind to both, their substrates and Ubc9 directly. While the SP-RING is required for Ubc9 interaction, less well defined areas N- and C-terminal of the RING are involved in target recognition (Hochstrasser 2001). Unrelated types of E3 ligases include not only Pc2 but also the already mentioned nucleoporin RanBP2.

In sumoylation, a preference for modification of lysines within a defined context, the originally identified Sumo consensus motif (Ψ -K-x-[E/D], Ψ - hydrophobic branched amino acid, x – any amino acid), can be attributed to the fact that Ubc9 recognizes this motif directly (Bernier-Villamor et al. 2002). The consensus motif has to be present in an extended structural conformation for recognition by Ubc9; lysines within helical structures can also be sumoylated, here however, the sequence context differs and a consensus motif has not yet been defined (Pichler et al. 2005).

Corresponding to the ability of Sumo to mediate protein-protein interactions, a Sumo interacting/binding motif (SIM/SBM) has been identified. SIMs feature a β sheet hydrophobic core ([V/I]-x-[V/I]-[V/I] and [V/I]-[V/I]-x-[V/I/L]) often flanked by acidic stretches at the N or C terminus (Minty et al. 2000; Song et al. 2004; Hannich et al. 2005; Hecker et al. 2006). The interaction between Sumo and the SIM is rather weak (Song et al. 2005; Hecker et al. 2006) and supposedly requires contribution from further interaction sites for efficient binding. SIMs have been identified in many E3 ligases

including the PIAS family and RanBP2 where the motif seems to be important for the functionality as E3 ligase (Song et al. 2004; Reverter and Lima 2005). Furthermore, some Sumo targets have been shown to harbor a SIM crucial for modification (Takahashi et al. 2005; Lin et al. 2006; Knipscheer et al. 2008; Meulmeester et al. 2008; Zhu et al. 2008). In this case, the SIM is likely to direct the Ubc9~Sumo thioester for modification to the substrate (Hochstrasser 2007; Zhu et al. 2008); often non-consensus lysines are being targeted by this mechanism and modification with Sumo seems to be more promiscuous in terms of the acceptor lysine specificity (Meulmeester et al. 2008; Zhu et al. 2008). Sumoylation is a very dynamic process due to the action of specific Sumo isopeptidases (the Senp family in mammals) that efficiently cleave the Sumo moiety off the target protein (Hay 2007; Mukhopadhyay and Dasso 2007). As a consequence, sumoylation of a substrate is controlled by both, modification and demodification and the steady state level of the sumoylated species of a given target protein is often very low.

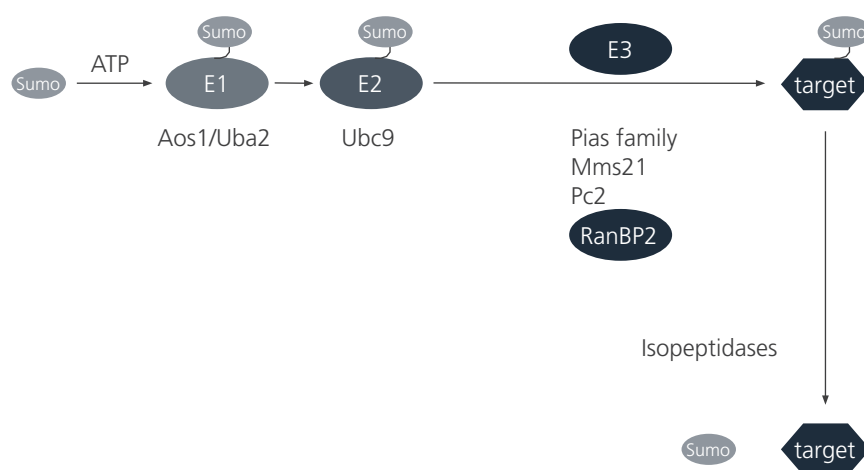


Fig. 5: Sumoylation – a schematic overview. the Sumo E1 enzyme, a heterodimer of Aos1 and Uba2, activates the mature Sumo molecule by covalently attaching an adenyl group to the C-terminal carboxyl group of Sumo; the activated Sumo then forms a thioester with the catalytic cysteine of Uba2. In the second step, Sumo is transferred to the catalytic cysteine of the Sumo E2 enzyme Ubc9 again forming a thioester linkage. In the final step, the Sumo moiety is covalently conjugated to the ϵ amino group of the target lysine; this process is in some cases catalyzed by Ubc9 alone (e.g. RanGAP1) or is supported by a Sumo E3 ligase (most other Sumo targets). Sumo modification is very dynamic due to specific Sumo isopeptidases that cleave the Sumo moiety off the target.

6. Sumo modification of RanGAP1

RanGAP1 was the first and to date one of the most prominent Sumo substrates identified, however it is special in two respects. First, modification of RanGAP1 is unusually efficient and is catalyzed by the Sumo E1 and E2 enzymes alone. No E3 ligase

is required due to a stable interaction of Ubc9 directly with the C terminus of RanGAP1 that allows for rapid modification of the consensus lysine (Bernier-Villamor et al. 2002). Second, once RanGAP1 becomes conjugated to Sumo, it binds very efficiently and stably to the nucleoporin RanBP2, which protects RanGAP1*Sumo1 from demodification by isopeptidases. Together, these properties lead to very stable modification of RanGAP1 with Sumo1.

So far, sumoylation of RanGAP1 has been shown to be essential for complex formation with RanBP2. While the exact details of this interaction still await further clarification, published and ongoing work suggest that Ubc9 is also required as a stable component to build a ternary complex of RanGAP1*Sumo1, RanBP2 and Ubc9 (Zhu et al. 2006, Andreas Werner, unpublished). Importantly, although RanGAP1 and RanBP2 build a stable complex involving a covalently attached Sumo1 molecule, RanBP2 is not an E3 ligase for RanGAP1 (Pichler et al. 2002).

7. The Sumo E3 ligase RanBP2

The most important Sumo E3 ligase for this work is the 358 kD nuclear pore protein RanBP2 (Pichler et al. 2002). Crucial for its activity as an E3 ligase is a very small domain of 79 amino acids in the C-terminal half of the protein, the so-called IR1+M domain that is flanked by a number of FG repeats (binding sites for transport receptors) and the Ran binding sites 3 and 4 (Fig. 6); the active stretch is natively unfolded and adopts its structure upon wrapping around Ubc9 (Pichler et al. 2004). RanBP2 is thought to catalyze the transfer of Sumo to a substrate protein by positioning the Ubc9 thioester for optimal transfer to the acceptor lysine (Reverter and Lima 2005). While catalytic fragments of RanBP2 such as IR1+M or RanBP2 Δ FG act on many substrates *in vitro*, the first and so far only known *bona fide in vivo* substrate of RanBP2 is Topoisomerase II α (TopoII α) (Dawlaty et al. 2008). A hypomorphic allele of RanBP2 in mouse embryonic fibroblasts leads to loss of TopoII α sumoylation and to displacement of the protein from the inner centromere concomitant with severe aberrations in chromosome segregation. These defects can be rescued by overexpression of the catalytic RanBP2 Δ FG fragment. Overall, mice with low levels of RanBP2 show a tendency towards aneuploidy, a hallmark of cancer, and are prone to the development of spontaneous and induced tumors suggesting that the E3 ligase activity of RanBP2 plays an important role in cell division.

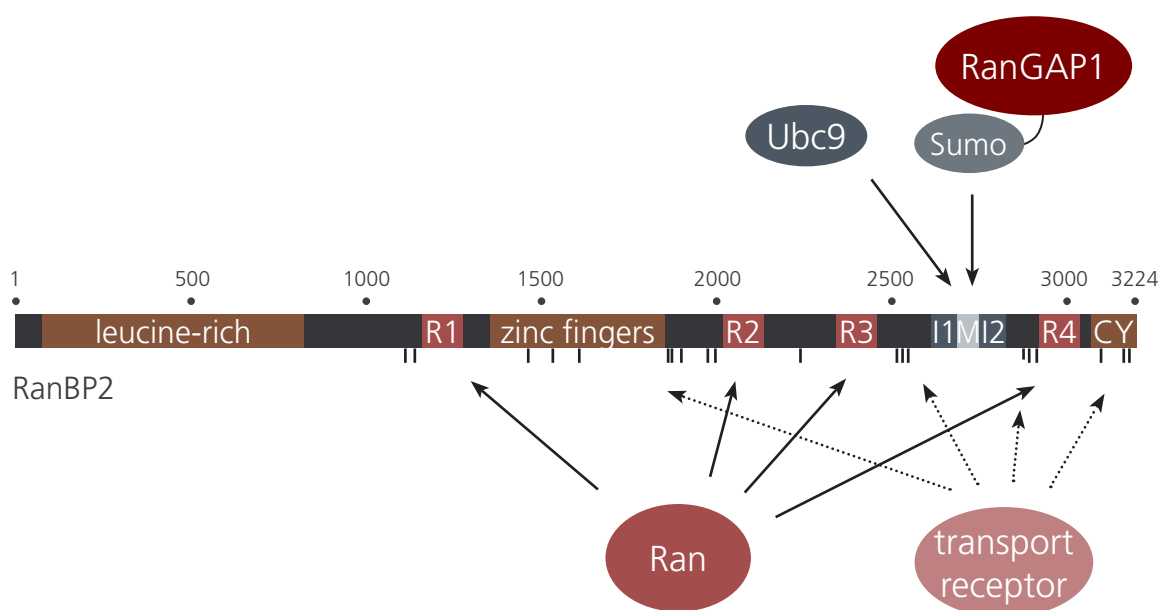


Fig. 6: RanBP2 domain structure. RanBP2 is a 358 kD large nucleoporin comprising a N-terminal leucine-rich domain, a number of zinc fingers, a domain of internal repeats IR1 and IR2 (I1, I2) interspersed by a middle segment (M) and a C-terminal cyclophilin domain (CY); a number of Ran binding domains (R 1-4) and FG repeats (dashes) line the protein mediating interaction with Ran and nuclear transport receptors, respectively. The IR1+M domain harbors the Sumo E3 ligase activity and is also the region of RanBP2 that interacts with RanGAP1*Sumo1 and Ubc9.

8. Regulation of the RanGAP1-RanBP2 complex

Taken all presented features together the RanGAP1-RanBP2 complex represents a fascinating assembly: on one hand it contains the RanGTP hydrolysis promoting activity of RanGAP1 in concert with RanBP2, on the other hand RanBP2 together with Ubc9 harbors Sumo conjugating activity. Given that RanGAP1 and RanBP2 play important roles during both, interphase and mitosis, a better understanding of the regulation of the RanGAP1-RanBP2 complex is instrumental to dissecting its presumably diverse functions.

To date, knowledge on RanBP2 or RanGAP1 regulation is rather limited. By mass spectrometric analysis, both RanGAP1 and RanBP2 have been reported to be phosphorylated (Beausoleil et al. 2004; Swaminathan et al. 2004; Takeda et al. 2005; Beausoleil et al. 2006; Nousiainen et al. 2006). In interphase cells phosphorylation of RanGAP1 at serine 358, possibly catalyzed by casein kinase II, has been suggested to influence ternary complex assembly with Ran and RanBP1; a non-phosphorylated variant is inefficient in co-immunoprecipitating these two components of the Ran system

(Takeda et al. 2005).

During mitosis, RanGAP1 is quantitatively phosphorylated on three different sites (Swaminathan et al. 2004) in the C-terminal tail, T409, S428 and S442 in human RanGAP1. Using specific phosphopeptide antibodies, RanGAP1 phosphorylation can first be detected in early prophase cells when the nuclear envelope is still present. It persists throughout mitosis until the nuclear envelope starts to reform. A quantitative shift towards the triply phosphorylated form can be detected upon arrest of the cells in mitosis with the microtubule destabilizing drug nocodazole (see Fig. 7). While phosphorylation occurs simultaneously on all three sites, dephosphorylation occurs in a more sequential fashion.



Fig. 7: RanGAP1 phosphorylation in mitosis. In mitosis, RanGAP1 is phosphorylated on three closely spaced residues in the C-terminal tail, T409, S428 and S442. Two of the phosphorylation events, pT409 and pS428, give rise to a size shift in SDS PAGE and antibodies specific for the phosphorylated forms of RanGAP1 only detect the modified form (I - interphase, M - mitotic arrest with nocodazole). Two of the phosphorylation sites are highly conserved (S428, S442 in human RanGAP1 are also present in *Xenopus laevis*) while the first site (T409 in human RanGAP1) is absent from *Xenopus* RanGAP1.

It remains to be determined what RanGAP1 phosphorylation means for RanGAP1 function. As phosphorylation of many nucleoporins is thought to act as a signal for the disassembly of the NPCs (Macaulay et al. 1995; Favreau et al. 1996), a putative function of the mitotic RanGAP1 phosphorylation could be to dissociate the RanGAP1-RanBP2 complex; however, phosphorylated RanGAP1 remains tightly associated with both, RanBP2 and Ubc9 in mitosis. Moreover, phosphorylation of RanGAP1 does also not

abolish its GTPase activating function towards Ran, at least not when purified from a detergent-containing HeLa cell lysate. Likewise there are no indications that RanGAP1 phosphorylation may influence protein stability (Swaminathan et al. 2004).

9. Aim of this work

The task of this work was to further elucidate the role of the RanGAP1-RanBP2 complex specifically in mitotic cells. The fact that RanGAP1 becomes phosphorylated at the onset of mitosis served here as a starting point. While previous studies from our and other laboratories have investigated mitosis-specific localization and the GTPase activating function of the RanGAP1-RanBP2 complex this study rather focusses on the sumoylation activity with an emphasis on mitosis-specific *in vivo* substrates and mechanisms of substrate specificity.

MATERIALS & METHODS

1. Materials

1.1. Technical equipment

General laboratory equipment was obtained from various common suppliers, some selected ones are listed below:

Thermomixer compact	Eppendorf, Hamburg
Powersupplies EPS301 und EPS 300	GE Healthcare, München
Elektrophoresis and blotting chambers	Workshop MPI of Biochemistry, Martinsried
Water purification system Ultra Clear	SG, Barsbüttel
Sonicator Sonopuls HD2070	Bandelin, Berlin
Photometer DU640	Beckman, München
Photometer SmartSpec Plus	Bio-Rad, München
Centrifuge J6MI	Beckman Coulter, München
Centrifuge Avanti J30I	Beckman Coulter, München
Centrifuge Allegra X-15R	Beckman Coulter, München
Ultracentrifuge OptimaMax	Beckman Coulter, München
Ultracentrifuge Optima L-80 XP	Beckman Coulter, München
Rotors JS 4.2, JA 30.50Ti, SX4750, TLA 100.3	Beckman Coulter, München
Rotors Type45, Type60Ti, Type70.1Ti	Beckman Coulter, München
Table centrifuge 5415C, 5424	Eppendorf, Hamburg
Bacterial incubator Kelvitron t	Heraeus, Hanau
Shaking incubator Innova 4230	New Brunswick Scientific, Edison, NJ (USA)
Sterile cell culture hood Hera safe	Heraeus, Hanau
Cell culture incubator Hera cell	Heraeus, Hanau
Cell culture incubator Incucell	MMM Medcenter, Planegg
Power supply Variomag Biomodul 40B	H+P Labortechnik, München
Stir plates Biosystem	H+P Labortechnik, München
SpeedVac Concentrator SPD111V	Thermo Electron Corporation, Milford, MA (USA)
Vacuum pump LABOPORT N480.3FTP	KNF Neuberger, Freiburg

Chromatography system Äkta Purifier	GE Healthcare, München
Fluorescence microscope Axioskop 2	Carl Zeiss MicroImaging, Jena
Axiocam	Carl Zeiss MicroImaging, Jena
Documentation system Gel Jet Imager	Intas, Göttingen
Documentation system LAS 3000	Fujifilm, Tokyo (Japan)
Film developing machine Curix 60	Agfa, Köln
Scanner 4990 Photo	Epson, Meerbusch

1.2. Consumable supply

Consumables were obtained from various common suppliers, some selected ones are listed below:

ANTI-FLAG M2 agarose, mouse	Sigma
Autoradiography films (Hyperfilm ECL, BioMax)	GE Healthcare; Kodak
Cell culture consumables	Sarstedt, TPP
Centrifugal filter units	Millipore, Vivaspin
Coverslips (12 mm diameter)	Marienfeld
Cyanogen-activated sepharose 4B	Sigma
Dialysis tubing Spectra-Por	Roth
Disposable plastic columns Bio-Spin, Poly-Prep, Econo-Pac	Bio-Rad
EAH sepharose 4B	GE Healthcare
Filter paper 3MM Whatman	Whatman
Glutathione sepharose FastFlow 4B	GE Healthcare
Monoclonal Anti-HA agarose, mouse clone HA-7	Sigma
Ni-NTA agarose	Qiagen
NuPAGE system	Invitrogen
Protein G agarose, Protein A agarose	Roche
PROTRAN nitrocellulose	Schleicher & Schuell
Reaction tubes	Sarstedt, Eppendorf
Slides	Menzel
Sterile filters and – membranes (0.22 – 0.45 µM)	Millipore, Pall, Renner, Sartorius

1.3. Chemicals, reagents and enzymes

Common chemicals were obtained from AppliChem (Darmstadt), CARL ROTH GmbH (Karlsruhe), Merck (Darmstadt), Serva (Heidelberg) and Sigma-Aldrich (Taufkirchen).

Selected chemicals, reagents and enzymes are listed below:

Acrylamide solution (30 %, 37.5:1 AA:bisAA)	AppliChem, Roth
Aprotinin	Biomol
ATP, disodium salt	Sigma
Benchmark protein marker	Invitrogen
BSA, fraction V	AppliChem
Digitonin, high purity	Calbiochem
DMEM (high glucose)	PAA
DNA ladder	Fermentas
dNTPs	Fermentas
ECL (Pico, Immobilon)	Pierce, Millipore
Fetal bovine serum, FBS	Gibco
FuGENE6	Roche
Glutamine (cell culture grade)	Gibco
GTP and GDP, sodium salt	Sigma
Fluorescent mounting medium	DakoCytomation
Hoechst 33258	Sigma
IPTG	Fermentas
Joklik's modified minimal essential medium	Sigma
Leupeptin	Biomol
Newborn calf serum, NCS	Gibco
Nocodazole	AppliChem
Oligofectamin	Invitrogen
Oligonucleotides	MWG, Operon, Sigma
OptiMEM	Invitrogen
Ovalbumine	Sigma
Pefa bloc	Roth, Sigma
Pepstatin	Biomol

Pfu Ultra, Pfu Turbo polymerase	Stratagene
Phusion polymerase	Finnzymes/NEB
PMSF	Sigma
Poly-lysine	Sigma
Puromycin	Clontech
Restriction enzymes	Fermentas, New England Biolabs
RNase inhibitor	Fermentas
siRNA oligonucleotides	Ambion
T4 DNA ligase	Fermentas
Taxol (Paclitaxel)	Alexis
Thymidine	Sigma
Trypsin/EDTA	Gibco, PAA
Vent polymerase	NEB

1.4. Kits

NucleoBond® PC100, PC500	Macherey & Nagel
NucleoSpin® Extract II	Macherey & Nagel
QIAquick® Gel Extraction Kit	Qiagen
QIAquick® PCR Purification Kit	Qiagen
NucleoSpin RNAII	Macherey & Nagel
RevertAid™ First Strand cDNA Synthesis Kit	Fermentas
BigDye Terminator v1.1 cycle sequencing kit	Applied Biosystems
Factor Xa Cleavage Capture Kit	Novagen

1.5. Buffers and stock solutions

Buffers and stock solutions were prepared using deionized H₂O as solvent unless noted otherwise. Stock solutions were stored at –20 °C or were prepared freshly. HEPES buffers were titrated with potassium hydroxide, other buffers were titrated with sodium hydroxide and hydrochloride.

Stock solutions

Ampicillin	100 mg/ml
Aprotinin, 1000x	1 mg/ml
ATP	100 mM ATP, 100 mM magnesium acetate, 20 mM HEPES pH 7.4
Chloramphenicol	30 mg/ml
Digitonin	10 % (w/v) in DMSO
Dithiothreitol (DTT)	1 M
Hoechst 33258	0.1 mg/ml
Iodoacetamide	0.5 M, prepared freshly
Kanamycin	50 mg/ml
Leupeptin/Pepstatin, 1000x	1 mg/ml each, in DMSO
N-ethylmaleimide	0.5 M in DMSO, prepared freshly
Nocodazole	5 mg/ml in DMSO
Pefa bloc, 100x	100 mM
PMSF	100 mM in 2-propanol
Puromycin	1 mg/ml in PBS
Taxol	10 mM in DMSO
Thymidine	200 mM in PBS, sterile-filtered

Commonly used buffers

Phosphate buffered saline (PBS)	140 mM sodium chloride, 2.7 mM potassium chloride, 10 mM di-sodium hydrogen phosphate, 1.8 mM potassium di-hydrogen phosphate, pH 7.5
PBS/MgCl ₂	PBS supplemented with 1 mM MgCl ₂
PBST	PBS supplemented with 0.2 % (v/v) Tween 20
Transport buffer (TB)	110 mM potassium acetate, 2 mM magnesium acetate, 1 mM EGTA, 20 mM HEPES pH 7.3 titrated with potassium hydroxide
Sumoylation assay buffer (SAB)	transport buffer supplemented with 0.2 mg/ml ovalbumine, 0.05 % (v/v) Tween 20, 1 mM DTT, aprotinin, leupeptin, pepstatin
GPT (lysis) buffer	6 M guanidine hydrochloride, 100 mM sodium

	phosphate, 10 mM Tris-HCl pH 8
UPT (wash) buffer	8 M urea, 100 mM sodium phosphate, 10 mM Tris-HCl pH 8 or pH 6.3
RIPA buffer	150 mM sodium chloride, 1 % (v/v) nonidet P-40, 0.5 % (w/v) sodium desoxycholate, 0.1 % (w/v) SDS, 50 mM Tris-HCl, pH 8
DNA loading dye (stock 6x)	10 mM Tris-HCl pH 8, 50 mM EDTA, 1 % (w/v) SDS, 30 % (w/v) glycerol, 0.1 % (w/v) bromophenol blue, 0.1 % (w/v) xylencyanol
SDS sample buffer	50 mM Tris-HCl pH 6.8, 2 % (w/v) SDS, 0.1 % (w/v) bromophenol blue, 10 % (v/v) glycerol, 100 mM DTT final, prepared as 1x, 2x, 4x stock solutions

1.6. Media

Bacterial media were sterilized by autoclaving, mammalian cell culture media were sterile-filtered.

Bacterial cell culture media

LB	1 % (w/v) bacto-tryptone, 0.5 % (w/v) yeast extract, 1 % (w/v) sodium chloride, pH 7, LB was supplemented with 1.5 % (w/v) bacto-agar for plates
SOC	2 % (w/v) tryptone, 5 % (w/v) yeast extract, 50 mM sodium chloride, 2.5 mM potassium chloride, 10 mM magnesium chloride, 10 mM magnesium sulfate
Autoinducing medium	1 % bacto-tryptone, 0.5 % yeast extract, 25 mM di-sodium hydrogen phosphate, 25 mM potassium di-hydrogen phosphate, 50 mM ammonium chloride, 5 mM sodium sulfate, 2 mM magnesium sulfate, 0.5 % glycerol, 0.05 % glucose, 0.2 % lactose, 10 μ M ferric chloride, 2 μ M manganese chloride, 0.4 μ M cobalt chloride, 2 μ M zinc chloride

Mammalian cell culture media

Jokliks medium was prepared by dissolving Jokliks MEM powder for 10 l together with 20 g sodium hydrogen carbonate and 23.8 g HEPES (cell culture grade) in 10 l autoclaved ultrapure H₂O. The pH was titrated to pH 7.1 with sodium hydroxide, the medium was filter-sterilized and stored at 4 °C in the dark.

Other cell culture media and supplements were obtained commercially.

1.7. Cell lines

Bacterial strains

DH5 α	F- ϕ 80dlacZM15 (lacZYA-argF) U169 deoR recA1 endA1 hsdR17(r _k ⁻ , m _k ⁺) phoA supE44 thi-1 gyrA96 relA1 λ -
INV110	F' {tra Δ 36 proAB lacI ^q Z Δ M15} rpsL (Str ^R) thr leu endA thi-1 lacY galK galT ara tonA tsx dam dcm supE44 Δ (lac-proAB) Δ (mcrC-mrr) 102::Tn10 (Tet ^R)
Bl21 (DE3)	F- ompT hsdS _B (r _B ⁻ m _B ⁻) gal dcm (DE3)
Bl21 gold (DE3)	F- ompT hsdS _B (r _B ⁻ m _B ⁻) dcm+ Tet ^R gal λ (DE3) endA Hte
Rosetta (DE3)	F- ompT hsdS _B (r _B ⁻ m _B ⁻) gal dcm (DE3) pRARE (Cm ^R)
Rosetta2 (DE3)	F- ompT hsdS _B (r _B ⁻ m _B ⁻) gal dcm (DE3) pRARE2 (Cm ^R)

Mammalian cell lines

HeLa (obtained from Francis Barr)	human cervix carcinoma cell line
HeLa (obtained from Mary Osborn)	human cervix carcinoma cell line
HeLa suspension cells (CSH HeLa strain)	human cervix carcinoma cell line
HEK293T cells	human embryonic kidney cell line

1.8. Oligonucleotides, vectors and plasmids

DNA oligonucleotides for cloning		
#	name	sequence (5' – 3')
AP1	Ubch9-s BamHI	TTAAGGATCCGATGTCGGGGATCGCCCTCAGC
AP2	Ubch9-as HindIII	TTAAAAGCTTTGAGGGCGCAAACCTCTTGCTTG
577	5-NdeI-GAP	GGAATTCCATATGGCCTCGGAAGACATTGCCAAGC
578	3-BamHI-stop-GAP	GCGGATCCTAGACCTTGTACAGCGTCTGCAGCAGACT

672	5-BglIII-GAP	GATAGATCTATGGCCTCGGAAGACATTGCC
673	3-GAP 600	GGTCCCGATGACCCTAAAAGC
689	Dralll-AH-XhoI	GTGTTAAGCGTAATCTGGAACATCGTATGGGTAC
690	XhoI-HA-Dralll	TCGAGTACCCATACGATGTTCCAGATTACGCTTAACACTAA
694	Clal-MCS-NotI	CGATATCGCTAGCTTAAGAATTCGGATCCGC
695	NotI-SCM-Clal	GGCCGCGGATCCGAATTCTTAAGCTAGCGATAT
882	NcoIcut-HA-SacIcut	CATGGGATACCCATACGATGTTCCAGATTACGCTAGCTTGCCCGAGCT
883	SacIcut-AH-NcoIcut	CGGGCAAGCTAGCGTAATCTGGAACATCGTATGGGTATCC
1123	5-BamHI-hUbc9	GTGGATCCGATGTCGGGGATCGCCCTCAGC
1183	3-EcoRI-stop-8xHis	GTGAATTCTTAGTGATGGTGATGGTGATG
1316	5-EcoRI-Pias1	ATGAATTCCATGGCGGACAGTGC GG AAC
1317	3-XhoI-stop-8xHis-KpnI-Pias1	TACTCGAGTCAATGGTGATGGTGATGATGGTGGTGGGTACCGTCC AATGAAATAATGTCTGGTATGATGCC
1321	5-SacI-hTACC2i5	ATGAGCTCATGGGCAATGAGAACAGCACC
1322	3-XhoI-stop-hTACC2	TACTCGAGTTAGCTTTTCCCCATTTTGGC
1364	5-SacI-hTACC2i2	ATGAGCTCATGCCCTGAGGAGGCCAAAG
DNA oligonucleotides for mutagenesis		
534	5-GAPL263sil	GACCTTGAAGACC CT CCGGCAGGTGGAGGT
535	3-GAPL263sil	ACCTCCACCTGCCG GAG GGTCTTCAAGGTC
536	5-GAPT409E	GGAGAGAAGTCAGCC GAG CCCTCACGGAAGATTC
537	3-GAPT409E	GAATCTCCGTGAGGG CT CGGCTGACTTCTCTCC
538	5-GAPT409A	AGAGAAGTCAGCC GCG CCCTCACGGAAG
539	3-GAPT409A	CTCCGTGAGGG GCG GGCTGACTTCTCT
540	5-GAPS428D	CTCCCGTGCTGTCC GAC CCACCTCCTGCAGAC
541	3-GAPS428D	GTCTGCAGGAGGTGG GTC GGACAGCACGGGAG
542	5-GAPS428A	CGTGCTGTCC GCCC ACCTCCTG
543	3-GAPS428A	CAGGAGGTGG GGC GGACAGCACG
544	5-GAPS442D	CTTCTGGCTTTTCCC GAT CCAGAGAAGCTGCTGC
545	3-GAPS442D	GCAGCAGCTTCTCTGG ATC GGGAAAAGCCAGGAAG
546	5-GAPS442A	TTCCTGGCTTTTCCC GCT CCAGAGAAGCTGCTG
547	3-GAPS442A	CAGCAGCTTCTCTGG AGC GGGAAAAGCCAGGAA
575	5-GAPK524R	CATGGGTCTGCTC AGG AGTGAAGACAAGG
576	3-GAPK524R	CCTGTCTTCACT CCT GAGCAGACCCATG
895	5-hUbc9K14R	CTCGCCAGGAGAGG AGAG CATGGAGGAAAAGAC
896	3-hUbc9K14R	GTCTTCTCCATGCT CT CCTCTCTGCGCGAG
926	5-hUbc9K153R	GTCCGAGCACAAGCC AGG AAGTTTGCGCCCTC
927	3-hUbc9K153R	GAGGGCGCAAAC CT TGGCTTGCTCGGAC
1223	5-hUbc9HisK159A	GAAGTTTGCGCCCTC AGCG CTTGC GGCCGCACAG
1224	3-hUbc9HisK159A	CTGTGCGGCCGCAAG CGCT GAGGGCGCAAAC CT C
1329	5-Pias1 stop538Y	GACACCCATGC CTTAC GACTTACAAGGATTAG

1330	3-PIAS1stop538Y	CTAATCCTGTAAAGTC GTA AGGCATGGGTGTC
1431	5-PIK1K556R	CTACATCGACGAG AGG CGGGACTTCCGCAC
1432	3-PIK1K556R	GTGCGGAAGTCCCG CCT CTCGTCGATGTAG
1433	5-PIK1K601R	CCAGCAACCGTCTC AGG GCCTCCTAACTCGAG
1434	3-PIK1K601R	CTCGAGTTAGGAGGC CCT GAGACGGTTGCTGG

Vectors for bacterial expression		
name	features	origin
pGEX-6P3	N-term. GST, Precission cleavage site	GE Healthcare
pETDuet1	bicistronic expression	Novagen
pET11a		Novagen
pET28a	N-term. His	Novagen
pETDuet-His	N-term. His	this work
Vectors for mammalian expression		
pHHS10B	N-term. HA	Furukawa and Hotta, 1993
pQE TriSystem HisStrep1	C-term. Strep and His	Qiagen
pQE TriSystem His-HA	N-term. His, C-term. HA	this work
pcDNA4TO	CMV promoter under control of tet operator	Invitrogen
pIRESpuro2-MCS	IRES-coupled puromycin	this work
Plasmids for bacterial expression		
pGEX-6P-PIAS1-His	GST-hPIAS1-His	this work
pETDuet-His-TACC2i2	His-hTACC2 isoform 2	this work
pETDuet-His-TACC2i7	His-hTACC2 isoform 7	this work
pET11a-hRanGAP1 wt	hRanGAP1 wt	this work
pET11a-hRanGAP1 EDD	hRanGAP1 EDD	this work
pET11d-mRanGAP1	mRanGAP1	Mahajan et al., 1997
pET28a-His-Aos1	His-hAos1	Pichler et al., 2002
pET11d-Uba2	hUba2	Pichler et al., 2002
pET23a-Ubc9	mUbc9	Pichler et al., 2002
pGEX-3X-RanBP2 Δ FG	GST-hRanBP2 Δ FG	Pichler et al., 2002
pET11a-Sumo1 Δ C4	hSumo1 Δ C4	Pichler et al., 2002
pET11a-Sumo2 Δ C11	hSumo2 Δ C11	Meulmeester et al., 2008
pEYFP-Sumo1 Δ C4	EYFP-hSumo1 Δ C4	Pichler et al., 2002
pET28a-His-Sumo1 Δ C4	His-hSumo1 Δ C4	Meulmeester et al., 2008
pET28-YFP-Sp100	YFP-hSp100	Tina Lampe, unpublished*

Plasmids for mammalian expression	
pDsRed-hRanGAP1	Joseph et al., 2002
pDsRed-hRanGAP1 wt (L263 sil mut)	this work
pDsRed-hRanGAP1 T409E	this work
pDsRed-hRanGAP1 T409A	this work
pDsRed-hRanGAP1 S428D	this work
pDsRed-hRanGAP1 S428A	this work
pDsRed-hRanGAP1 S442D	this work
pDsRed-hRanGAP1 S442A	this work
pDsRed-hRanGAP1 S428/442D	this work
pDsRed-hRanGAP1 S428/442A	this work
pDsRed-hRanGAP1 T409E/S428/442D	this work
pDsRed-hRanGAP1 T409A/S428/442A	this work
pDsRed-hRanGAP1 K524R	this work
pHA-hRanGAP1 wt	this work
pHA-hRanGAP1 AAA	this work
pHA-hRanGAP1 EDD	this work
pHA-hRanGAP1 KR	this work
pIRES-HA-hRanGAP1 wt	this work
pIRES-HA-hRanGAP1 AAA	this work
pIRES-HA-hRanGAP1 EDD	this work
pIRES-HA-hRanGAP1 KR	this work
pQE TriSystem-His-TACC2i2	this work
pQE TriSystem-His-TACC2i7	this work
pcDNA-Flag-Plk1	Hanna Vörsmann*
pcDNA-HA-Plk1 wt	this work
pcDNA-HA-Plk1 K556R	this work
pcDNA-HA-Plk1 K601R	this work
pQE TriSystem-hUbc9-StrepHis	Andrea Pichler*
pcDNA-hUbc9-His wt	this work
pcDNA-hUbc9-His K14R	this work
pcDNA-hUbc9-His K153R	this work
pcDNA-hUbc9-His K14/153R	this work
pcDNA-HA-Sumo1	Desterro et al., 1998

1.9. Proteins

Protein	Source
His-Aos1/Uba2 (Sumo E1)	common stock [#]
Ubc9 (Sumo E2)	common stock [#]

RanBP2 Δ FG	this work
PIAS1-His	this work
Sumo1 Δ C4	common stock [#]
Sumo2 Δ C11	common stock [#]
YFP-Sumo1 Δ C4	common stock [#]
His-Sumo1 Δ C4	Erik Meulmeester*
YFP-Sp100	Andreas Werner*
His-TACC2 isoform 2	this work
mRanGAP1 wt	common stock, Florian Kiendl*
mRanGAP1 TSS 411,430,444 EEE	Florian Kiendl*
mRanGAP1 K526R	Florian Kiendl*
His-Crm1	Ralph Kehlenbach*
Sumo3 vinylmethylester (Sumo Vme)	Lukasz Kozackiewicz, Erik Meulmeester*

* These people are current or former members of the Melchior lab.

[#] These proteins were purified alternately by members of the Melchior lab and are available as common protein stocks in the lab.

1.10. Antibodies

Primary antibodies

Antibody	Immunogen	Origin/reference	Concentration	Dilution
goat α RanGAP1	mRanGAP1	Melchior lab Pichler et al., 2002	0.8 mg/ml	WB 1:3000 IF 1:2000 - 1:1000
goat α RanGAP1	mRanGAP1	Melchior lab Pichler et al., 2002	1.6 mg/ml	WB 1:6000 IF 1:1000
goat α RanGAP1 pT409	mRanGAP1, peptide comprising pT411 (T409 in human)	Melchior lab Swaminathan et al., 2004	1 mg/ml	WB 1:1000

goat α RanGAP1 pT409 (pre-absorbed against non- phospho peptide)	mRanGAP1, peptide comprising pT411 (T409 in human)	Melchior lab Swaminathan et al., 2004	0.22 mg/ml	IF 1:500
goat α RanBP2	hRanBP2 Δ FG	Melchior lab Hutten et al., 2008	0.35 mg/ml	WB and IF 1:1000 - 1:500
goat α Crm1 N-15	hCrm1, N-term. peptide	Santa Cruz	0.2 mg/ml	WB 1:200
rabbit α Crm1	hCrm1, C-term. peptide GIFNPHEIPEEMCD	Ralph Kehlenbach Kehlenbach et al., 1998	serum, diluted 1:2 with glycerol	WB 1:2500 IF 1:1000
mouse α Ran	hRan aa 7-171	BD Biosciences	0.25 mg/ml	WB 1:5000 - 1:2000
goat α Ubc9	h/mUbc9	Melchior lab Pichler et al., 2002	1.5 mg/ml	WB 1:500 IF 1:200
mouse α Sumo1 (α GMP-1) clone 21C7	Sumo1	Zymed Matunis et al., 1996	0.5 mg/ml	WB 1:500
mouse α Sumo1 (α GMP-1) clone 21C7	Sumo1	Mike Matunis Matunis et al., 1996	ascites, diluted 1:2 with glycerol	WB 1:500
goat α Sumo2/3	RanGAP1 tail conjugated to Sumo2	Melchior lab, Bossis and Melchior, 2006	n.d.	WB 1:500

rabbit α TopoII α H-231	hTopoisomerase II α , aa 1301 – 1531	Santa Cruz	0.2 mg/ml	WB 1:50
goat α PIAS1 C-20	hPIAS1, C-term. peptide	Santa Cruz	0.2 mg/ml	WB 1:500 - 1:200
rabbit α TACC2	GST-hTACC2 aa2230-2630	ProteinTech Group, Inc.	0.43 mg/ml	WB 1:1000 -1:500
rabbit α CKAP-5	hCKAP-5, C-term. 301 aa	Duane A. Compton Dionne et al., 2000	serum, diluted 1:2 with glycerol	WB 1:500
rabbit α Plk1	hPlk1, C-term. peptide	Cell Signaling	n.d.	WB 1:1000 - 1:250 IF 1:500 - 1:100
mouse α Plk1 clone F-8	hPlk1, aa 261-412	Santa Cruz	0.2 mg/ml	WB 1:200 IF 1:100 - 1:50
mouse α USP7 1G7	N-terminus of USP7	Madelon M. Maurice Meulmeester et al., 2005	0.5 mg/ml	WB 1:500
mouse α USP7 7G9	C-terminus of USP7	Madelon M. Maurice Meulmeester et al., 2005	0.5 mg/ml	WB 1:500
mouse α tubulin α clone DM1A	chicken brain microtubules, specific for tubulin α	Sigma Blöse et al., 1984	ascites	WB 1:10000
mouse α HA clone HA.11	CYPYDVPDYASL	Covance	2.5 - 3.5 mg/ml	WB 1:1000 - 1:500 IF 1:500

mouse α HA clone 12CA5	X47 HA1, aa 76 – 111 (epitope YPYDVPDYA)	Niman et al., 1983	0.4 mg/ml	used for IP only
mouse α Hec1	hHec1, aa 56-642	GeneTex	0.5 mg/ml	WB 1:1000 - 1:500 IF 1:400
rabbit α YFP (GFP) (FL)	GFP, aa 1-238	Santa Cruz	0.2 mg/ml	WB 1:1000

Secondary antibodies

Generally, the secondary antibodies used were raised in donkey against the constant region of goat, mouse and rabbit immunoglobulines and were highly cross-absorbed against other species. Horseradish peroxidase-conjugated secondary antibodies for western blot analysis were obtained from Dianova and were used at a dilution of 1:10000 – 1:5000. Secondary antibodies for immunofluorescence conjugated to Alexa 488 and Alexa 594 were obtained from Molecular Probes and were used at a dilution of 1:500.

1.11. Software

Adobe Creative Suite 3 (Photoshop, InDesign, Acrobat)	Adobe®
AxioVision (LE) Rel. 4.7	Zeiss
BioEdit v. 7	Hall, T.A., 1999
BLAST	Altschul et al., 1990
Blast2Sequences	Tatusova and Madden, 1999
FASTA and SSEARCH - Protein Similarity Search	http://www.ebi.ac.uk/Tools/fasta33
Image Reader LAS 3000	Fuji
SUMOSP 2.0	SUMOSP 2.0: an updated WWW service for sumoylation sites prediction. Jian Ren, Longping Wen, Xinjiao Gao, Changjiang Jin, Yu Xue and Xuebiao Yao. Submitted.

2. Methods

2.1. Molecular biological techniques

Standard procedures in molecular biology were performed on the basis of Molecular Cloning. A Laboratory Manual. Maniatis, T., Fritsch, E.F. & Sambrook, J. (Cold Spring Harbor Laboratory, New York, 1982).

2.1.1. *Culturing and storage of bacteria*

Bacteria were propagated in LB at 37 °C for standard cultures, supplemented with antibiotics as required (ampicillin 100 µg/ml, kanamycin 60 µg/ml, chloramphenicol 30 µg/ml for liquid cultures, half the concentration was used for plates). Liquid cultures were shaken at 180 rpm.

For storage liquid cultures were supplemented with 50 % (v/v) glycerol and stored at –80 °C.

2.1.2. *Plasmid preparation*

For most purposes including cloning, clone screening, mutagenesis, sequencing and DNA storage, DNA was prepared from DH5α bacteria at small scale (mini prep) by alkaline lysis (Birnboim and Doly 1979) and DNA precipitation according to a standard protocol. In short, cells equivalent to 4 ml of an overnight culture were harvested, resuspended in 300 µl P1 (50 mM Tris-HCl pH 8, 10 mM EDTA, 100 µg/ml RNase A), lysed by addition of 300 µl P2 (200 mM sodium hydroxide, 1 % (v/v) SDS) and protein and debris was precipitated by addition of 300 µl P3 (3 M potassium acetate pH 5.5). The soluble fraction was cleared by centrifugation and plasmid DNA was precipitated by addition of 0.8 volumes of 2-propanol. The precipitated DNA was collected by centrifugation, washed with 70 % (v/v) ethanol, was dried and was reconstituted in 50 µl TE buffer (10 mM Tris-HCl pH 8, 0.1 mM EDTA).

For transfection and in instances where problems arose due to DNA impurity, DNA was prepared at larger scale using midi or maxi prep kits from Qiagen or Macherey & Nagel according to the manufacturers' instructions. DNA was generally reconstituted in sterile H₂O. DNA concentration and purity was assessed by measuring absorption at 260 and 280 nm.

2.1.3. Cloning

DNA constructs were documented and handled virtually using the software tool BioEdit v. 7 (Hall 1999).

DNA restriction, agarose gel electrophoresis and DNA ligation

The enzymes and buffer system of Fermentas were used for DNA restriction. The conditions were chosen according to the manufacturer's instructions. In some instances the buffer system of New England Biolabs was used for double restrictions. 10 µl mini prep DNA or 1 µg of midi/maxi prep DNA was used in a volume of 100 µl for preparative restrictions using approximately 20 – 30 units of enzyme for 2 – 6 h, 3 – 5 µl of mini prep DNA in a volume of 20 µl for control restrictions using 3 – 5 units of enzyme for 1 – 2 h. The volume of the enzyme never exceeded 1/10 of the reaction volume.

After restriction the DNA fragments were separated on 1.3 % or 2 % (w/v) agarose gels in TAE buffer (1 mM EDTA, 40 mM Tris acetate pH 7.7) at 70 V. DNA was stained in a bath with 1 µg/ml ethidiumbromide and was visualized with UV light. For preparative purposes UV light of 365 nm was applied.

DNA fragments were extracted from agarose gels using a DNA extraction kit from Qiagen or Macherey & Nagel according to the manufactureres' instructions. DNA was eluted in a volume of 30 µl of the elution buffer.

Ligations were set up at a vector to insert ratio of approximately 1:7. For triple ligations a ratio of 1:3.5:3.5 of vector:insert:insert was used. 1 Weiss unit of T4 DNA ligase (Fermantas) was used in a total volume of 10 µl adding some ATP in addition to the supplied ligation buffer. Ligation was performed cycling 100 times between 10 °C and 30 °C for 30 seconds each step, for 1 h at room temperature or at 16 °C overnight. Generally, the ligase was heat inactivated at 65 °C for 20 minutes before transforming half of the reaction into DH5α.

mRNA and cDNA preparation

mRNA was prepared from cycling or nocodazole-arrested HeLa cells using the NucleoSpin RNAII kit from Macherey & Nagel according to the manufacturer's instructions. mRNA was transcribed into cDNA using the First-strand cDNA Synthesis with RevertAid™ kit from Fermentas.

PCR techniques

PCR reactions were set up in a final volume of 50 μ l using 0.5 μ l or 50 – 100 ng template DNA or 1 – 2 μ l cDNA, 500 μ M of each, forward and reverse primer, 200 μ M of each dATP, dTTP, dGTP, dCTP and 1 units Phusion (Finnzymes), Vent (NEB) or 1.25 units PfuUltra or PfuTurbo for most site-directed mutagenesis reactions (Stratagene). In some instances, especially for amplification from cDNA and for site-directed mutagenesis 2 – 4 % (v/v) DMSO were added to the reaction. The annealing temperature was calculated for the annealing part of the oligonucleotide according to online calculators (Phusion: https://www.finnzymes.fi/tm_determination.html, other polymerases: <http://www.basic.northwestern.edu/biotools/oligocalc.html>). 3 $^{\circ}$ C were added to the calculated temperature for Phusion, 5 – 6 $^{\circ}$ C were subtracted when DMSO was added. The amplification time was chosen according to the given processivity of the polymerase. Amplification was performed according to the following program: initial denaturation for 2 – 3 minutes at 95 $^{\circ}$ C or 98 $^{\circ}$ C (Phusion), during cycling 15 – 30 seconds denaturation at 95 $^{\circ}$ C or 98 $^{\circ}$ C (Phusion), 15 – 30 seconds annealing at the calculated temperature, elongation at 72 $^{\circ}$ C for the calculated time, standardwise 35 cycles, including a final elongation step at 72 $^{\circ}$ C for 2 – 10 minutes. Primers for site-directed mutagenesis were chosen with the help of the web-based software tool PrimerX (<http://www.bioinformatics.org/primerx/>).

Oligonucleotide cloning

To introduce some affinity tags or restriction sites, oligonucleotides were designed with the appropriate overhangs to match the restriction sites of the target vector; the oligonucleotide pair was annealed in annealing buffer (30 mM HEPES pH 7.4, 100 mM potassium acetate, 2 mM magnesium acetate) at a concentration of 6 μ M per oligonucleotide by boiling the reaction for 5 minutes at 95 $^{\circ}$ C in a 0.5 – 1 l water bath. The reaction was then allowed to cool down slowly. The annealed oligonucleotide pair was then phosphorylated with polynucleotide kinase (Fermantas) according to the manufacturer's instructions and approximately 250 nM of the annealed oligonucleotide pair was used in a standard ligation reaction.

Preparation and transformation of competent bacteria

Transformation competent E. coli were prepared from a growing culture of OD₆₀₀ 0.4

– 0.5. The cells were incubated on ice for 10 minutes, then collected with 5000 x g at 4 °C. The pellet was resuspended in an equal volume of sterile ice cold TFB-I (100 mM rubidium chloride, 50 mM manganese chloride, 30 mM potassium acetate, 10 mM calcium chloride, 15 % (v/v) glycerol, 0.5 mM lithium chloride; the pH was adjusted to pH 5.8 with acetic acid) and incubated on ice for 2 h. The cells were again collected with 5000 x g at 4 °C and resuspended in 1/25 of the original culture volume of TFB-II (10 mM MOPS, 10 mM rubidium chloride, 75 mM calcium chloride, 15 % (v/v) glycerol; the pH was adjusted to pH 7 with sodium hydroxide). 100 ml aliquots were frozen in liquid nitrogen and stored at –80 °C.

For transformation, competent *E. coli* were thawed and incubated with the DNA for 20 – 60 minutes on ice. The cells were heat-shocked at 42 °C for 1.5 minutes, then incubated on ice for 3 minutes before LB or SOC medium was added. The cells were allowed to recover for 1 h at 37 °C before antibiotics were added for selection.

2.1.4. Sequencing

All plasmids constructed via PCR amplification were verified by sequencing. The sequencing reactions were based on BigDye Terminator v1.1 cycle sequencing kit (Applied Biosystems) and were set up and purified according to the protocol given by the respective sequencing facility (Department Osterhelt, MPI of Biochemistry, Martinsried; Department Pieler, University of Göttingen). The sequences were analyzed using the web-based software tool Blast 2 Sequences (<http://www.ncbi.nlm.nih.gov/blast/bl2seq/wblast2.cgi>) or comparable applications.

2.1.5. Vectors and plasmids constructed in this work

pQE TriSystem His-HA: The His tag of pQE TriSystem StrepHis1 was deleted via XhoI-DraIII and was replaced by an oligonucleotide (#689/690) coding for the HA epitope. The C-terminal Strep tag was deleted via the PmlI-XhoI sites and the ends were religated after Klenow fill-in yielding pQE TriSystem HA. pQE TriSystem His-HA was created by inserting an oligonucleotide coding for 8 histidines (#882/883) into the NcoI-SacI sites of pQE TriSystem HA.

pETDuet-His: Note that pETDuet-His only exists as a plasmid coding for a His-tagged protein, in the following designated as spacer. pETDuet-His was constructed by

swapping a 8-fold histidine tag oligonucleotide fused to a 1.5 kb spacer (equivalent to the pQE TriSystem His-HA including a 1.5 kb spacer cloned into the SacI-BamHI sites) via NcoI-BamHI. This vector allows expression of 8-fold His tagged proteins cloned in frame with the SacI site. The second multiple cloning site is being removed by cloning with 3' XhoI.

pIRESpuro2-MCS: pIRESpuro2-MCS was created by cloning an oligonucleotide (#694/695) into the ClaI-NotI sites of pIRESpuro2-His-Sumo1 construct from Guillaume Bossis (unpublished); the resulting vector is equivalent to cloning the oligonucleotide into pIRESpuro2 directly.

pQE TriSystem-hUbc9-StrepHis wt and K14R: Human Ubc9 amplified by PCR (#AP1/2) from pET28b-HisUbc9 (Bernier-Villamor et al. 2002) was cloned into the BamHI-HindIII of pQE TriSystem StrepHis1 (Knipscheer et al. 2008); K14 was changed to R by site-directed mutagenesis (#895/896).

pcDNA-hUbc9-His wt and variants: pcDNA-hUbc9-His was constructed by deleting the Strep tag of pQE TriSystem-hUbc9-StrepHis via the PmlI - XhoI sites followed by religation after Klenow fill-in. The created hUbc9-His was PCR amplified (#1123/1183) and cloned into the BamHI-EcoRI sites of pcDNA4TO. Since the HindIII site used in the first cloning step introduced a lysine at position 159 it was changed to an alanine by site-directed mutagenesis (#1223/1224). The mutations in hUbc9-His (K14R, K153R and K14R/K153R) were introduced by site-directed mutagenesis (#895/896, #926/927).

pDsRed-hRanGAP1 wt and variants: Human RanGAP1 in pDsRed-N1 (Joseph et al. 2002) was subjected to site-directed mutagenesis (#534/535) to first introduce a silent mutation at position 263. A panel of variants was created by site-directed mutagenesis (#536-547, #575/576), in which T409 was changes to E or A, S428 and S442 to D or E, and K524 to R; single, double and triple mutations were introduced stepwise.

pET11-hRanGAP1 wt and variants: hRanGAP1 was PCR amplified (#577/578) from pDsRed1-N1-hRanGAP1 introducing a 5' NdeI site and a 3' stop codon and BamHI site and was cloned into pET11a. The triple variants (T409 S428 S442 to EDD or to AAA) were constructed by swapping a SacI fragment from the respective pDsRed1-N1-hRanGAP1 variants into pET11-hRanGAP1.

pHA-hRanGAP1 wt and variants: BglII-EcoRI fragments carrying hRanGAP1 were swapped from pET11-hRanGAP1 wild type, EDD and AAA variant, into pHHS10B

yielding pHHS-hRanGAP1. Nucleotides 1 – 627 were PCR amplified (#672/673) from pHHS-hRanGAP1 EDD introducing a 5' BglIII site and a BglIII-AflIII fragment (including the silent mutation at L263) was swapped into pHHS-hRanGAP1 yielding pHA-hRanGAP1 wild type and variants. The K524R variant was constructed by swapping an AflIII-DraIII fragment from pDsRed1-N1-hRanGAP1 K524R into pHA-hRanGAP1 in a triple ligation.

pIRESpuro-HA-hRanGAP1 wt and variants: pIRESpuro-HA-hRanGAP1 was constructed by swapping a XbaI-BamHI fragment from pHA-hRanGAP1 wildtype, the triple variants (T409 S428 S442 to EDD or to AAA) and the Sumo-deficient variant (K524R) into the NheI-BamHI sites of pIRESpuro2-MCS.

pGEX-6P-PIAS1-His: PIAS1 was PCR amplified (#1316/1317) from pGEX-PIAS1 (Schmidt and Muller 2002) including the absolute C-terminus and introducing a C-terminal His tag; PIAS1-His was cloned into the EcoRI-XhoI of pGEX-6P3. A mutation (Y538stop) present in some PIAS1 constructs commonly used in the Sumo field leads to a truncation of the C terminus. This nonsense mutation was reverted back to Y by site-directed mutagenesis (#1329/1330) yielding pGEX-6P-PIAS1-His.

pETDuet-His-TACC2: pETDuet-His-TACC2 was cloned by PCR amplification of TACC2 including the stop codon (#1321/1322 for isoform 2, #1364/1322 for isoform 7) from HeLa cDNA. The PCR products were cloned via SacI-XhoI into pETDuet-His and were introduced into pQE TriSystem His-HA using the same restriction sites.

pcDNA-HA-Plk1: pcDNA-HA-Plk1 was constructed by swapping the Plk1 gene from pcDNA-Flag-Plk1 (Vörsmann 2007) into pcDNA-HA-Sumo1 via BamHI-XhoI. The K556R and K601R variants were introduced by site-directed mutagenesis (#1431-1434).

2.2. Cell biological techniques

2.2.1. Culturing and storage of mammalian cells

Adherent HeLa and HEK293T cells were propagated in DMEM supplemented with 10 % (v/v) FBS at 37 °C and 5 % CO₂. Usually, cells were split at a 1/10 ratio just before reaching confluency. For this purpose the cells were washed with sterile PBS, detached from the culture dishes with trypsin/EDTA and diluted with fresh medium. HeLa suspension cells were propagated in Joklik's medium supplemented with 5 % (v/v) NCS, 5 % (v/v) FBS. 2 mM glutamine was added if the medium was older than two weeks.

The cells were cultured in spinner flasks at 100 rpm in a 37 °C incubator at 3 – 10 x 10⁵ cells/ml. The typical doubling time ranged between 16 – 24 h. The cell density was determined using a Neubauer counting chamber and cell density was adjusted daily. For long term storage cells, exponentially growing cells were trypsinized and diluted in serum-containing medium to inactivate the protease; the cells were collected at 70 x g, resuspended in FBS or NCS in case of suspension cells and were then supplemented dropwise with 7 – 10 % (v/v) DMSO under gentle agitation. Aliquots were frozen slowly enclosed in a 2-propanol insulation at –80 °C. Eventually the cells were transferred to liquid nitrogen tanks for long term storage.

2.2.2. *Cell cycle arrest and synchronization*

Exponentially growing cells were arrested in prometaphase by addition of 75 ng/ml nocodazole for 18 h. If adherent cells were used the mitotic cells were collected by washing them off the dishes.

For cell cycle synchronization exponentially growing cells were exposed to 2 mM thymidine for 19 h before thymidine was removed thoroughly and the cells were released into fresh medium for 10 h. The peak of the mitotic index was determined in a pilot experiment by counting the ratio of mitotic cells with condensed chromosomes after Hoechst staining.

2.2.3. *Transfection*

Transient transfections for small scale applications such as immunofluorescence were carried out using FuGENE6, a cationic lipid-based transfection reagent, according to the manufacturer's instructions.

For biochemical purposes and larger scale experiments such as the establishment of stable cell lines calcium phosphate precipitation was applied. 10 µg DNA for 10 cm dishes or 30 µg for 15 cm dishes were supplemented with 200 mM calcium chloride and mixed with equal parts of 2-fold concentrated HBS buffer pH 6.95 – 6.97 (50 mM HEPES, 250 mM sodium chloride, 1.5 mM di-sodium hydrogen phosphate, pH titrated with potassium hydroxide, sterile-filtered) either by pipetting vigorously or by adding the HBS dropwise onto a large surface of the DNA/calcium chloride solution in order to yield small calcium phosphate/DNA precipitates. The mixture was incubated for 10 – 20

minutes and then added to the cells. Generally the medium was exchanged 6 – 24 h after transfection.

To downregulate the levels of RanBP2 cells were transfected with validated siRNA oligonucleotides directed against RanBP2 (RanBP2-1, CACAGACAAAGCCGUUGAAuu) according to an established protocol (Hutten and Kehlenbach 2006). In short, siRNA was obtained from Ambion (standard purity) as single stranded oligonucleotides and pairs were annealed according to manufacturer's instructions. HeLa cells (source Mary Osborn) were transfected with 100 nM siRNA on day 1 and the cells were split and retransfected on day 3; the analysis was performed on day 5. A typical transfection mix for a 24-well format contained 1 µl Oligofectamin diluted in 9 µl OptiMEM. After mixing and 5 minutes of incubation at room temperature 1.75 µl of double-stranded siRNA were added and incubated again for 20 – 40 minutes. The transfection mixture was added to the cells in a volume of 300 µl medium.

2.2.4. Selection of stable HeLa cell lines expressing HA-hRanGAP1

HeLa cells (source Francis Barr) were transfected with pHA-hRanGAP1 wt, pHA-hRanGAP1 AAA, pHA-hRanGAP1 EDD, or pHA-hRanGAP1 KR by calcium phosphate using 20 µg DNA per 15 cm dish. The cells were split the day after transfection, selection with 1 µg/ml puromycin was started 2 days after transfection. The efficiency of selection was controlled on untransfected HeLa cells. The selection medium was renewed after 2 weeks. The transfected cells were cultured under selection until single cells expanded to visible cell colonies. The colonies were examined under the microscope for normal cell morphology and single colonies were scraped off the dish with a sterile pipet tip and transferred into a drop of trypsin to separate the cells. Single clones were expanded to a 10 or 15 cm format and tested for expression of HA-RanGAP1 by western blot analysis of SDS cell lysates. Selection with puromycin was maintained until the clones were frozen for long term storage. Approximately 100 clones were screened for each HA-RanGAP1 variant.

2.2.5. Immunofluorescence and fluorescence microscopy

Cells for immunofluorescence analysis were seeded onto coverslips at least one day in advance, in the case of siRNA knock-down of RanBP2 the coverslips were coated

with poly-lysine beforehand. In most instances the cells were pre-extracted for 10 minutes at room temperature in transport buffer supplemented with protease inhibitors (aprotinin, leupeptin, pepstatin, Pefa bloc), 1 mM DTT and 0.005 % (w/v) digitonin prior to fixation. Digitonin perforates the plasma membrane by preferential binding to cholesterol without solubilizing membranes in general. This allows for removal of the soluble cytoplasmic protein pool. The cells were fixed with 4 % (w/v) formaldehyde in a buffer containing 20 mM PIPES pH 6.8, 0.2 % (v/v) Triton X-100, 4 mM EGTA, 1 mM magnesium chloride for 10 minutes (Stucke et al. 2002). After a washing step with PBS supplemented with 1 mM magnesium chloride (PBS/MgCl₂) unspecific binding sites were blocked with 2 % (w/v) BSA in PBS/MgCl₂ (blocking buffer) for 30 – 60 minutes. The cells were incubated with the primary antibody diluted in blocking buffer for at least 2 h at room temperature or overnight at 4 °C. After two washing steps in PBST and one in PBS/MgCl₂ the cells were incubated with the secondary antibody diluted in blocking buffer and supplemented with 0.2 µg/ml Hoechst 33258 for 2 h at room temperature. The washing procedure was repeated and the coverslips were mounted onto glass slides with flurescent mounting medium (DakoCytomation) after a short rinse with H₂O. Fluorescence was analyzed on a Axioskop 2 fluorescence microscope from Zeiss using apochromatic oil immersion objectives with an enlargement factor of 10, 40 or 63. Pictures were taken with an AxioCam camera (Zeiss) set up with the software AxioVision Rel. 4.6 using the 63x objective with a numerical aperture of 1.4 and the following filter set: #43 (BP 545/25, FT 570, BP 605/70) for Hoechst, #50 (BP 640/30, FT 660, BP 690/50) for Alexa488 and YFP, #1 (BP 365, FT 395, LP 397) for Alexa594, #10 (BP 450-490, FT 510, BP 515-565) for Alexa630/647. Pictures were processed using AxioVision Rel. 4.7 LE and Adobe Photoshop.

2.2.6. *In situ* sumoylation

To detect sumoylation activity in cells they were seeded on coverslips and were pre-extracted with 0.007 % digitonin in transport buffer supplemented with 5 µM Taxol, 1 mM DTT, and protease inhibitors for 5 minutes on ice. The digitonin was removed by two washing steps in the same buffer devoid of digitonin and the cells were incubated with 50 µl of a sumoylation mix for 30 minutes at 37 °C in a humid chamber. For the sumoylation mix 200 µl cytosol of cycling cells were incubated for 20 minutes with

0.2 μ l Sumo3 Vme at 30 °C to inhibit all isopeptidase activity. The amount of Sumo3 Vme required to inhibit isopeptidase activity had previously been titrated by Lukasz Kozaczekiewicz in a FRET-based assay using CFP-GAPtail*YFP-Sumo deconjugation as reference. Half of the cytosol was incubated for 10 minutes with 4 units of hexokinase reconstituted in 30 μ l 250 mM glucose in transport buffer at room temperature. The other half received 30 μ l ATP (final concentration 23 mM ATP) just before added to the cells. Both the hexokinase and the ATP treated cytosol were supplemented with 4 μ g YFP-Sumo1 and 25 μ M Taxol before addition to the cells. The cells were washed three times in PBS/MgCl₂ after sumoylation to remove non-incorporated YFP-Sumo1, and were then fixed and processed as described for other immunofluorescence samples.

2.3. Biochemical techniques

2.3.1. SDS PAGE and analysis

SDS PAGE

SDS polyacrylamide gel electrophoresis was performed essentially according to the system described by Laemmli (Laemmli 1970). In most instances 5 – 20 % continuous gradient gels were used; occasionally 6 % gels were preferred. The gels were prepared in a casting block fitting eight gels at once, equipped with an inlet at the lower border of the glass plates and connecting the batch of gels via a rim at the central bottom of the casting block allowing to fill a batch of gels simultaneously starting from the bottom. Equal volumes of 5 % and 20 % (w/v) polyacrylamide solutions in 0.4 M Tris-HCl pH 8.8, 0.1 % (w.v) SDS were prepared together fitting the casting block. Polymerization was started by adding APS and TEMED (each 0.06 % (w/v)/(v/v) for the 5 % solution and 0.05 % (w/v)/(v/v) for the 20 % solution). The solutions were filled into the casting block using a double-cylindrical gradient mixer yielding a polyacrylamide gradient of 5 % at the top to roughly 20 % towards the bottom of the gel; an overlay of 2-propanol was applied from the top. The 2-propanol was removed thoroughly after polymerizing and the stacking gel (4 % (w/v) polyacrylamide, 50 mM Tris-HCl pH 6.8, 0.1 % (w/v) SDS, 0.1 % (w/v) APS, 0.1 % (v/v) TEMED) was poured; the gels were allowed to polymerize for at least 2 h before running. Gels were run with Laemmli

buffer (25 mM Tris, 192 mM glycine, 0.05 % (w/v) SDS) at 20 mA/300 V per gel at room temperature.

Sample preparation

Samples were adjusted to approximately 50 mM Tris-HCl pH 6.8, 2 % (w/v) SDS, 0.1 % (w/v) bromophenol blue, 10 % (v/v) glycerol, 100 mM DTT with one-, two-, or four-fold concentrated SDS sample buffer and were boiled at 95 °C for some minutes before loading. For storage samples were flash-frozen in liquid nitrogen and kept at –80 °C in most cases. In case samples were too dilute to fit the gel pocket or if the sample contained guanidine, protein was precipitated by methanol-chloroform extraction. 1 volume of sample was mixed with 1 volume of chloroform and 3 volumes of methanol; after mixing 3 volumes of H₂O were added and the mixture was vortexed vigorously. Protein was collected at the water-organic solvent interface by centrifugation at 8000 x g. The water phase was aspirated and 3 volumes of methanol were added again. After mixing protein was collected at the bottom of the tube by centrifugation, was dried and reconstituted in SDS sample buffer.

SDS PAGE analysis

For Coomassie staining, gels were fixed in a solution of 40 % ethanol and 10 % acetic acid in H₂O for 20 – 30 minutes, the gels were rehydrated for 10 minutes in H₂O and were stained in a solution of 0.005 % Coomassie R-250 in 10 % acetic acid. Gels were dried for documentation; for this, they were incubated for 30 – 60 minutes in a gel drying preservative (20 % (v/v) ethanol, 1 % (v/v) glycerol); the gels were mounted between cellophane sheets and clamped between two plastic frames for drying. For immunoblot analysis, gels were transferred on nitrocellulose membranes after SDS PAGE. The gel was mounted between Whatman paper stacks soaked in western blot buffer (25 mM Tris, 193 mM glycine, 20 % (v/v) methanol, 0.036 % (w/v) SDS) and proteins were transferred onto the membrane at 200 mA/300 V for 2 h in a semi-dry western blot apparatus. The transfer was controlled by staining protein with 0.5 % (w/v) PonceauS in 1 % (v/v) acetic acid; excess dye was removed by washing with 1 % acetic acid. Unspecific binding sites on the membrane were blocked by incubating for 30 – 60 minutes in 5 % (w/v) skim milk in PBST. Primary and secondary horseradish peroxidase-coupled antibodies were applied diluted in blocking buffer; the membrane

was incubated with the primary antibody for at least 2 h at room temperature or overnight at 4 °C and with the secondary antibody for 2 h at room temperature. The membrane was washed extensively with at least three changes of PBST after each antibody incubation. Bound antibody was detected by chemiluminescence using ECL kits from Pierce and Millipore; exposed films were developed using an automatic developing machine. In case a single membrane was used to detect several proteins consecutively, old signals were quenched by adding 2 mM sodium azide to the following primary antibody; azide irreversibly inhibits horseradish peroxidase thereby erasing the previous signal. The order of incubation was chosen according to the expected strength of the signal (starting with weak signals) and the size of the protein (starting with lower molecular weight proteins). Alternatively, membranes were cut to separate specific molecular weight ranges (e.g. top to 120 kD, 120 – 50 kD, 50 kD to bottom).

2.3.2. *Antibody purification*

All lab-made antibodies used in this study were affinity-purified against the original antigen based on an established lab protocol. Antibodies that I purified include goat α RanGAP1, goat α RanGAP1 pT409, goat α RanBP2, goat α Ubc9, and mouse α HA (clone 12CA5) antibodies.

For protein matrices, recombinant protein was dialyzed against 0.2 M sodium carbonate pH 9 (carbonate buffer) to remove all traces of primary amines except for the protein itself. Cyanobromide-activated sepharose was swollen in 1 mM hydrochloric acid and washed with several changes of H₂O and one short change of carbonate buffer. The protein was incubated with the sepharose for 1 h at room temperature and overnight at 4 °C, irreversibly immobilizing the antigen on the sepharose beads. The antigen matrix was washed several times with carbonate buffer, remaining active groups were blocked for 1 h with 0.1 – 0.2 M ethanolamine pH 8.9, and the matrix was again washed with carbonate buffer and equilibrated with 0.5 M sodium chloride in PBS before proceeding to antibody binding.

Peptide matrices were prepared using EAH sepharose. EAH sepharose was swollen in 0.5 M sodium chloride, washed several times with PBS and was activated by adding Sulfo-SMCC (Sulfosuccinimidyl 4-[N-maleimidomethyl]cyclohexane-1-carboxylate, Pierce), a bifunctional amine- and sulfhydryl-reactive cross-linker; the N-hydroxysuccinimide ester

reacts with primary amines of the sepharose. Excess cross-linker was removed by several washes with PBS and reduced peptide containing an N-terminal cysteine reconstituted in PBS was added to the activated matrix overnight at room temperature forming a thioether bond with the maleimide group. The peptide matrix was washed extensively and was equilibrated in 0.5 M sodium chloride in PBS before proceeding to antibody binding.

In general, the antigen was coupled at 0.5 – 1 mg/ml and 1 – 3 mg antigen were used for purification from 50 ml of serum or hybridoma cell supernatant. The antibody source was diluted approximately 1:1 with PBS and the antibody was allowed to bind overnight at 4 °C. The antigen/antibody matrix was collected in a column and washed with 100 column volumes 0.5 M sodium chloride in PBS. Bound antibody was eluted with 0.2 M acetic acid pH 1.9 – 2.7 depending on the antigen (RanGAP1 requires a lower pH (pH 2.2) for optimal elution, approximately 1/10 of the antibody remains bound at pH 2.7). The eluted antibody fractions were neutralized by supplementing with 1 M Tris base to a final concentration of ~0.2 M and the antibody was dialyzed against PBS and concentrated using centrifuge concentrators. The antibody concentration was determined by absorption at 280 nm using an extinction factor of 1.25 l g⁻¹ cm⁻¹ and the antibody was diluted 1:1 with 87 % (v/v) glycerol for storage at –20 °C.

2.3.3. Protein expression and purification

Protein expression

E. coli strains suited for protein expression (e.g. BL21(DE3), BL21 gold(DE3), Rosetta(DE3), Rosetta2(DE3)) were transformed with the plasmid for protein expression. Pre-cultures in LB supplemented with antibiotics to select for the maintenance of all desired plasmids were grown over night at 37 °C. Cells were collected by centrifugation and diluted 1:100 into fresh medium supplemented with antibiotics to maintain the expression plasmid. Expression of recombinant proteins in *E. coli* was induced with IPTG or by autoinduction. Autoinduction was obtained by diluting the pre-culture 1:100 into autoinducing medium; the cultures were grown for at least 24 h or to maximal density at 16 – 18 °C shaking 1 l cultures with 130 rpm in 5 l chicane flasks. The optimal induction time may vary depending on the recombinant protein and the bacterial strain

used for expression.

Purification of RanBP2 Δ FG

RanBP2 Δ FG in pGEX-3X was purified according to an established lab protocol (Pichler et al. 2002). In short, RanBP2 Δ FG was expressed as a GST fusion protein by IPTG induction in BL21 gold, and was purified by a GST pull-down in 50 mM Tris-HCl pH 8, 300 mM sodium chloride, 1 mM EDTA, 1 mM EGTA, 1 mM DTT, aprotinin, leupeptin, pepstatin; Pefa bloc was added only to the bacterial lysate but not in later washing steps. GST-RanBP2 Δ FG was further purified by molecular sieving over a preparative Superdex 200 and the GST tag was cleaved by treatment with Factor Xa protease (Novagen). The protease was removed using X arrest agarose (Novagen), and free GST and uncleaved GST-RanBP2 Δ FG was trapped using glutathione sepharose. Cleaved RanBP2 Δ FG was further purified by molecular sieving over a preparative Superdex 200 in transport buffer supplemented with 1 mM DTT, aprotinin, leupeptin, pepstatin and was concentrated in centrifuge concentrators.

Purification of Pias1-His

GST-PIAS1-His in pGEX-6P3 was expressed in Rosetta by autoinduction for 24 h at 17 °C. The cells were lysed in 20 ml PIAS buffer (50 mM Tris-HCl pH 8, 300 mM sodium chloride, 10 % (v/v) glycerol, 50 μ M zinc chloride) with 0.2 % (v/v) Triton X-100, 1 mM DTT, aprotinin, leupeptin, pepstatin, Pefa bloc per liter culture. The cells were lysed with the EmulsionFlex and the lysates were cleared by centrifugation for 1 h with 100,000 x g at 4 °C. The lysates were diluted to 0.1 % (v/v) Triton X-100 and were subjected to a GST pull-down over a column using 2 ml glutathione sepharose (Fast Flow 4B, GE Healthcare) per liter culture. The beads were washed with PIAS buffer supplemented with 0.1 % Triton X-100, 1 mM DTT, aprotinin, leupeptin, pepstatin, and bound protein was eluted with 30 mM glutathione in PIAS buffer devoid of zinc chloride (can inhibit Precission) supplemented with 0.1 % Triton X-100, 1 mM DTT, aprotinin. Eluted GST-PIAS1-His was mixed with 30 μ g Precission and was dialyzed over night against PIAS buffer devoid of zinc chloride supplemented with 0.1 % (v/v) Triton X-100, aprotinin, 1 mM β -mercaptoethanol at 4 °C. Precipitated protein was removed by centrifugation, uncleaved protein, free GST and Precission was removed by a subsequent GST pull-down using 100 μ l glutathione sepharose. PIAS1-His was enriched from the

flow-through on 100 μ l Ni-NTA agarose (Qiagen). The Ni²⁺ beads were washed with PIAS buffer devoid of zinc chloride supplemented with 0.1 % Triton X-100, 1 mM β -mercaptoethanol, aprotinin, leupeptin and bound protein was eluted in the same buffer in the presence of 250 mM imidazole. This protocol allows for purification of 30 μ g full-length PIAS1-His per liter culture, which is active towards p53, His-TACC2 and Plk1, however further optimization is required.

Purification of His-TACC2

His-TACC2 in pETDuet1 was expressed in Rosetta by autoinduction for 24 h at 17 °C. The cells were lysed in 50 mM sodium phosphate pH 8, 300 mM sodium chloride, 1 mM DTT, and aprotinin, leupeptin, Pefa bloc using the EmulsionFlex. The lysates were cleared by centrifugation for 1 h with 100,000 x g at 4 °C. The lysates were diluted 5-fold in lysis buffer supplemented with aprotinin, leupeptin, pepstatin and 20 mM imidazole. His-TACC2 was bound to Ni-NTA agarose over a column using 1 ml beads per liter culture. The column was washed with lysis buffer supplemented with aprotinin, leupeptin, pepstatin and 20 mM imidazole. His-TACC2 was eluted with 250 mM imidazole in lysis buffer supplemented with aprotinin, leupeptin, pepstatin and 1 mM β -mercaptoethanol. His-TACC2 containing fractions were pooled and dialyzed against transport buffer supplemented with aprotinin, leupeptin, pepstatin and 1 mM DTT. The dialyzed protein was cleared by centrifugation at 100,000 x g.

2.3.4. Mammalian cell lysate and extract preparation

Whole cell lysates were prepared by lysing cells in 1x or 2x SDS sample buffer after several washes with PBS at room temperature; the lysates were sonicated and boiled before SDS PAGE analysis. In a few instances whole cell lysates were prepared by lysing cells in 6 M guanidine-HCl in 100 mM sodium phosphate, 10 mM Tris pH 8; the lysates were sonicated and cleared for 30 – 60 minutes by centrifugation at 100,000 x g. Protein was precipitated by methanol-chloroform extraction (see sample preparation) and reconstituted in SDS sample buffer for analysis by SDS PAGE. For standard experiments cell extracts were prepared from cycling or nocodazole-arrested HeLa suspension cells; mitotic adherent cells were washed off the dishes by pipetting. The cells were collected by gentle centrifugation at room temperature with

70 x g and were washed two times with PBS at room temperature. The cell pellet was weighed and resuspended in 2 volumes of cold transport buffer supplemented with 1 mM DTT, aprotinin, leupeptin, pepstatin, Pefa bloc, 50 mM sodium fluoride and phosphatase inhibitor cocktail I (Sigma; for serine/threonine-directed phosphatases). The cells were lysed in a douncer using the S pestle for the preparation of cytosol; for regular cell extracts cell lysis was achieved by adding 0.21 – 0.23 % digitonin (65 – 70 μ L of a 10 % digitonin solution per gram of cells) after resuspension of the cells followed by a 20 minute incubation on ice. Cytosol and cell extracts were cleared by centrifugation at 4 °C: 10 minutes at 300 x g, 30 minutes at 25,000 x g, 60 minutes at 100,000 x g; aliquots were flash-frozen in liquid nitrogen and stored at –80 °C. For most immunoprecipitation experiments the cell extracts were prepared freshly.

2.3.5. Immunoprecipitation

Immunoprecipitations were typically performed from 0.5 to 1 ml cell extract using 10 – 30 μ g affinity-purified antibodies or pre-immune serum as IgG control (assuming a concentration of 10 mg/ml IgG); 48 μ g were used for the immunoprecipitation performed for MS analysis. The antibody was incubated with the cell extracts for 2 –3 h rotating slowly at 4 °C; if required a clearing centrifugation step was included before adding 0.17 μ l Protein G agarose (Roche) per μ g antibody or a minimum of 2.5 μ l. The samples were rotated at 4 °C for another 2 h, aggregates built eventually during incubation were removed and the beads were collected by centrifugation in a swing-out rotor with 70 x g at 4 °C. The immunoprecipitates were washed three times with transport buffer supplemented with 1 mM DTT and protease inhibitors, were transferred to fresh tubes (which minimizes unspecific background substantially!) and bound protein was eluted with 1x SDS sample buffer. One sample was generally sufficient for loading of 3 – 5 gels.

2.3.6. Cross-linking of proteins

Cell extracts of cycling and nocodazole-arrested HeLa suspension cells were adjusted to approximately pH 9 with 1 N potassium hydroxide for cross-linking with dimethyl pimelimidate (DMP; Pierce) and dimethyl suberimidate (DMS; Pierce); the pH was left at pH 7.3 for treatment with ethylene glycol bis[succinimidylsuccinate] (EGS; Pierce). Stock

solutions of the cross-linkers were prepared freshly in transport buffer adjusted to pH 8.1 (DMP, DMS) or in DMSO (EGS) and the cross-linkers were added to the cell extracts at the indicated concentrations. The cross-linkers were allowed to react for 20 minutes at room temperature or at 4 °C. The reactions were quenched by supplementing with 100 mM Tris-HCl pH 8.1 (DMP, DMS) or pH 7.5 (EGS) for 15 – 20 minutes on ice. The samples were mixed with 2x SDS sample buffer for further analysis.

2.3.7. Pull-down with peptide affinity matrices

RanGAP1 peptides (T409: H-CEKSAT(PO₃H₂)PSRKI-OH/H-CEKSATPSRKI-OH; S428: H-CAFPS(PO₃H₂)PEKLLR-OH/H-CAFPSPEKLLR-OH; S442: H-CPVLSS(PO₃H₂)PPPAD-OH/H-CPVLSSPPPAD-OH) were dissolved in PBS at 2 mg/ml and coupled to EAH sepharose at 1 mg/ml (salt elution) or at 0.1 mg/ml (peptide elution). The pull-down assays were performed from commercial HeLa cell pellets (5 x 10⁹ cells/pellet); the cells were resuspended in 2 volumes transport buffer supplemented with 1 mM DTT, 50 mM sodium fluoride, aprotinin, leupeptin, pepstatin, Pefa bloc and were lysed by douncing. The lysates were cleared for 15 minutes by centrifugation with 5000 x g and for 1 h with 100,000 x g at 4 °C.

In case of eluting with stepwise increasing salt concentrations, 7 ml (equivalent to 1/8 cell pellet) cell extract supplemented with phosphatase inhibitor cocktail I (Sigma) and 200 µl of peptide affinity matrix were used per pull-down. The affinity matrix was washed with 1 M sodium chloride in transport buffer supplemented with 1 mM DTT and inhibitors, was equilibrated with transport buffer and was filled into a column. Proteins were bound to the matrix by passing the extract over the columns; the columns were washed with transport buffer and bound protein was eluted with 3 column volumes of each 0.2 M, 0.5 M and 1 M sodium chloride in transport buffer supplemented with 1 mM DTT and inhibitors.

In case of eluting with peptide, 12 ml of HeLa cell extracts were pre-cleared with 1 ml S442 peptide matrix. 6 ml pre-cleared extract and 200 µl affinity matrix were used per pull-down. Protein was bound over a column, the columns were washed with transport buffer supplemented with 1 mM DTT and inhibitors and bound protein was eluted with 3 column volumes of the respective peptide at 1 mg/ml in inhibitor-supplemented transport buffer.

Eluted protein was precipitated by methanol-chloroform precipitation (see sample preparation) and was reconstituted in 1x SDS sample buffer for further analysis.

2.3.8. *In vitro* interaction of recombinant Crm1 and sumoylated RanGAP1

5 μg recombinant mouse RanGAP1 (wild type, phosphomimetic EEE variant, Sumo-deficient KR variant) were incubated for 40 minutes in a sumoylation reaction at 1.6 μM using 300 nM Aos1-Uba2, 550 nM Ubc9, 3.3 μM Sumo1 and 5 mM ATP in sumoylation assay buffer (SAB) at 30 °C. The reaction mix containing sumoylated RanGAP1 was incubated for 1 h with 5 μg His-Crm1 in 0.5 ml SAB at 4 °C (corresponding to 90 nM His-Crm1 and 135 nM RanGAP1). RanGAP1 and associated proteins were recovered by immunoprecipitation using 16 μg goat α RanGAP1 antibodies and 5 μl Protein G agarose; the immunoprecipitates were washed with SAB.

2.3.9. *In vitro* sumoylation with recombinant proteins

Typically 200 – 500 ng of a recombinant sumoylation substrate were incubated in a sumoylation reaction with the following recombinant factors: 68 nM Sumo E1 enzyme (His-Aos1/Uba2), 55 nM Sumo E2 enzyme (Ubc9), 9 – 19 μM Sumo1 or Sumo2 and where indicated with 16 nM Sumo E3 ligase RanBP2 Δ FG or 17 – 68 nM PIAS1-His in sumoylation assay buffer (SAB) in a total volume of 20 μl . The reaction was started by adding 5 mM ATP and was stopped after a 30 – 60 minute incubation at 30 °C with 1.5 volumes 2x SDS sample buffer.

For Plk1 sumoylation, the recombinant protein was produced in HEK293T cells and was enriched by immunoprecipitation with M2 Flag or with HA.7 agarose (Sigma) from cell extracts prepared essentially as described before except that the cells were lysed by adding 0.1 % (v/v) Triton X-100 instead of digitonin. The sumoylation reaction was carried out on the beads to avoid sumoylation of the Flag epitope. Approximately 2.5 – 4 μl beads equivalent to 125 – 250 μl extract were used per reaction. For sumoylation assays with immunoprecipitated proteins, the sumoylation assay buffer was supplemented with Pefa bloc. The reaction was mixed at 600 – 700 rpm at 30 °C in a thermo mixer using an air bubble as stir bar.

2.3.10. *In vitro* sumoylation of recombinant proteins with endogenous RanBP2 E3 ligase

For *in vitro* sumoylation of recombinant YFP-Sp100 with the endogenous RanGAP1-RanBP2-Ubc9 complex, the complex was immunopurified from cell extracts prepared from nocodazole-arrested HeLa suspension cells using 2 ml of extract and 30 μ g of goat α RanGAP1 antibodies and 10 μ l of Protein G agarose. The immunoprecipitates were split into four reactions after washing. To strip off Crm1, the beads were incubated on ice for 30 minutes with RIPA buffer or with transport buffer (supplemented with 1 mM DTT, aprotinin, leupeptin, pepstatin, Pefa bloc) as control; the beads were washed with another change of transport buffer to remove the detergent and were finally split into the sumoylation reactions. The reactions were performed by adding a typical sumoylation mix of recombinant proteins as described in the previous section. The reaction was performed for 45 minutes at 30 °C in a thermo mixer and was stopped by adding 1.5 volumes of 2x SDS sample buffer.

2.3.11. *In vitro* sumoylation and purification of endogenous RanGAP1-RanBP2 associated proteins

Mitotic RanGAP1-RanBP2 complex was purified from freshly prepared nocodazole-arrested HeLa cell extracts by immunoprecipitation with goat α RanGAP1 or goat α RanBP2 antibodies. Typically, 1 – 2 ml of extract and 30 – 60 μ g of antibody were used per sample. The immunoprecipitates were treated for 5 minutes at 4 °C with Sumo3 Vme (e.g. 200 – 250 ng/sample) diluted in transport buffer (supplemented with 1 mM DTT, aprotinin, leupeptin, pepstatin, Pefa bloc) to inhibit eventually associated isopeptidase activity. Excess Sumo3 Vme was removed in an additional wash step. A sumoylation mix was added to the immunoprecipitates typically containing 68 nM His-Aos1/Uba2, 55 nM Ubc9 where indicated (not required for efficient sumoylation), 23 μ M Sumo1 and 5 mM ATP in SAB supplemented with Pefa bloc in a volume of 20 – 40 μ l. The reaction was performed in a thermo mixer for 60 minutes at 30°C and 600 – 700 rpm using an air bubble as stir bar and was stopped by adding 1.5 volumes 2x SDS sample buffer.

For MS analysis, 7.5 – 8 ml extract and 200 μ g goat IgG or α RanGAP1 antibodies were used per sample. Eventual associated isopeptidases were inactivated with 500 ng Sumo3 Vme diluted in 200 μ l transport buffer (supplemented with 1 mM DTT, aprotinin,

leupeptin, pepstatin, Pefabloc) for 5 minutes at room temperature and excess Sumo3 Vme was removed in an additional wash step. The sumoylation reaction containing 164 nM His-Aos1/Uba2, 18 μ M His-Sumo1 in the absence or presence of 5 mM ATP was performed in 50 μ l SAB devoid of ovalbumine. After 1 h incubation in a thermo mixer at 30 °C with 650 rpm the reaction supernatant was transferred to a new tube and both, the bead and the supernatant fraction were denatured by adding 0.2 and 0.5 ml GPT buffer, respectively. The guanidine-soluble fractions were subjected to a denaturing Ni²⁺ pull-down using 30 μ l Ni-NTA agarose (Qiagen) in a spin column. The beads were washed with 3 x 0.5 ml GPT buffer, 3 x 0.5 ml UPT buffer pH 8, and 3 x 0.5 ml UPT buffer pH 6.3 for the first MS screen. Bound protein was eluted with 2x SDS sample buffer and 1/16 of the samples were analyzed by western blotting, the remaining samples were sent to Henning Urlaub (MPI for Biophysical Chemistry, Göttingen) for separation on a NuPAGE gel and for MS analysis. For the second MS screen, the Ni-NTA beads were washed with 3 x 1 ml GPT buffer supplemented with 0.1 % Triton X-100, 5 mM β -mercaptoethanol, 10 mM imidazole, 3 x 1 ml UPT buffer pH 8 supplemented with 0.1 % Triton X-100, 3 x 1 ml UPT buffer pH 6.3 supplemented with 0.1 % Triton X-100, and finally with 1 ml UPT buffer pH 8. Bound protein was eluted with 4 x 100 μ l 250 mM imidazole in 6 M Urea, 75 mM sodium phosphate, 7.5 mM Tris pH 8. Eluted protein was precipitated by methanol-chloroform extraction and was reconstituted in sample buffer fitting the NuPage gel electrophoresis system (Invitrogen). The samples were sent to Henning Urlaub (MPI for Biophysical Chemistry, Göttingen) for separation on a NuPAGE gel (Invitrogen) and for MS analysis.

2.3.12. MS analysis

MS analysis of RanGAP1 interaction partners

Proteins purified by immunoprecipitation with α RanGAP1 antibodies were eluted with SDS sample buffer and separated by gel electrophoresis over a 5 – 20 % gradient gel. After staining with Coomassie or silver (SilverQuest, Invitrogen), bands of interests were excised and in-gel digested with trypsin (Promega) in principle as published by Shevchenko et al. (Shevchenko et al. 1996).

Desalted peptide mixtures were analyzed on an Ultraflex MALDI-ToF/ToF instrument

(Bruker Daltonics, Bremen) in such way that the two most intense peptide ions identified from a previously recorded peptide finger print were selected for confirmation by fragmentation.

MASCOT generic data file were created using FlexControl (Bruker) and searched against the human NCBI nr protein database using MASCOT Server. The following settings were used: Digestion with trypsin allowing 1 miss cleavage, carbamylation of cysteine as fixed modification, oxidation of methionine as variable, 100 ppm peptide mass accuracy and 0.7 Da for fragmentation masses.

The tryptic digestion, MS and MASCOT analysis were carried out by Guido Sauer using the MS facility of the proteomics group at the MPI of Experimental Medicine, Göttingen.

MS analysis of Sumo targets

First MS screen: The gel lanes of both the IgG and the α RanGAP1 bead-bound fraction after sumoylation were cut into 23 gel slices. Each gel slice was subjected to in-gel digestion with trypsin (Roche) and peptides were extracted according to Shevchenko et al. (Shevchenko et al. 1996). The extracted peptides were analyzed in a liquid chromatography-coupled electrospray ionization quadrupole time of flight (Q-ToF Ultima Waters) mass spectrometer under standard conditions.

Data analysis was performed in two batches: The data of samples from the top half of the gel (samples 1-12) were merged as well as the data from the bottom half of the gel (samples 13-23). The created data sets of fragment spectra of sequenced peptides were searched against the mammalian NCBI nr protein database using the MASCOT search engine. The following settings were used: Digestion with trypsin allowing 1 miss cleavage carbamylation of cysteine as fixed and oxidation of methionine as variable modification, 0.3 Da peptide mass accuracy and 0.3 Da for fragmentation masses. The IgG data set obtained for samples 1-12 was subtracted from the α RanGAP1 data set obtained for samples 1-12; the same procedure was applied to samples 13-23. Selected were proteins of the bead-bound fraction from the goat α RanGAP1 samples identified with a score higher than 40 after subtracting trypsin and keratins, all proteins from the IgG control sample, all antibody- and immune system-related proteins, casein and albumin derivatives, and heat shock proteins.

Second MS screen: The bead-bound fractions after sumoylation $-/+$ ATP (second MS screen) were processed as described above. Data sets for each gel slice were analyzed by MASCOT against the mammalian NCBI nr protein database allowing for carbamylation of cysteine and oxidation of methionine as variable modification, 0.0003 Da peptide mass accuracy and 300 mmu for fragmentation masses. Selected were all proteins of the bead-bound fraction + ATP identified with an additive score higher than 40 after subtracting trypsin and keratins, all antibody- and immune system-related proteins, casein and albumin derivatives, heat shock proteins, proteins identified in the IgG control from the first MS screen and in corresponding or directly neighboring bands of the $-$ ATP sample of the second MS screen. In case proteins were also found in the absence of ATP, they were only considered if their score was at least 2-fold as high as the control and a further hit with a score higher than 40 was found in a higher MW band. The additive score corresponds to the sum of all single scores, from which $-$ ATP scores were subtracted.

The tryptic digestion and MS analysis were carried out by Monika Raabe (Urlaub lab, MPI for Biophysical Chemistry, Göttingen; the MASCOT search and data analysis was carried out by myself.

*2.3.13. Double step affinity purification of Ubc9*Sumo*

5 15 cm dishes HEK293T cells co-transfected by calcium phosphate with pQE TriSystem-Ubc9-StrepHis and pcDNA or pcDNA-HA-Sumo1 were washed with PBS at room temperature and were lysed in GPT lysis buffer (6 M guanidine-HCl, 100 mM sodium phosphate, 10 mM Tris pH 8; 5 ml/dish) 40 h after transfection. The lysates were sonicated and were cleared by centrifugation for 1 h with 100,000 x g at 4 °C. In the first purification step, Ubc9-StrepHis was bound to 100 μ l Ni-NTA agarose (Qiagen) over a column and was washed with 4 x 1 ml GPT lysis buffer supplemented with 20 mM iodoacetamide, 20 mM N-ethylmaleimide and 25 mM imidazole and with UPT wash buffer (8 M urea, 100 mM sodium phosphate, 10 mM Tris) supplemented with 20 mM iodoacetamide and 10 mM β -mercaptoethanol, 4 x 1 ml at pH 8 and 4 x 1 ml at pH 6.3. Bound protein was eluted with 50 μ l SDS elution buffer (50 mM Tris-HCl pH 6.8, 2 % (w/v) SDS, 10 % (v/v) glycerol). The SDS eluates were diluted 20-fold to RIPA buffer conditions (0.1 % SDS with RIPA devoid of SDS) supplemented with 20

mM iodoacetamide, 20 mM N-ethylmaleimide, aprotinin, leupeptin, pepstatin, Pefabloc for the second purification step. HA-Sumo1 conjugated species were purified by immunoprecipitation using 15 μ l HA.7 agarose (Sigma), the immunoprecipitates were washed with 4 x 1 ml RIPA buffer and bound protein was eluted with SDS elution buffer. The samples were supplemented with 100 mM DTT and some bromophenol blue prior to SDS PAGE.

2.3.14. *In vivo analysis of the Ubc9 sumoylation site*

HEK293T cells were co-transfected by calcium phosphate with pcDNA-HA-Sumo1 and the indicated hUbc9-His variants (wild type, K14R, K153R, K14/153R, or no Ubc9) in pcDNA4TO. The cells were lysed in GPT buffer (3 ml per P10 dish), the lysates were sonicated and cleared by centrifugation for 1 h with 100,000 x g. Ubc9-His was bound to 50 μ l Ni-NTA agarose over spin columns, the beads were washed with 2 x 1 ml GPT buffer and 1 ml GPT buffer supplemented with 10 mM β -mercaptoethanol, 3 x 1 ml UPT buffer pH 8 and 3 x 1 ml UPT buffer pH 6.3 and bound protein was eluted with 50 μ l 2x SDS sample buffer. Input samples were precipitated by methanol-chloroform extraction (see sample preparation) and reconstituted in 1x SDS sample buffer. The pull-down samples were adjusted to approximately equal levels of unmodified Ubc9-His as the efficiency of recovery was not absolutely equal for all variants tested.

RESULTS

Chapter I: Characterizing the RanGAP1-RanBP2 complex in mitosis

1. Establishing stable cell lines expressing RanGAP1 phospho-variants

Starting point of this work was the observation that RanGAP1 is phosphorylated on three sites in its C-terminal vertebrate-specific domain in mitosis (Swaminathan et al. 2004, for details see introduction). Previous work has failed to reveal a function for this modification in GAP activity, sumoylation and association with RanBP2.

To gain further insights into putative functions, I aimed to undertake a detailed localization and function analysis in cells. Two properties of RanGAP1 hamper its analysis. First, RanGAP1 is a very stable protein forming a tight complex with RanBP2. It therefore takes several rounds through the cell cycle to efficiently replace or downregulate endogenous RanGAP1. Secondly, cells are very sensitive to changes in RanGAP1 protein levels and tolerate neither overexpression nor downregulation because the protein plays crucial roles during interphase and mitosis. Therefore, I wanted to generate stable cell lines expressing wild type and mutant derivatives of HA-tagged human RanGAP1 at or below endogenous levels. Silent mutations were introduced into the HA-RanGAP1 constructs as I hoped to also use these cell lines for replacement of endogenous RanGAP1 by siRNA.

To facilitate selection of stable clones, the HA-RanGAP1 constructs were introduced into a vector that allows for expression of the selection marker under control of the same promoter via an internal ribosome entry site (Fig. 8A). HeLa cells were transfected with these constructs coding for HA-RanGAP1 wild type, a variant that potentially mimics phosphorylation (T409E, S428D, S442D), or that can not be phosphorylated (T409A, S428A, S442A). Additionally, as the functional relevance of RanGAP1 sumoylation is still matter of debate, a variant of RanGAP1 that can not be sumoylated (K524R) was included. After selection with puromycin, single clones were isolated and tested for expression of HA-RanGAP1.

Approximately 100 clones were screened for each, wild type, phosphomimetic, phosphodeficient and Sumo-deficient HA-RanGAP1; only few of them expressed HA-

RanGAP1 at levels comparable to the endogenous levels by western blot analysis with α HA antibodies (Fig. 8B, top panel, and 8C). Most clones were obtained for wild type HA-RanGAP1 and only one for the Sumo-deficient variant. As fusion to the HA tag leads to a size shift of the unsumoylated form of RanGAP1 detectable by SDS PAGE, western blot analysis of the overall RanGAP1 levels in the cell lysates allowed to estimate the maximal expression of HA-RanGAP1 to approximately a third of the endogenous protein (Fig. 8B, middle panel, lane 5).

Even at low expression levels, a striking difference in the ratio of sumoylated versus non-sumoylated RanGAP1 could be observed for the HA-tagged form by comparison to endogenous RanGAP1 from a mother cell line: whereas endogenous RanGAP1 is predominantly sumoylated, the ratio for most HA-tagged forms is shifted towards the unsumoylated species (Fig. 8B, compare lane 1 of the middle panel to lanes 2-11 of the top panel). Complex formation with RanBP2 protects RanGAP1 from desumoylation; considering a limiting number of binding sites for RanGAP1 at RanBP2, this result suggests that even wild type HA-RanGAP1 is limited in its ability to replace endogenous RanGAP1 within the RanGAP1-RanBP2 complex. One possible reason for this is that the N-terminal tag may lead to slightly impaired binding (see also p. 77).

In summary, several stable cell lines could be established for wild type, phosphomimetic and phosphodeficient HA-RanGAP1. These can be used to study the localization below endogenous levels. Due to low expression levels, replacement of endogenous RanGAP1 was not possible.

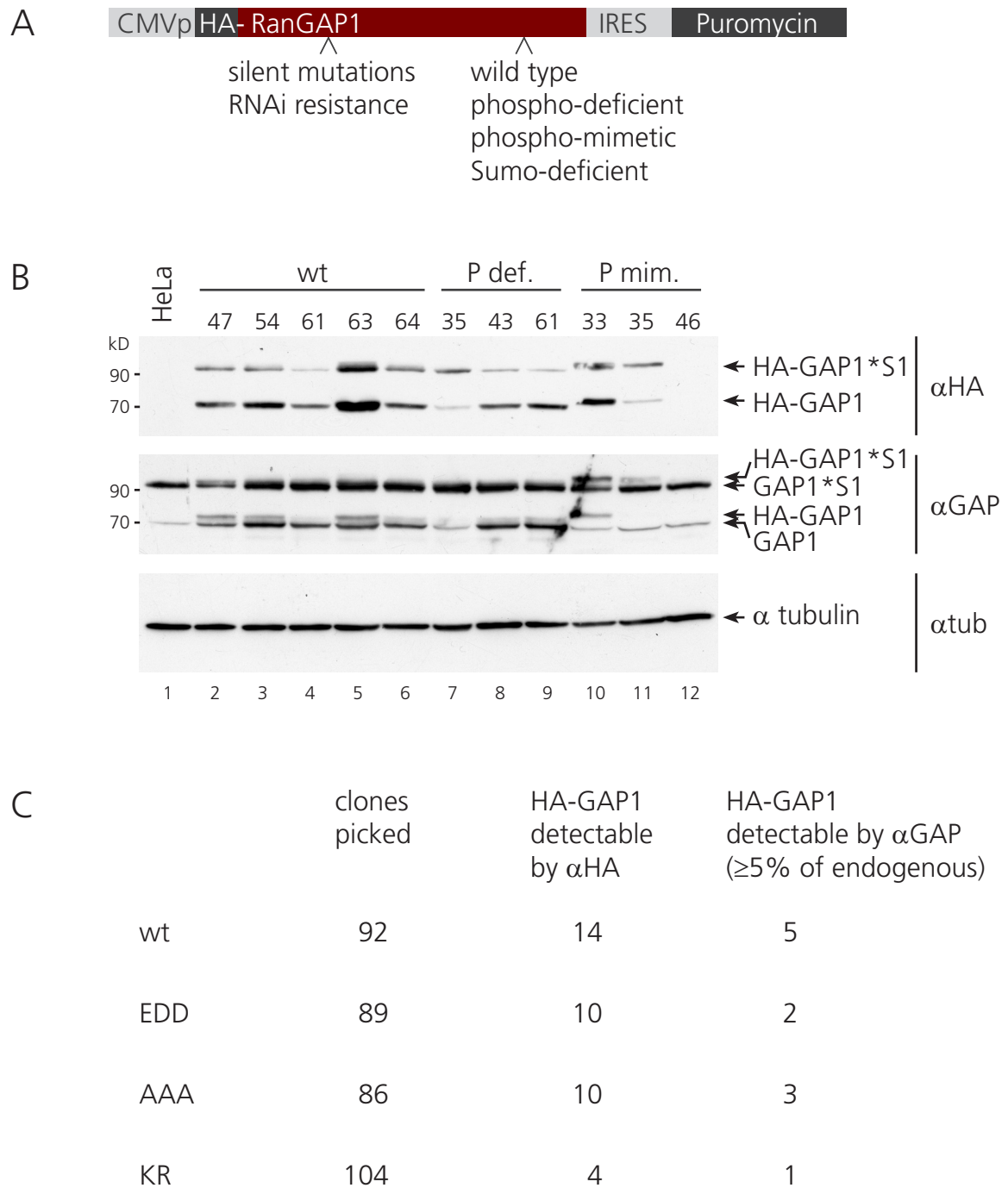


Fig. 8: HeLa cell lines stably expressing HA-RanGAP1 wild type and variants. (A) Replacement strategy. HA-RanGAP1 wild type and the indicated variants (phosphomimetic T409E, S428D, S442D; phosphodeficient T409A, S428A, S442A; Sumo-deficient K524R), all carrying additional silent mutations to confer RNAi resistance compared to the endogenous RanGAP1, were introduced into a vector, in which the puromycin resistance gene for selection is expressed from an internal ribosome entry site (IRES) and is therefore under control of the same CMV promoter as the HA-RanGAP1 gene. Theoretically this strategy allows for the selection of cell lines stably expressing HA-RanGAP1, in which the endogenous RanGAP1 may then become downregulated by RNAi. (B) Selected HeLa cell lines stably expressing HA-RanGAP1 wild type and variants. Cells were lysed in SDS sample buffer and analyzed by western blot with mouse αHA (top), goat αRanGAP1 (middle), mouse αalpha-tubulin (bottom) antibodies. (C) The table shows an overview of how many clones were originally picked for each RanGAP1 species, how many of these expressed HA-RanGAP1 detectable with αHA antibodies, and how many expressed HA-RanGAP1 at levels that could be detected with αRanGAP1 antibodies in comparison to endogenous levels; most clones expressed so little that the endogenous RanGAP1 signal obscured the HA-RanGAP1 signal.

2. RanGAP1 localization to kinetochores in mitosis does not depend on RanGAP1 phosphorylation

To gain insight into RanGAP1 localization during mitosis, I first assessed localization of the endogenous protein. Towards this goal, cells were pre-extracted with digitonin to remove the soluble RanGAP1 pool prior to fixation. By immunofluorescence with α RanGAP1 antibodies, a pool of RanGAP1 relocates from the nuclear envelope in interphase and early prophase to kinetochores in prometaphase represented by the kinetochore marker Hec1 (Fig. 9 and not shown). At later mitotic stages when the mitotic spindle has formed, RanGAP1 can additionally be detected at spindle microtubules. Furthermore the protein also appears to reside at the spindle poles of many meta- and anaphase cells and at central spindle microtubule-like structures in late ana- and telophase cells. In telophase both proteins associate again with the reassembling nuclear envelope. These observations correspond nicely with published data showing that RanGAP1 together with RanBP2 localizes to the spindle and kinetochores in mitosis (Joseph et al. 2002) where they have been shown to be important for stable kinetochore-microtubule attachment (Joseph et al. 2004).

To address the question whether phosphorylation of RanGAP1 is required for its mitosis-specific localization when expressed at levels below the endogenous ones, HeLa cell lines stably expressing human wild type HA-RanGAP1 or the phosphodeficient variant were permeabilized prior to fixation to remove the soluble and therefore mostly unsumoylated pool of HA-RanGAP1. Immunofluorescence analysis of HA-RanGAP1 in these cells showed that the phosphodeficient variant of RanGAP1 localized to kinetochores in prometaphase, to kinetochores and the spindle in metaphase, and to the reforming nuclear envelope in telophase comparable to the wild type protein (Fig. 10). Likewise there were also no discernable differences in localization of overexpressed human RanGAP1 C-terminally fused to DsRed carrying the phosphomimicking or phosphodeficient mutations singly or in combination when compared to wild type (not shown). Thus, mitotic RanGAP1 phosphorylation is not required to localize the protein to kinetochores, the mitotic spindle and the reforming nuclear envelope.

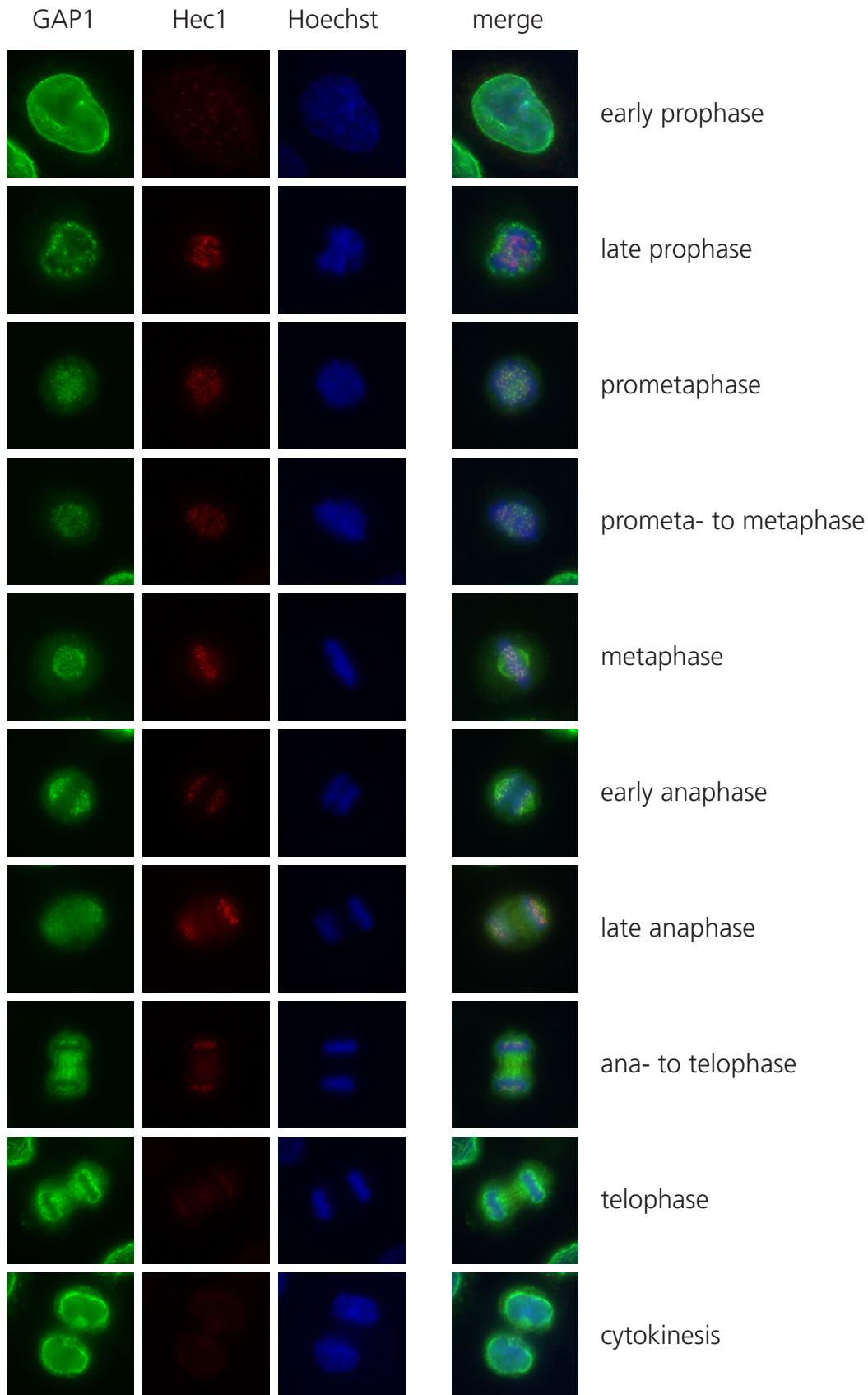


Fig. 9: RanGAP1 localizes to the spindle and kinetochores in mitosis. HeLa cells were permeabilized prior to fixation. Immunostaining was performed with goat α RanGAP1/donkey α goat Alexa488 and mouse α Hec1/donkey α mouse Alexa594 as kinetochores marker, DNA was stained with Hoechst. The samples were analyzed by fluorescence microscopy.

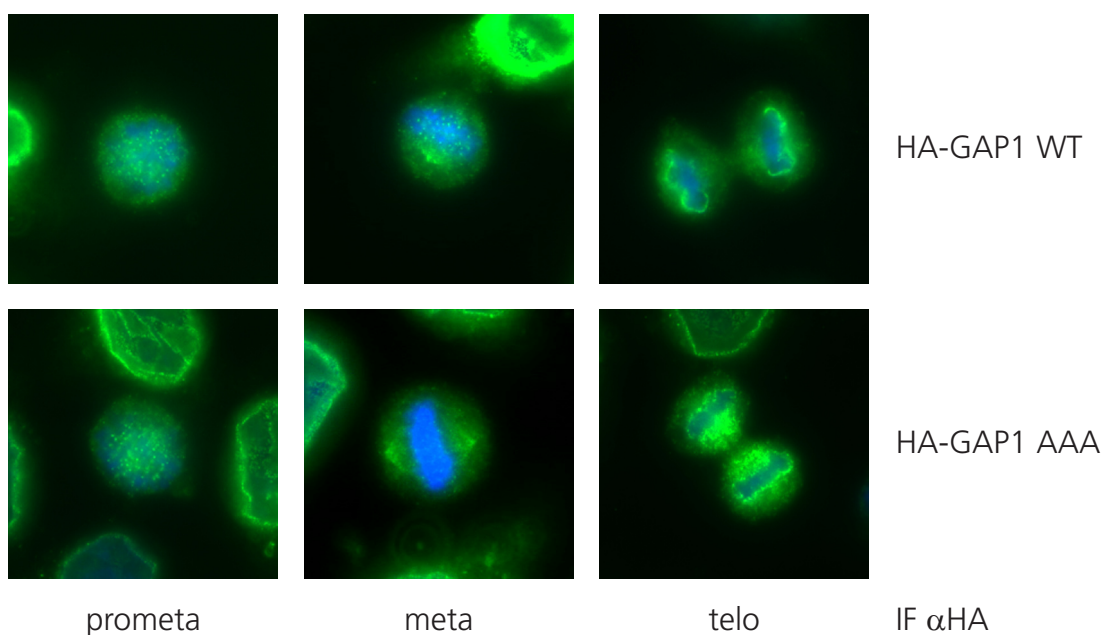


Fig. 10: Non-phosphorylated RanGAP1 localizes to kinetochores in mitotic HeLa cells. HeLa cell lines stably expressing HA-RanGAP1 wild type or a phosphodeficient (T409 S428 S442 to AAA) variant were permeabilized prior to fixation. Immunostaining was performed with mouse α HA/donkey α mouse Alexa488 (green) and DNA was stained with Hoechst (blue). The samples were analyzed by fluorescence microscopy. Note, the metaphase cell in the HA-GAP1 WT panel is tilted in comparison to the AAA panel, therefore only one half of the spindle is visible.

3. Crm1 and Ran are stable components of the mitotic RanGAP1-RanBP2-Ubc9 complex

Many proteins are recruited to their respective binding partner in dependence of a phosphorylation event. An obvious function for mitotic RanGAP1 phosphorylation would be regulation of unknown protein interactions. To follow this idea, several strategies were explored: 1) Cross-linking of interacting proteins; 2) Pull-down with phosphorylated RanGAP1 peptides; 3) immunoprecipitation from mitotic cell extracts. These approaches will be described in the following sections.

3.1. Searching for RanGAP1 interacting proteins

To test the possibility whether RanGAP1 interacts with other proteins in mitosis, cell extracts of mitotic HeLa cells were treated with increasing concentrations of the irreversible bifunctional amino-reactive cross-linker dimethyl pimelimidate (DMP). Indeed, treatment with the cross-linker resulted in α RanGAP1-reactive bands of higher molecular weight when analyzed by SDS PAGE (Fig. 11A). A comparable pattern was also observed

upon treatment with other bifunctional amino-reactive cross-linkers of different spacer length (Fig. 11B; DMP 9.2 Å, DMS 11 Å, EGS 16.1 Å). An α RanGAP1-reactive double band migrating 20 kD bigger than sumoylated RanGAP1 itself was detected preferentially in mitotic cell extracts in comparison to interphase extracts; the cross-linked species also reflected the size shift due to RanGAP1 phosphorylation. For RanBP2, no specific cross-linked species were detectable, as the protein did not migrate into the resolving gel after treatment with cross-linker (not shown). Together, these results suggest that RanGAP1 interacts with other proteins, some of which may be mitosis-specific.

To investigate whether the mitotic phosphorylations of RanGAP1 may provide binding sites for putative interacting proteins, RanGAP1 peptides comprising one phosphorylation site each were immobilized in their unphosphorylated or phosphorylated form and used for pull-down assays. As described in Materials and Methods, 7 ml of extracts from cycling HeLa cells were used for 200 μ g of immobilized peptides. Bound protein was eluted with stepwise increasing concentrations of NaCl (0.2 M, 0.5 M, 1 M NaCl) assuming that potential phospho-specific interactions were of ionic nature. Coomassie staining of the eluted proteins after SDS PAGE showed no discernable differences when comparing the unphosphorylated versus the respective phosphorylated peptides (Fig. 12A, 0.2 M NaCl elution is given as an example). The same held true when the background resulting from unspecifically binding protein was minimized by eluting with the respective unphosphorylated or phosphorylated peptide (shown with the S442 peptide, Fig. 12B). An attempt to fish for interacting proteins with immobilized recombinant RanGAP1 and different phosphomimetic variants did also not lead to the identification of a binding partner (Vörsmann 2007). While technical tricks significantly decreased the unspecific background, it still remained too strong to detect significant differences in bound proteins; these experiments would likely be amenable to a SILAC approach.

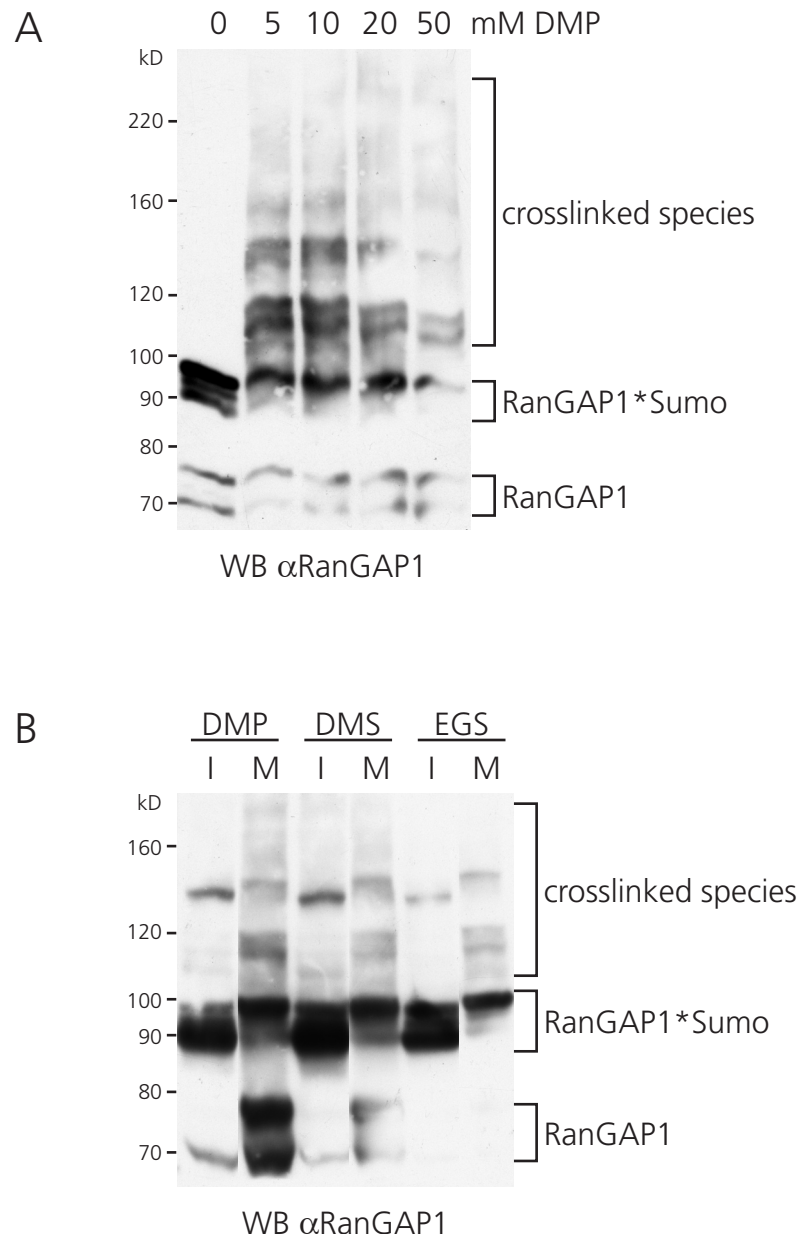


Fig. 11: RanGAP1 can be cross-linked to unknown proteins. (A) Cell extracts from nocodazole-arrested HeLa CSH cells were treated with increasing amounts of DMP, a bifunctional amino-reactive cross-linker. Proteins were separated by SDS PAGE and analyzed by immunoblotting with goat α RanGAP1 antibodies. (B) Cell extracts from cycling (I) and nocodazole-arrested (M) HeLa CSH cells were treated with 5 mM DMP, 5 mM DMS, or 1 mM EGS, all bifunctional amino-reactive cross-linkers of varying length. Proteins were separated by SDS PAGE and analyzed by immunoblotting with goat α RanGAP1 antibodies. Note: not directly neighboring lanes were spliced together from one single blot.

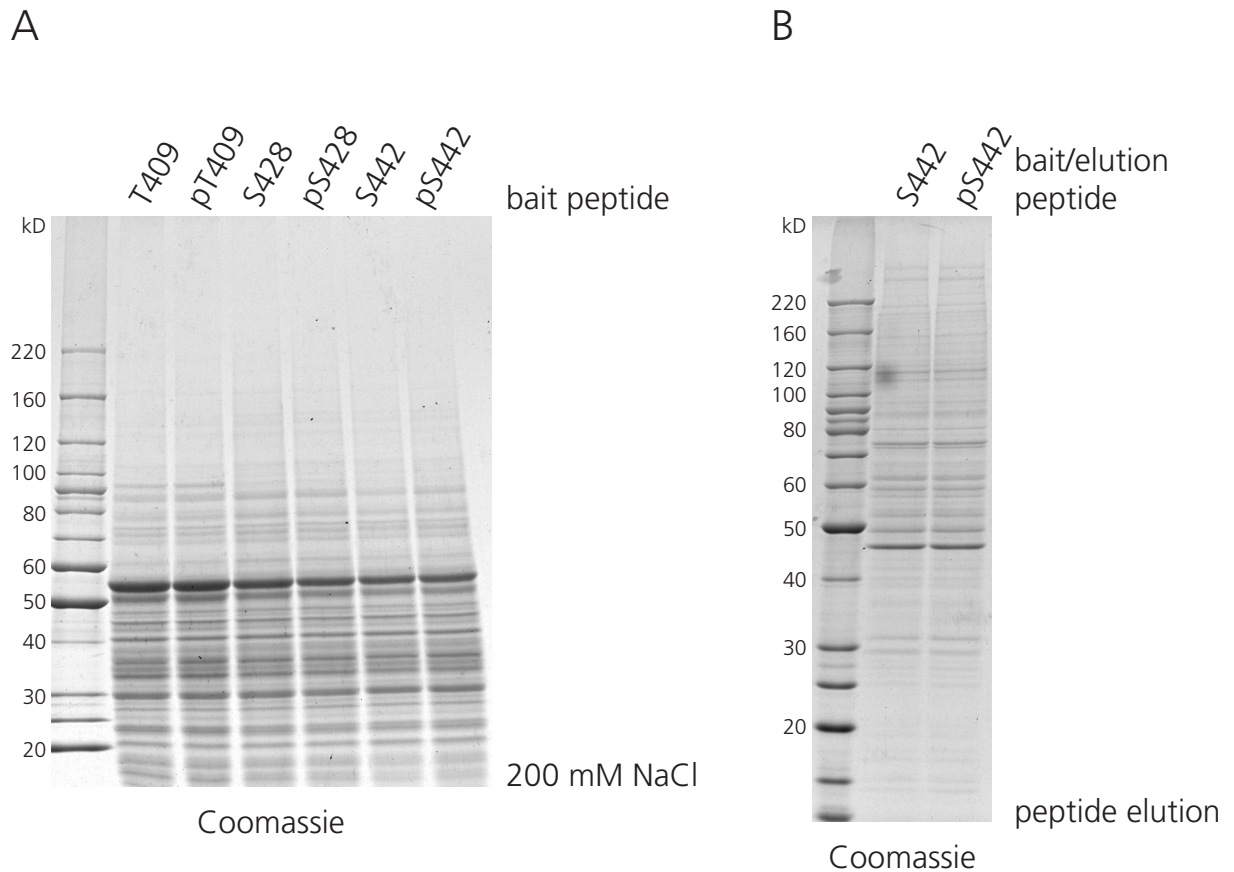


Fig. 12: Pull-down with RanGAP1 phospho-peptides from HeLa cell extracts. (A) Cell extracts of cycling HeLa cells were run over a column of immobilized RanGAP1 peptide comprising the RanGAP1 phosphorylation sites, either in their unphosphorylated or phosphorylated forms. Bound protein was eluted with stepwise increasing concentrations of NaCl. The eluates were separated by SDS PAGE and stained with Coomassie. (B) Cell extracts of cycling HeLa cells were run over columns of immobilized RanGAP1 S442 peptide in its unphosphorylated or phosphorylated form. Bound protein was eluted with either unphosphorylated or phosphorylated RanGAP1 S442 peptide, respectively. Eluted proteins were separated by SDS PAGE and stained with Coomassie.

3.2. The export receptor Crm1 constitutes a major component of the RanGAP1-RanBP2 complex

A more successful strategy to identify proteins associated with the RanGAP1-RanBP2 complex was to purify mitotic RanGAP1 from nocodazole-arrested HeLa cell extracts by immunoprecipitation. 1 ml cell extract and 48 μ g polyclonal α RanGAP1 antibodies were used for the IP of which 1/3 was loaded on gels to visualize co-purifying proteins by Coomassie staining after SDS PAGE (Fig. 13A). A band of about 110 kD represented the most striking difference to the IgG control besides the expected proteins RanGAP1, RanBP2, and Ubc9. This band was excised from the gel, subjected to tryptic digestion and analyzed by MS in collaboration with Guido Sauer. The identified peptide masses in combination with sequencing of selected peptides identified this protein as the nuclear export receptor Crm1. Western blot analysis of RanGAP1 immunoprecipitates confirmed that considerable amounts of Crm1 co-purified with mitotic RanGAP1 next to RanBP2 and Ubc9 but not with the IgG control (Fig. 13B).

To test whether Crm1 is part of the mitotic RanGAP1-RanBP2-Ubc9 complex, RanBP2 (Fig. 13C) and Crm1 (Fig. 13D) were immunopurified from cycling and nocodazole-arrested HeLa cell extracts (100.000 x g supernatant) prepared in transport buffer by digitonin lysis. Of note, nuclear pore complexes do not disassemble under these conditions; consequently, interphase extracts have very little RanBP2 compared to mitotic extracts. All three components, RanGAP1, RanBP2 and Crm1, were recovered specifically with α RanBP2 and α Crm1 antibodies in these experiments from both, cycling and mitotic extracts indicating that Crm1 is indeed a component of the RanGAP1-RanBP2-Ubc9 complex. Of note, purification of Crm1 and RanBP2 from cycling cells resulted in an enrichment of phosphorylated RanGAP1 compared to the respective IP supernatants. In the case of RanBP2, this likely results from the fact that most soluble RanBP2 in these extracts is being contributed by the 5 % mitotic cells present in a growing culture. For Crm1, this result suggests that either Crm1 preferentially associates with phosphorylated RanGAP1 or that the interaction between Crm1 and RanGAP1 is mediated by RanBP2.

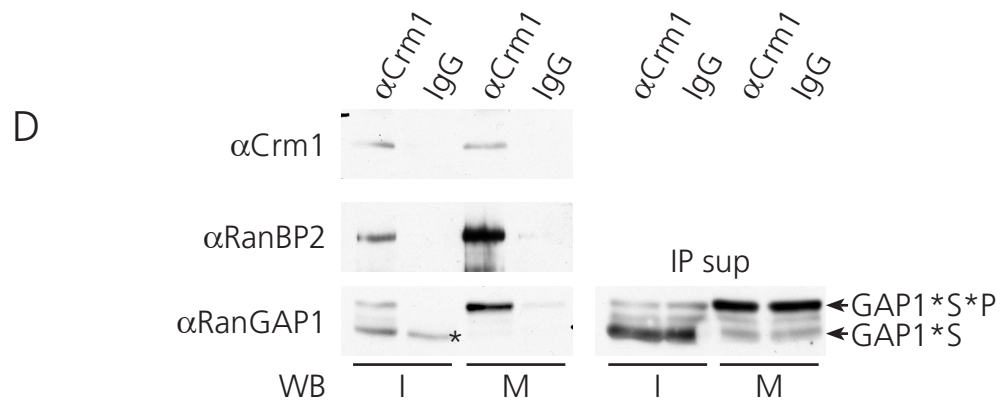
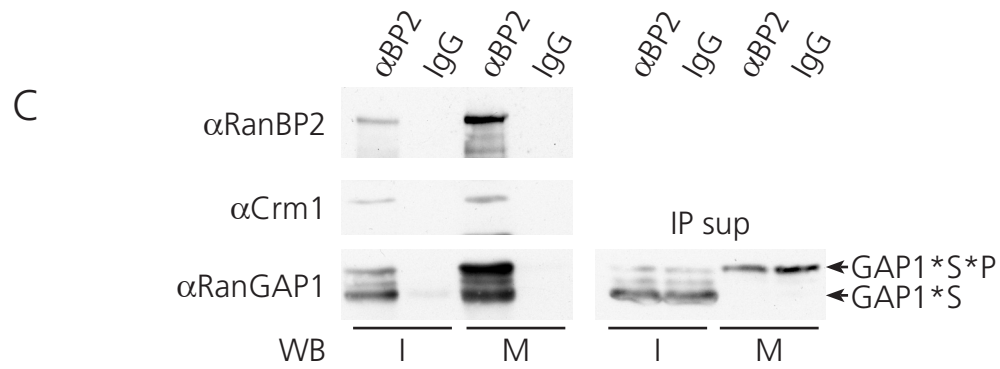
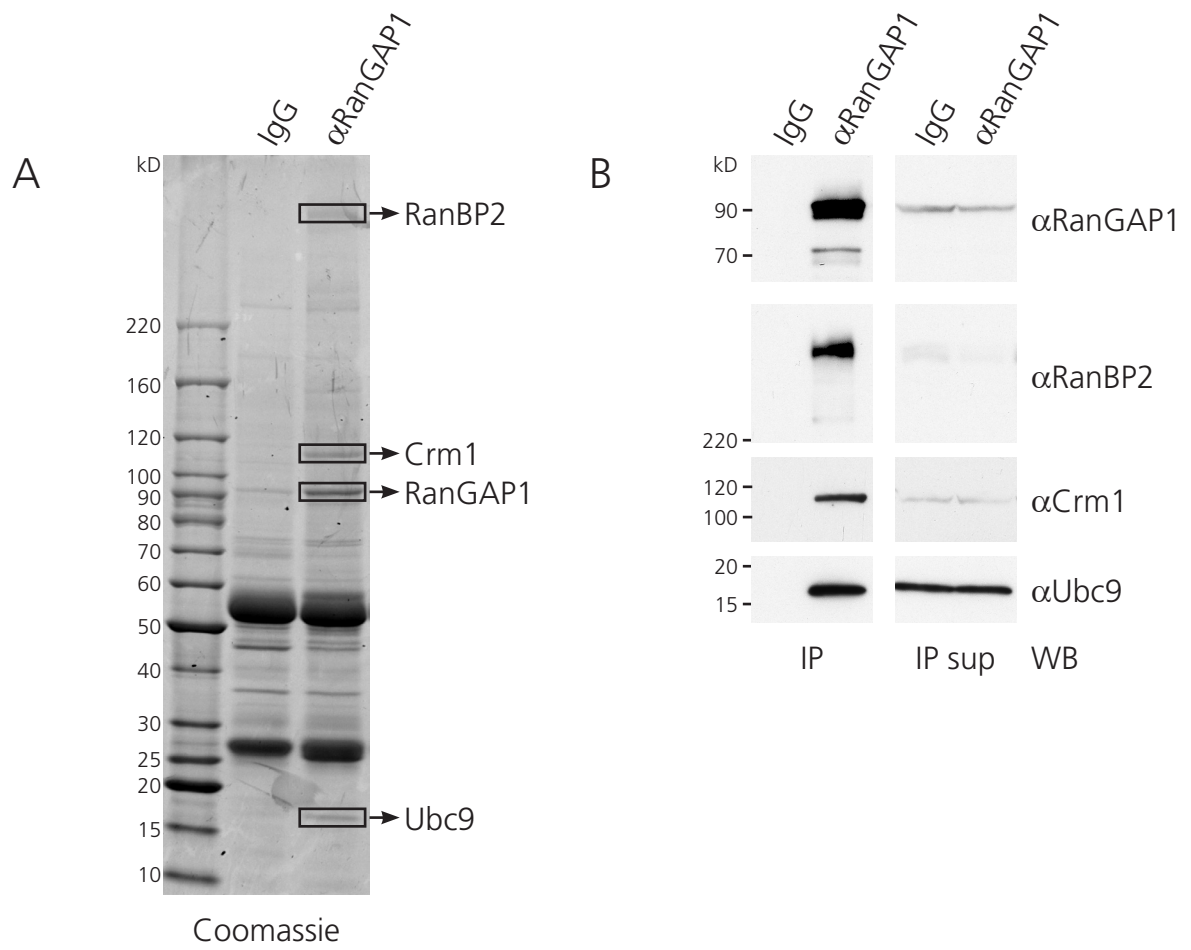


Fig. 13: Crm1 associates with the mitotic RanGAP1-RanBP2 complex. (A) Identification of Crm1 as a RanGAP1 co-purifying protein in mitosis. Representative IgG and goat α RanGAP1 immunoprecipitates from nocodazole-arrested HeLa CSH cells were separated by SDS PAGE and stained with Coomassie. Selected corresponding gel slices were excised from both, the control and α RanGAP1 samples and analyzed by MS. (B) Confirmation of Crm1 as a RanGAP1 co-purifying protein. Western blot analysis of IgG and goat α RanGAP1 immunoprecipitates from nocodazole-arrested HeLa CSH cells and 4.5% of the corresponding IP supernatants was performed with the indicated antibodies. (C, D) Crm1 is part of the mitotic RanGAP1-RanBP2 complex. The IP and corresponding IP supernatant samples were analyzed on the same gel and were spliced together from one western blot exposure. (C) IgG and goat α RanBP2 and (D) IgG and goat α Crm1 immunoprecipitates from cycling (I) and nocodazole-arrested (M) HeLa CSH cells prepared in transport buffer and 0.8% of the corresponding IP supernatants were separated by SDS PAGE on a 6 % gel and analyzed by western blot with the indicated antibodies. The asterisk indicates a contamination of non-phosphorylated RanGAP1*Sumo1 in the IgG control of this particular experiment.

In line with this, a study by Mary Dasso's lab published during the course of this work reported that Crm1 is needed for kinetochore localization of the RanGAP1-RanBP2 complex (Arnaoutov et al. 2005). I could confirm the finding that RanGAP1, RanBP2 and Crm1 co-localize at kinetochores and the mitotic spindle from prometaphase until telophase; Crm1 however does not appear to localize the the central spindle of telophase cells (Fig. 14, RanBP2 data not shown). Likewise, Crm1 did not co-localize with RanGAP1 at the nuclear envelope in early prophase and only a small fraction appeared to reside at reforming nuclear envelopes while a pool of Crm1 can easily be detected at the nuclear envelope in interphase cells (Hutten and Kehlenbach 2006 and not shown). In conclusion, Crm1 seems to be a stable partner in the mitotic RanGAP1-RanBP2-Ubc9 complex.

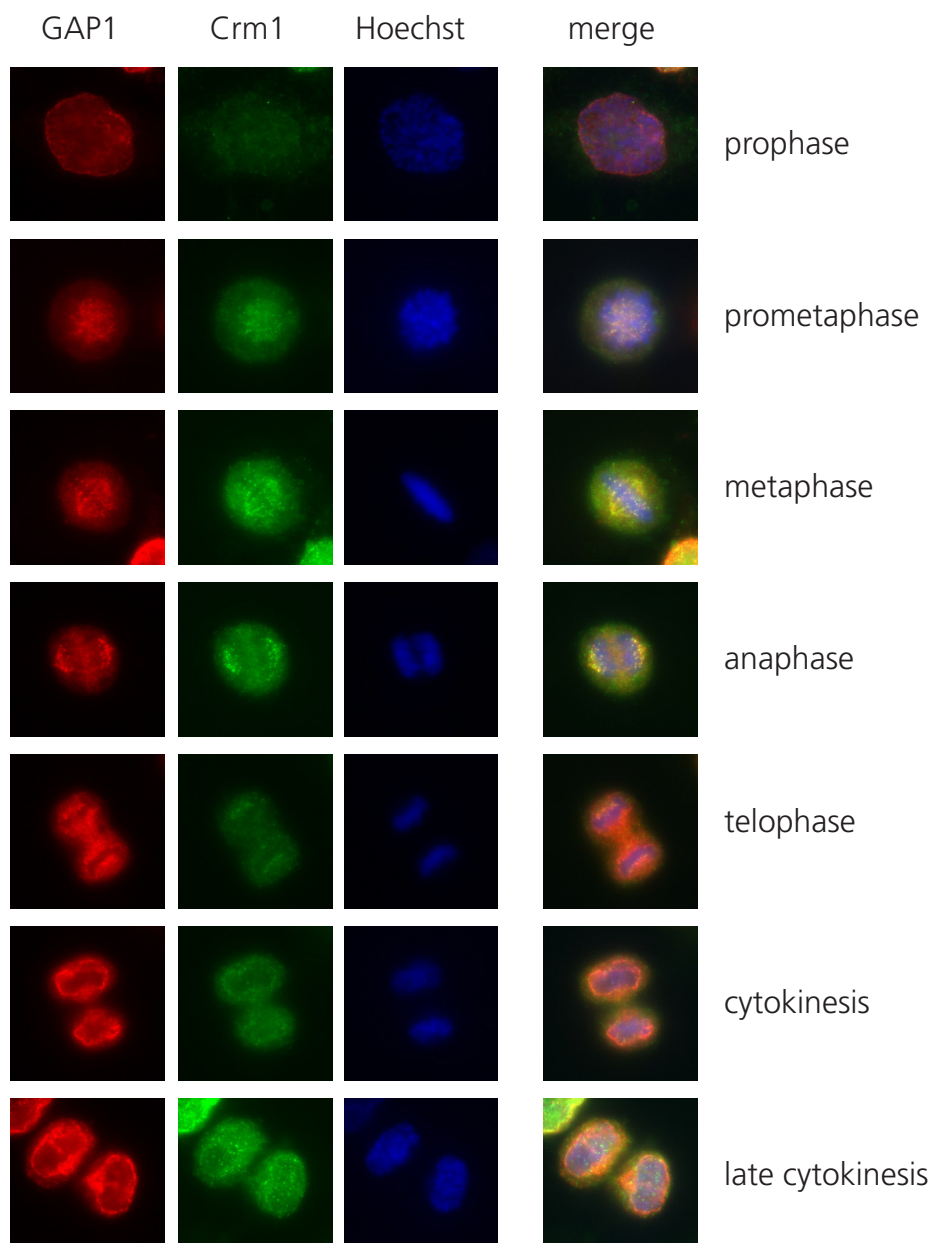


Fig. 14: Crm1 co-localizes with RanGAP1 at the mitotic spindle and kinetochores. HeLa cells were permeabilized prior to fixation. Immunostaining was performed with rabbit α Crm1/donkey α rabbit Alexa488 (green) and goat α RanGAP1/donkey α goat Alexa594 (red), DNA was stained with Hoechst (blue). The samples were analyzed by fluorescence microscopy.

To test whether Crm1 binds directly to RanGAP1, in dependence of phosphorylation and/or sumoylation, recombinant mouse wild type RanGAP1 (WT), the phosphomimicking (EEE), the Sumo-deficient variant (KR) or no RanGAP1 were incubated in a sumoylation reaction before equal amounts of recombinant His-Crm1 were added. The different RanGAP1 species and bound protein were recovered from the reaction mix by immunoprecipitation with polyclonal goat α RanGAP1 antibodies and analyzed by SDS PAGE. However, no significant co-purification of Crm1 with any of

the tested RanGAP1 species was detectable by Coomassie staining in this experiment (Fig. 15, compare input with the purified samples) or when immobilized His-Crm1 was used as affinity matrix for the recombinant Sumo-modified RanGAP1 variants (not shown). Thus, Crm1 does not directly interact with sumoylated, phosphomimetic or unsumoylated RanGAP1, at least not under the conditions tested.

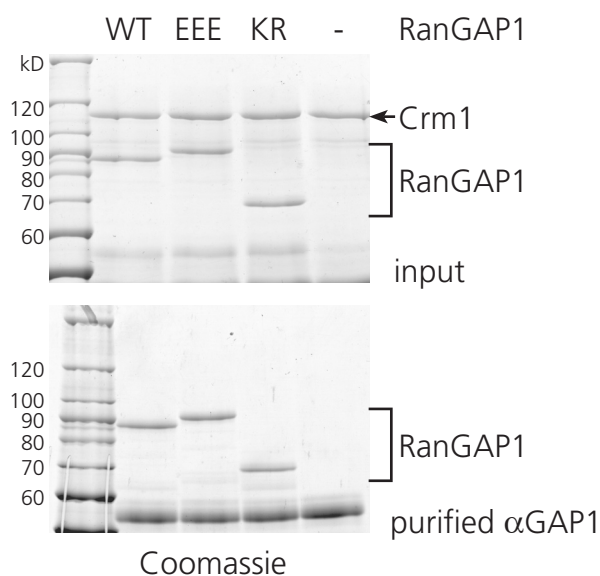


Fig. 15: Crm1 does not bind to RanGAP1 directly. 5 μ g recombinant wild type (wt), phospho-mimetic (EEE), or Sumo-deficient (KR) mouse RanGAP1 or no RanGAP1 were incubated in a sumoylation reaction with Aos1-Uba2, Ubc9, Sumo1 and ATP in sumoylation assay buffer including ovalbumine for 45 min. at 30°C. After sumoylation, each reaction mix was incubated in the presence of 5 μ g recombinant His-Crm1 for 1 h at 4°C. RanGAP1*Sumo1-bound proteins were immunopurified with polyclonal goat α RanGAP1 antibodies. The recovered proteins and 16 % of the input were separated by SDS PAGE and visualized by Coomassie staining.

The before described experiments do not exclude the possibility that RanGAP1 phosphorylation influences binding of Crm1 to the RanGAP1-RanBP2-Ubc9 complex by indirect means. Therefore, wild type and phosphodeficient HA-RanGAP1 were purified with α HA antibodies from mitotic stable HA-RanGAP1 HeLa cell lines. Two different clones were used for each RanGAP1 variant and the immunoprecipitates were analyzed for co-purifying Crm1. Although more wild type HA-RanGAP1 was recovered compared to the phosphodeficient variant, comparable amounts of Crm1 relative to the respective HA-RanGAP1 co-purified with phospho-deficient RanGAP1 (Fig. 16) indicating that phosphorylation is not required for association of Crm1 with mitotic RanGAP1-RanBP2-Ubc9.

Of note, only a small fraction of Crm1 co-purified with the stably expressed HA-RanGAP1 compared to endogenous RanGAP1 (Fig. 16, compare the ratio of the western

blot signals for RanGAP1 and Crm1 from lanes 3-6 to lane 1) again suggesting that HA-RanGAP1 does not efficiently compete with endogenous RanGAP1 (see also above).

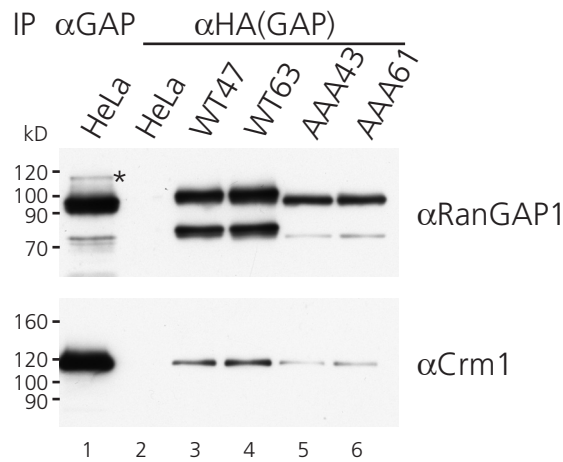


Fig. 16: Association of Crm1 with the mitotic RanGAP1-RanBP2 complex does not depend on RanGAP1 phosphorylation. goat α RanGAP1 (5 μ g antibody/IP) and mouse α HA (clone 12CA5, 4 μ g antibody/IP) immunoprecipitates from nocodazole-arrested HeLa cells or mouse α HA immunoprecipitates from nocodazole-arrested HeLa cell lines stably expressing HA-RanGAP1 wild type (wt clones 47 and 63, lanes 3 and 4) or a phospho-deficient variant (AAA clones 43 and 61, lanes 5 and 6) were analyzed by western blot with the indicated antibodies.

3.3. The GTPase Ran stably interacts with the RanGAP1-RanBP2-Ubc9-Crm1 complex

Shortly after our discovery of Crm1 as part of the RanGAP1-RanBP2-Ubc9 complex, a study published by the group of Mary Dasso described kinetochore localization of Crm1 and the requirement for ternary complex assembly of Crm1 with Ran-GTP and a NES sequence to recruit RanGAP1-RanBP2 to kinetochores (Arnautov et al. 2005). The authors further showed that Crm1 and Ran-GTP are important to maintain discrete end-on attachments of kinetochores to single kinetochore fibers; inhibition of Crm1 with leptomyacin B disrupts mitotic progression and chromosome segregation at the meta- to anaphase transition.

This study and our MS analysis of RanGAP1 immunoprecipitates from mitotic cells suggested the GTPase Ran may also be present in complex with RanGAP1-RanBP2. Western blot analysis of corresponding immunoprecipitation experiments confirmed that Ran also specifically co-purifies with RanGAP1 in mitosis (Fig. 17).

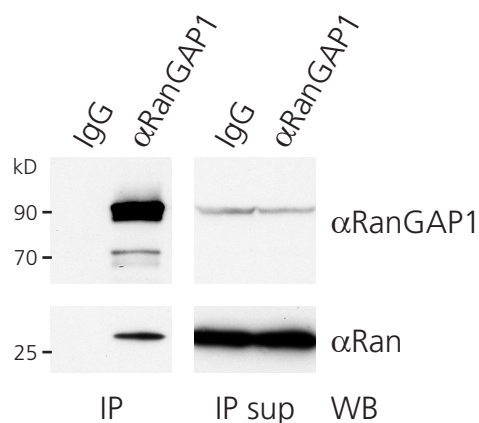


Fig. 17: Ran binds to the mitotic RanGAP1-RanBP2-Ubc9 complex. IgG and goat α RanGAP1 immunoprecipitates from nocodazole-arrested HeLa CSH cells and 4.5 % of the corresponding IP supernatants were analyzed by western blot with the indicated antibodies. The figure shows the same experiment as Fig. 13B. The IP and corresponding IP supernatant samples were analyzed on the same gel and were spliced together from one western blot exposure.

To further verify that Ran and Crm1 form one stable complex with RanGAP1-RanBP2-Ubc9, cell extracts from nocodazole-arrested HeLa cells were subjected to immunoprecipitation with control goat IgG, goat α RanGAP1, phosphospecific goat α RanGAP1 pT409, goat α RanBP2, and goat α Crm1 antibodies. The purified proteins were separated by SDS PAGE and RanBP2, RanGAP1, Ubc9, Crm1, and Ran were analyzed by immunoblotting. All five proteins were recovered specifically with all four antibodies tested indicating that RanBP2, RanGAP1, Ubc9, Crm1, and Ran are part of one stable protein complex (Fig. 18). Immunoprecipitation with RanGAP1 or RanBP2 antibodies led to a similar enrichment of RanBP2, Crm1, RanGAP1, Ran, and Ubc9 compared to the input samples with Ran being the least enriched protein compared to the entire protein pool present in the cell extracts; by contrast, enrichment of RanBP2, RanGAP1, Ran, and Ubc9 with Crm1 antibodies was less pronounced. These results suggests that only a fraction of Crm1 and Ran associate with the mitotic RanGAP1-RanBP2-Ubc9 complex. This is not surprising as Ran is one of the most abundant proteins, clearly much more abundant than RanGAP1 or RanBP2 (Gorlich et al. 2003). Localization of Ran to kinetochores or the spindle in mitosis comparable to RanGAP1, RanBP2 and Crm1 was not detectable by immunofluorescence analysis (not shown).

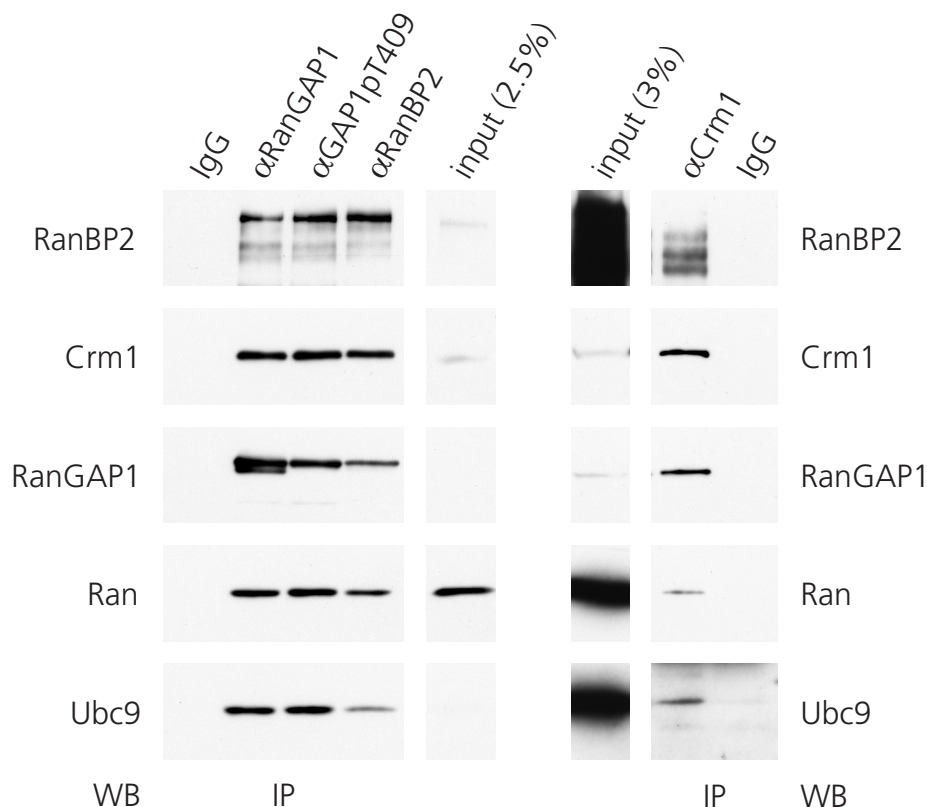


Fig. 18: Crm1 together with Ran are stable components of the mitotic RanGAP1-RanBP2-Ubc9 complex. Immunoprecipitation from nocodazole-arrested HeLa CSH cell was performed with control goat IgG (25 μ g/ml), goat α RanGAP1 (25 μ g/ml), goat α RanGAP1 pT409 (25 μ g/ml), goat α RanBP2 (25 μ g/ml), or goat α Crm1 (20 μ g/ml). The SDS eluates and the indicated amounts of the IP supernatants were separated by SDS PAGE and analyzed by immunoblotting with the indicated antibodies. The IP and corresponding IP supernatant samples were analyzed on the same gel and were spliced together from one western blot exposure.

Association of RanGAP1-RanBP2-Ubc9 with Crm1 and Ran was also observed when a growing culture of HeLa cells was cell cycle synchronized by a thymidine arrest-release protocol resulting in a mitotic index of approximately 20 % by the time of cell harvest. To enrich specifically for mitotic RanGAP1, the phospho-specific pT409 RanGAP1 antibody was used for immunoprecipitation. Together with RanGAP1 RanBP2, Crm1, Ran, and Ubc9 were specifically recovered from thymidine-synchronized cell extracts indicating that complex formation is not an artefact of the prolonged mitotic arrest caused by nocodazole treatment (Fig. 19). Corresponding to the lower percentage of phosphorylated mitotic RanGAP1 present upon thymidine synchronization, the associated proteins Crm1, Ran, and Ubc9 were less enriched in the purified sample compared to the IP supernatants. The soluble protein pool of RanBP2 is provided by the mitotic cells mostly, therefore an enrichment similar to purification from nocodazole-arrested cells was achieved (compare to Fig. 18).

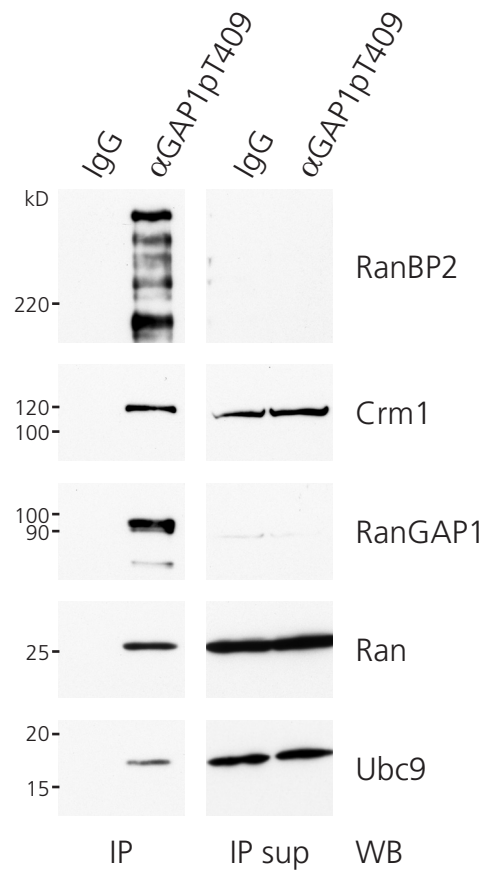


Fig. 19: The RanGAP1-RanBP2-Ubc9 complex including associated Crm1 and Ran can also be purified from mitotic cell cycle-synchronized cells. HeLa CSH cells were synchronized in mitosis by a thymidine arrest-release protocol. goat α RanGAP1 immunoprecipitates and 1.5 % of the corresponding IP supernatants were analyzed by western blot with the indicated antibodies. The IP and corresponding IP supernatant samples were analyzed on the same gel and were spliced together from one western blot exposure.

4. Does the Crm1-Ran subcomplex act as a substrate recruitment machinery for the mitotic RanGAP1-RanBP2-Ubc9 complex?

Considered from a functional point of view, the mitotic RanGAP1-RanBP2-Ubc9 complex comprises almost a complete set of two separate machineries. On one hand, Crm1 together with Ran, RanGAP1, and RanBP2 constitutes an entire system promoting nuclear protein export in interphase cells and on the other hand, Ubc9 together with RanBP2 represent the E2 and E3 components of the sumoylation machinery. One of the mysteries in sumoylation is how substrate specificity can be provided to a vast multitude of targets with only a single E2 enzyme and a limited set of E3 ligases.

In ubiquitination, one level of substrate selection is being installed by a modular build of some Ubiquitin E3 ligases: the SCF-type E3 ligases impart specificity for ubiquitination

of selected substrates by means of a specific substrate targeting subunit, the so-called F-box protein, which is linked to the core ubiquitination machinery via an adaptor protein (Ho et al. 2006; Bosu and Kipreos 2008). In nuclear protein export, the transport receptor Crm1 binds to a large set of NES-bearing cargoes in ternary complex with Ran-GTP. This export complex exhibits high affinity for the Ran binding domains of RanBP2. Applied to the mitotic RanGAP1-RanBP2-Ubc9 complex one can envision a scenario, in which Crm1-Ran act as a substrate targeting adaptor to recruit NES-containing proteins as substrates for sumoylation by RanBP2 (illustrated in Fig. 20).

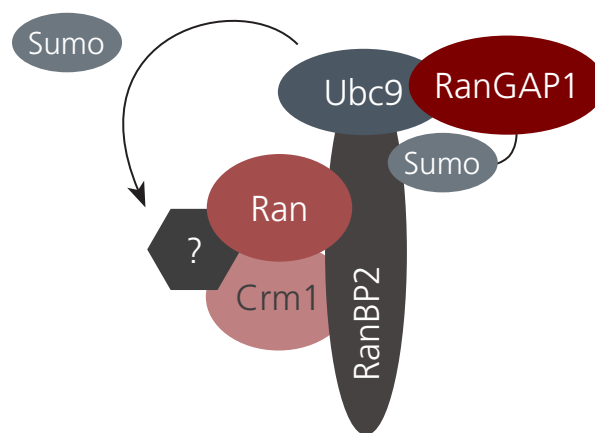


Fig. 20: Working hypothesis: Crm1 together with Ran may recruit NES containing proteins as substrates for sumoylation to RanGAP1-RanBP2-Ubc9. As an export receptor in nuclear transport, Crm1 binds to various NES containing proteins in complex with Ran-GTP. As part of the mitotic RanGAP1-RanBP2-Ubc9 complex, Crm1 together with Ran-GTP may potentially act as a recruitment machinery for NES containing proteins as sumoylation targets of RanBP2.

4.1. Proteins of unknown identity associate with and can be sumoylated by the mitotic RanGAP1-RanBP2-Ubc9 complex

A prediction of the afore presented model is that Crm1 and Ran, as they associate with RanGAP1-RanBP2-Ubc9, should carry along proteins that can be sumoylated by RanBP2. To address this hypothesis, the RanGAP1-RanBP2-Ubc9 complex was immunopurified from mitotic cells and was incubated in a sumoylation reaction with only the E1 enzyme Aos1-Uba2 and Sumo1; sumoylation under these conditions absolutely depends on complex-associated Ubc9 and likely RanBP2. Strikingly, in the presence of ATP, the appearance of a variety of α Sumo1-reactive bands could be detected with monoclonal α Sumo1 antibodies after SDS PAGE in comparison to the $-$ ATP control indicating that proteins of unknown identity became conjugated to Sumo1 (Fig. 21, compare lanes 1

and 3; please note that Sumo1 and YFP-Sumo1 have been added in the –ATP sample to serve as a combined control for lanes 1 and 2). When YFP-Sumo1 substituted for the untagged form, less Sumo1-reactive species became apparent migrating at a higher molecular weight compared to Sumo1 consistent with less efficient conjugation to the 27 kD bigger YFP-Sumo1. A similar but not identical pattern of associated sumoylated proteins was obtained when α RanBP2 immunoprecipitates were used as source of the E2 and E3 enzymes and of Sumo substrates (compare lanes 1 and 4). Thus, proteins of unknown identity associate with the mitotic RanGAP1-RanBP2-Ubc9 complex and can be sumoylated by the associated Ubc9, potentially in dependence of RanBP2.

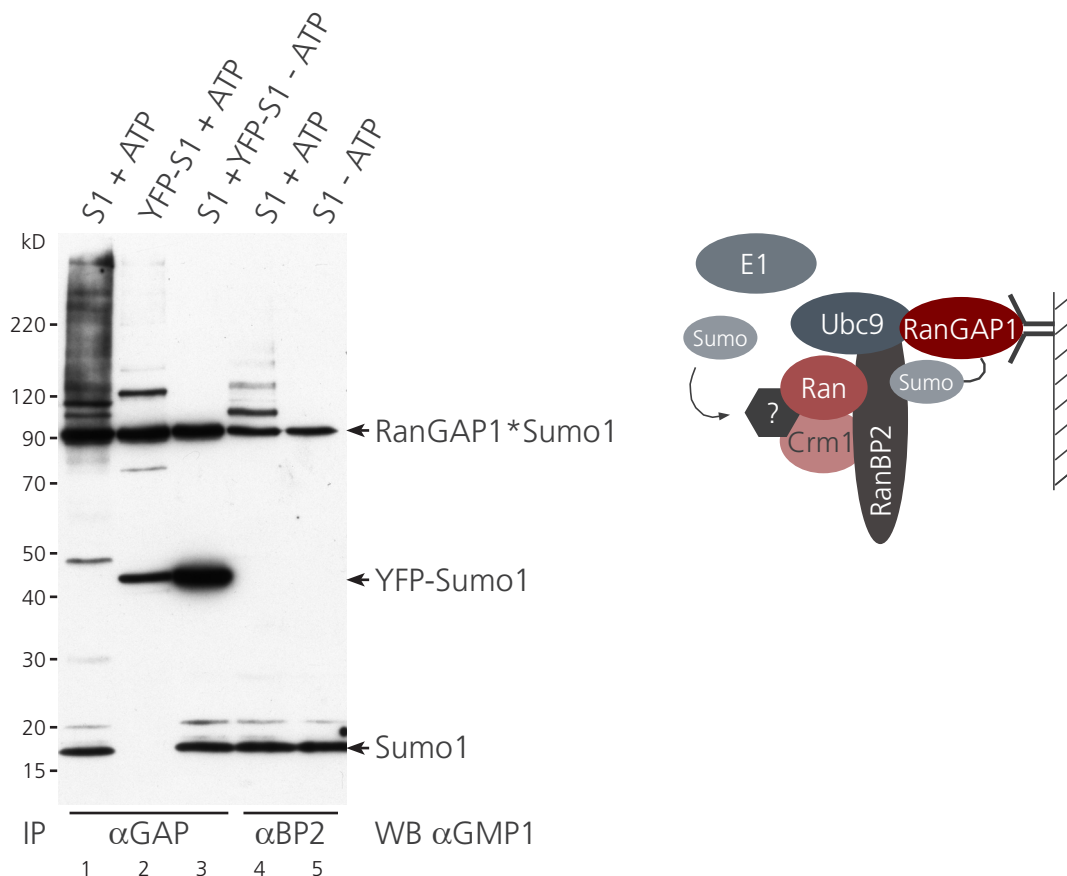


Fig. 21: The mitotic RanGAP1-RanBP2-Ubc9 complex carries along putative substrates that become sumoylated *in vitro*. RanGAP1-RanBP2-Ubc9 and associated proteins immunopurified with 20 μ g goat α RanGAP1 (lanes 1-3) or goat α RanBP2 antibodies (lanes 4-5) from 0.45 ml nocodazole-arrested HeLa CSH cell extracts were incubated in a sumoylation reaction with 68 nM recombinant Aos1-Uba2, 4.5 μ M Sumo1 and/or 1.3 μ M YFP-Sumo1 in the absence or presence of 5 mM ATP. The samples were separated by SDS PAGE and analyzed by immunoblotting with monoclonal α Sumo1 antibodies. The major Sumo1-reactive band in the absence of sumoylation besides Sumo1 itself represents sumoylated RanGAP1.

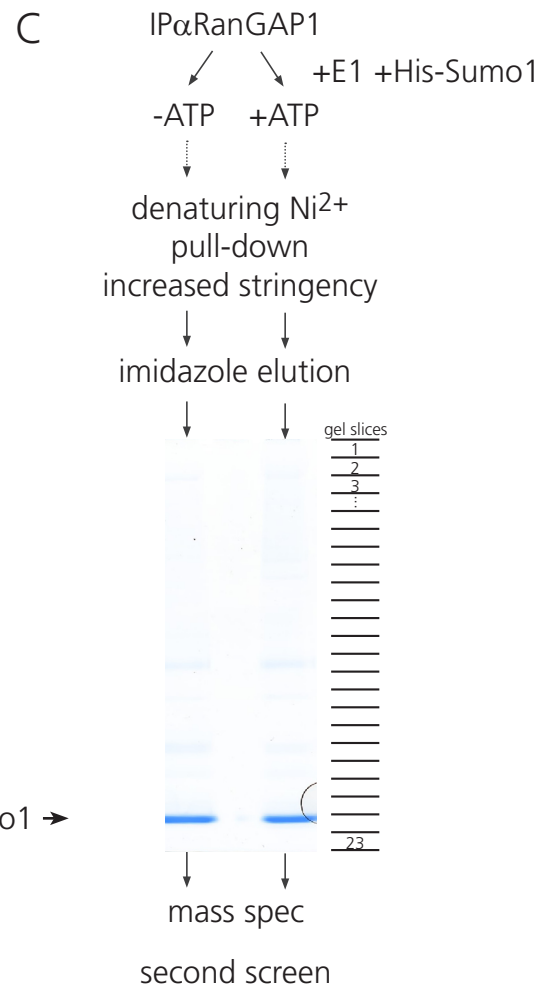
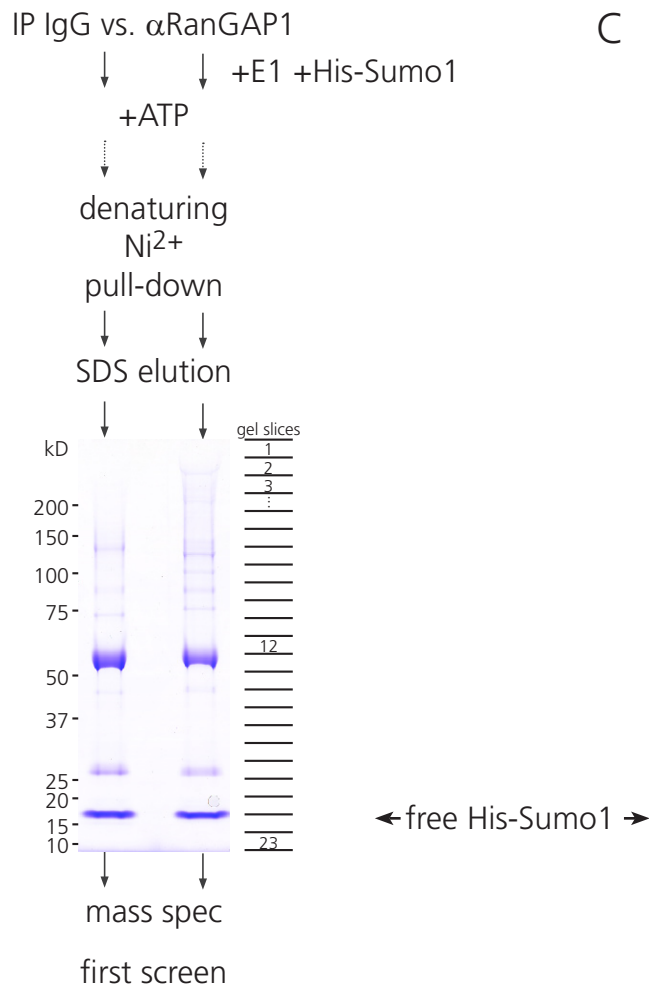
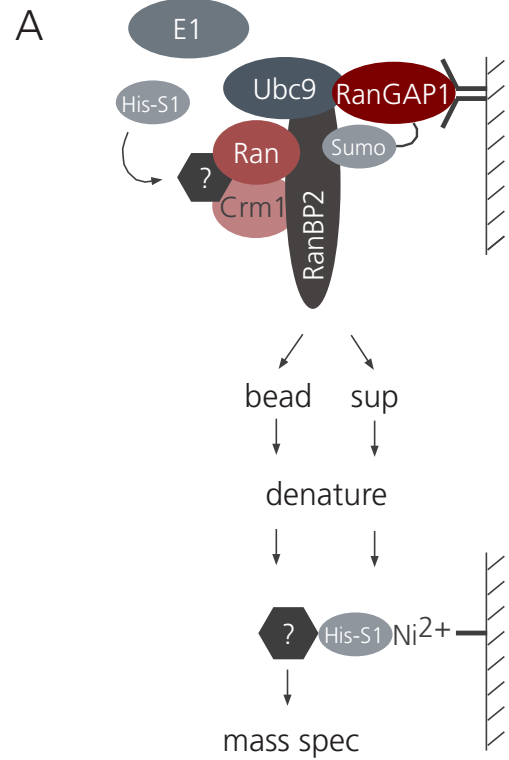
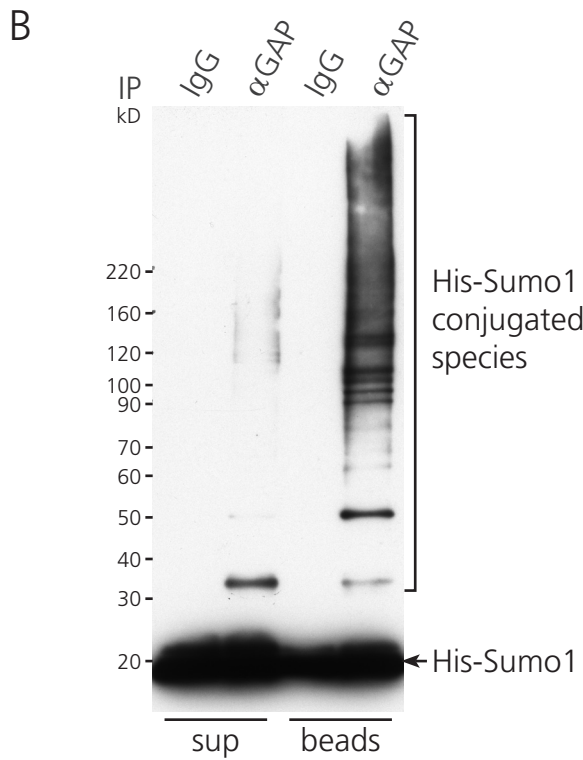
4.2. Unraveling the identity of RanGAP1-RanBP2-Ubc9-associated Sumo substrates

To further address the model of Crm1 as substrate targeting adaptor *a bona fide* RanBP2 Sumo substrate was essential. At the time no *in vivo* Sumo substrate of RanBP2 had been identified. I therefore decided to embark on the identification of Sumo targets that associated with the mitotic RanGAP1-RanBP2-Ubc9 complex.

For this purpose, control IgG and α RanGAP1 immunoprecipitates from 7.5 ml mitotic cell extracts were incubated in a sumoylation reaction with recombinant Aos1-Uba2 (E1 enzyme) and a His-tagged form of Sumo1 in the presence of ATP. Afterwards, the reactions were split into supernatant and bead-bound fraction to remove most non-incorporated His-Sumo1 and recombinant E1; the samples were denatured by addition of a buffer containing 6 M guanidine, and His-sumoylated proteins were enriched on Ni-NTA agarose, washed, and eluted with SDS sample buffer. Western blot analysis of a small fraction of the eluates with monoclonal α Sumo1 antibodies showed that most sumoylated proteins remained bead-bound (Fig. 22), suggesting that they are stably associated with the RanGAP1-RanBP2 complex even after modification.

Fig. 22: Identifying candidate Sumo targets of the mitotic RanGAP1-RanBP2-Ubc9 complex.

(A) General experimental setup. Mitotic RanGAP1-RanBP2 complex purified by α RanGAP1 immunoprecipitation was incubated in a sumoylation reaction with recombinant Sumo E1 enzyme and His-Sumo1 in the presence of ATP. Sumoylated bound proteins were purified by a denaturing Ni^{2+} pull-down and were identified by MS. (B) First MS screen. Control IgG or goat α RanGAP1 immunoprecipitates were incubated in a sumoylation reaction with 164 nM recombinant Aos1-Uba2 and 18 μM His-Sumo1 in the presence of 5 mM ATP. The reaction supernatant was transferred to a separate tube after the reaction and both, the beads and the supernatants were denatured in 6 M guanidine-HCl and subsequently subjected to a Ni^{2+} pull-down to enrich for His-Sumo1 modified proteins. Bound protein was eluted with SDS sample buffer and separated by SDS PAGE. (Top) Shown is a western blot analysis with monoclonal α Sumo1 antibodies. (Bottom) Shown is an experimental flow chart and the Coomassie gel subsequently analyzed by MS. The side bar indicates the approximate boundaries of the cut gel slices. (C) Second MS screen. For the second screen, the experiment was repeated with some modifications: goat α RanGAP1 immunoprecipitates were used for both, the control and the sample of interest. The sumoylation reaction was performed in the absence or presence of 5 mM ATP and the subsequent denaturing Ni^{2+} pull-down was performed with increased stringency in the presence of 0.1 % Triton X-100. Bound protein was eluted with imidazole. Shown is an experimental flow chart and the Coomassie gel subsequently analyzed by MS. The side bar indicates the approximate boundaries of the cut gel slices.



Identification of these proteins by MS was performed in collaboration with Henning Urlaub and Monika Raabe from the MPI-BPC, Göttingen. The bead-bound fractions were separated by SDS PAGE, stained with Coomassie and both entire gel lanes were sliced into 23 sections each. Single gel slices were subjected to tryptic digestion and were analyzed by ESI-MS. The MS data of samples from the top half of the gel (samples 1-12) were merged as well as the data from the bottom half (samples 13-23) and were analyzed by MASCOT against the mammalian database. Approximately 90 proteins were identified specifically in the sumoylation reaction of α RanGAP1 immunoprecipitates after manual sorting of the MASCOT data (compiled in Tab. 1, see Materials & Methods for more details). These covered a wide variety of molecular pathways in the cell comprising a number of nuclear transport receptors, various microtubule and centrosome-associated proteins, several kinases, ubiquitin specific proteases, and the known Sumo targets Parp-1 (Schmidt 2005) and Topoisomerase II α (Azuma et al. 2005; Dawlaty et al. 2008) among many other proteins. Unexpected was the identification of the Sumo E3 ligase PIAS1 and of all known core components of the RanGAP1-RanBP2-Ubc9 complex, of which Crm1, Ran and Ubc9 were known to not become modified in the reaction (see Fig. 23 for a representative example).

protein	score	queries
gi 6382079 RAN binding protein 2 [Homo sapiens]	4983	328
gi 4506411 Ran GTPase activating protein 1 [Homo sapiens]	4448	182
gi 57164942 colonic and hepatic tumor over-expressed protein isoform a [Homo sapiens] (or isoform b)	1403	98
gi 48255913 tripartite motif-containing 16 [Homo sapiens]#	1145	70
gi 42490984 SMT3 suppressor of mif two 3 homolog 1 (S. cerevisiae) [Homo sapiens]	1109	176
gi 4507943 exportin 1 [Homo sapiens]	983	68
gi 50897852 Hook-related protein 1 [Homo sapiens]	665	47
gi 3643107 protein inhibitor of activated STAT protein PIAS1 [Homo sapiens]	488	18
gi 28316815 mitotic spindle-associated protein p126 [Homo sapiens]	379	27
gi 55659360 PREDICTED: similar to Ran-specific GTPase-activating protein (Ran binding protein 1) (RanBP1) [Pan troglodytes]	370	27
gi 77539752 tubulin, alpha, ubiquitous [Pan troglodytes]	255	9
gi 10178313 nuclear factor of kappa light polypeptide gene enhancer in B-cells 2 (p49/p100) [Homo sapiens]	253	18

gi 32425497	RAN protein [Homo sapiens]	253	14
gi 37999716	Probable phospholipase DDHD1 (DDHD domain protein 1)	221	15
gi 12803441	MEN1 protein [Homo sapiens]	196	7
gi 17391008	URG4 protein [Homo sapiens]*	164	10
gi 38455439	cancer associated nucleoprotein [Homo sapiens]	164	2
gi 48734942	Bromodomain and WD repeat domain containing 2 [Homo sapiens]*	163	8
gi 55621594	PREDICTED: similar to eukaryotic translation initiation factor 4 gamma, 1 isoform 1; EIF4-gamma [Pan troglodytes]	158	21
gi 31543018	CP110 protein [Homo sapiens]*	141	7
gi 20306278	TBC1 domain family, member 15 [Homo sapiens]*	132	11
gi 56969191	RNA-binding region (RNP1, RRM) containing 3 [Homo sapiens]	127	8
gi 10863945	ATP-dependent DNA helicase II [Homo sapiens]	120	6
gi 59891448	rapamycin-insensitive companion of mTOR [Homo sapiens]	113	10
gi 20141248	ATP-citrate synthase (ATP-citrate (pro-S-)-lyase) (Citrate cleavage enzyme)	109	11
gi 12803339	SERPINE1 mRNA binding protein 1 [Homo sapiens]	109	5
gi 26996766	Leucine-rich repeats and IQ motif containing 2 [Homo sapiens]	102	8
gi 50604101	CEP170 protein [Homo sapiens]	101	2
gi 62088878	Protein 4.1 variant [Homo sapiens]	98	17
gi 19923142	karyopherin beta 1 [Homo sapiens]	96	10
gi 23272708	FLJ21945 protein [Homo sapiens]*	95	7
gi 12644130	Desmoplakin (DP) (250/210 kDa paraneoplastic pemphigus antigen)	91	18
gi 33943109	Grb10 interacting GYF protein 1 [Homo sapiens]	89	7
gi 21594340	Kinesin heavy chain member 2 [Homo sapiens]	89	5
gi 5107636	Karyopherin Beta2 [Homo sapiens]	87	2
gi 54673652	Transforming, acidic coiled-coil containing protein 2 [Homo sapiens]	85	18
gi 1174741	DNA topoisomerase 2-alpha (DNA topoisomerase II, alpha isozyme)	83	15
gi 21614544	S100 calcium-binding protein A8 [Homo sapiens]	82	3
gi 4507857	ubiquitin specific protease 7 (herpes virus-associated) [Homo sapiens]	80	12
gi 2392592	Murine/HUMAN UBIQUITIN-Conjugating Enzyme Ubc9	80	7
gi 4506411	Ran GTPase activating protein 1 [Homo sapiens]	76	8
gi 15341853	Ribosomal protein L8 [Homo sapiens]	75	3
gi 39795256	NFKBIE protein [Homo sapiens]	71	4
gi 21359873	polo-like kinase [Homo sapiens]	70	6

gi 4432754	ribosomal protein L27a [Homo sapiens]	69	1
gi 32171238	BAI1-associated protein 2-like 1 [Homo sapiens]	68	3
gi 5453549	thioredoxin peroxidase [Homo sapiens]	66	10
gi 33239445	eukaryotic translation initiation factor 3, subunit 9 eta, 116kDa [Homo sapiens]	64	2
gi 34783228	SKIV2L2 protein [Homo sapiens]	60	4
gi 63100468	Ankyrin repeat domain 28 [Mus musculus]	59	5
gi 2852125	S-adenosyl homocysteine hydrolase homolog [Homo sapiens]	58	6
gi 55661189	PREDICTED: similar to Molecule interacting with Rab13 (MIRab13) (MICAL-like protein 1) [Pan troglodytes]	58	5
gi 77812672	exosome component 9 isoform 1 [Homo sapiens]	58	2
gi 13606056	DNA dependent protein kinase catalytic subunit [Homo sapiens]	58	7
gi 4240171	KIAA0841 protein [Homo sapiens]	57	7
gi 21553095	NIMA-related expressed kinase 9 [Mus musculus]	55	2
gi 530049	14-3-3 protein	54	3
gi 4504897	karyopherin alpha 2 [Homo sapiens]	54	1
gi 55647627	PREDICTED: similar to hypothetical protein [Pan troglodytes]	53	2
gi 28374154	C15orf23 protein [Homo sapiens]	52	1
gi 1666075	ubiquitin hydrolase [Homo sapiens]	51	3
gi 4885615	signal transducer and activator of transcription 2 [Homo sapiens]	50	3
gi 68160922	ribosomal protein S14 [Homo sapiens]	50	2
gi 35493878	reticuloendotheliosis viral oncogene homolog B [Homo sapiens]	50	1
gi 4755142	inositol polyphosphate phosphatase-like 1 [Homo sapiens]	49	4
gi 18088719	Tubulin, beta [Homo sapiens]	49	3
gi 4501955	poly (ADP-ribose) polymerase family, member 1 [Homo sapiens]	49	2
gi 46255026	potassium channel tetramerisation domain containing 3 [Homo sapiens]	49	2
gi 12314268	novel S-100\ ICaBP type calcium binding domain and EF hand domain containing protein [Homo sapiens]	49	2
gi 3282239	rapamycin associated protein FRAP2 [Homo sapiens]	48	6
gi 21410211	Unknown (protein for MGC:32654) [Homo sapiens]	48	6
gi 62896685	TATA binding protein interacting protein 49 kDa variant [Homo sapiens]	48	3
gi 55662202	nuclear factor I/B [Homo sapiens]	47	5
gi 2118494	NF-kappa-B transcription factor subunit - human	47	3

gi 4505941 DNA directed RNA polymerase II polypeptide B [Homo sapiens]	47	2
gi 109482262 PREDICTED: hypothetical protein [Rattus norvegicus]	47	2
gi 4505941 DNA directed RNA polymerase II polypeptide B [Homo sapiens]	47	2
gi 56243583 WD repeat domain 18 [Homo sapiens]	47	2
gi 34193452 ZNF451 protein [Homo sapiens]	46	6
gi 4506773 S100 calcium-binding protein A9 [Homo sapiens]	45	4
gi 31657150 Tripartite motif-containing 16 [Homo sapiens]#	45	4
gi 4505713 period 1 [Homo sapiens]	45	2
gi 5453998 importin 7 [Homo sapiens]	45	2
gi 18676955 unnamed protein product [Homo sapiens]	45	2
gi 340026 tyrosine kinase*	45	1
gi 33392704 Unknown (protein for MGC:62037) [Homo sapiens]	44	5
gi 13699868 methylenetetrahydrofolate dehydrogenase 1 [Homo sapiens]	44	4
gi 45861372 200 kDa U5 snRNP-specific spliceosomal protein [Homo sapiens]	44	4
gi 13625162 jerky [Homo sapiens]	41	1

Tab. 1: Candidates identified in the first MS screen. Listed are all proteins of the bead-bound fraction from the α RanGAP1 sample after manual sorting (see Materials & Methods for further details); shown are also the accumulative MASCOT scores and the maximal accumulative number of peptides (queries) matched. The asterisk indicates that the respective set of peptides could also have matched a different protein. The data and list do not allow to distinguish between different isoforms of identified proteins. The Sumo1 score relates only to the accumulative score from samples 1-12, for which no significant hits for Sumo1 peptides were identified in the respective IgG control samples. # This protein was identified in the top (high score) and bottom part of the gel (low score).

The presence of Crm1, Ran and Ubc9 indicated that the Ni²⁺ pull-down had failed to unequivocally enrich for His-sumoylated proteins although high Sumo1 scores of the top part of the gel specifically with the α RanGAP1 immunoprecipitates suggested that a lot of conjugated Sumo1 had been purified. To foster identification of proteins modified in the reaction the experiment was repeated with two major changes. First, to start with the same set of proteins in both, the control and the sample of interest, α RanGAP1 immunoprecipitates were also used for the control. The only difference between the two samples was the absence or presence of ATP in the sumoylation reaction. Secondly, the enrichment of His-sumoylated proteins on Ni²⁺ beads was performed with increased stringency in the presence of 0.1 % Triton X-100 and bound protein was eluted with imidazole.

After MS analysis of the eluted samples of the bead-bound fraction in 23 gel slices,

the MASCOT data from each single slice were manually sorted subtracting proteins of the –ATP control from the +ATP sample (see Materials & Methods for more details). In this experiment 19 proteins were identified matching the sorting criteria (Tab. 2), of which 16 had already been identified in the first screen. Three proteins expected to be identified as they were known to be present and to be sumoylated were among these candidates (RanGAP1, RanBP2 and Uba2), and non-sumoylated proteins such as His-Aos1, Crm1, Ran or Ubc9 were absent. This indicated that the experimental and analytical setup was suitable to identify specifically sumoylated proteins. In addition, several members of the PIAS family were identified, PIAS1 being most prominent next to PIAS3 and PIAS2. The presence of PIAS E3 ligases in the RanGAP1 immunoprecipitates is surprising and it has implications for the interpretation of these and future data in respect to sumoylation. A third group of proteins comprises most spindle and centrosome-associated proteins already identified in the first MS screen and is consistent with the mitotic localization of RanGAP1-RanBP2 at the spindle. Only four proteins did not match any of these three categories, two of which were non-characterized open reading frames.

To test selected candidates in respect to specific binding and sumoylation, 10 proteins were chosen from the first and the second MS screen (Tab. 3). At least one antibody was obtained for each protein and tested in western blot analysis. Unfortunately, unequivocal signals for the selected proteins in HeLa cell lysates were detectable with only half of the antibodies (not shown, summarized in Tab. 3). These candidates were selected for further analysis.

protein	additive score	
gi 42490984 SMT3 suppressor of mif two 3 homolog 1 (S. cerevisiae) [Homo sapiens]	1859	proteins expected to be present
gi 4885649 SUMO-1 activating enzyme subunit 2 [Homo sapiens]	60	
gi 1009337 RanBP2 (Ran-binding protein 2) [Homo sapiens]	1333	
gi 4506411 Ran GTPase activating protein 1 [Homo sapiens]	2878	
gi 3643107 protein inhibitor of activated STAT protein PIAS1 [Homo sapiens]	967	PIAS E3 ligases
gi 56404447 E3 SUMO-protein ligase PIAS2 (Protein inhibitor of activated STAT2)	120	
gi 56405302 E3 SUMO-protein ligase PIAS3 (Protein inhibitor of activated STAT protein 3)	407	
gi 3121951 Cytoskeleton-associated protein 5 (Colonic and hepatic tumor over-expressed protein) (Ch-TOG protein)	497	centrosome and spindle-associated proteins
gi 66347361 transforming, acidic coiled-coil containing protein 2 [Homo sapiens]	66	
gi 28316815 mitotic spindle-associated protein p126 [Homo sapiens]	72	
gi 55962085 centrosomal protein 170kDa [Homo sapiens]	70	
gi 5353738 protein 4.1 [Homo sapiens]	137	
gi 1922313 kinesin-2 [Homo sapiens]	175	
gi 18088719 tubulin, beta [Homo sapiens]	62	
gi 37492 alpha-tubulin [Homo sapiens]	41	
gi 2282576 HsGCN1 [Homo sapiens]	43	
gi 33874022 HNRPM protein [Homo sapiens]	100	
gi 23272708 C2orf44 protein [Homo sapiens]	68	other
gi 28374154 C15orf23 protein [Homo sapiens]	46	

Tab. 2: Candidates identified in the second MS screen. Listed are all proteins of the bead-bound α RanGAP1 fraction + ATP after manual sorting (see Materials & Methods for further details). The additive score corresponds to the sum of all single scores, from which –ATP scores were subtracted.

List selected candidates:	selected from screen	antibody	MW [kD]
protein inhibitor of activated STAT 1, PIAS1	1 + 2	+	72
Cytoskeleton-associated protein 5, CKAP-5	1 + 2	+/-	226
transforming, acidic coiled-coil containing protein 2, TACC2	1 + 2	+	64 - 309
mitotic spindle-associated protein p126, Astrin	1 + 2	-	134
centrosomal protein 170kDa, Cep170	1 + 2	-	175
protein 4.1	1 + 2	-	63 - 97
Topoisomerase II alpha	1	+/-	174
Polo-like kinase 1, Plk1	1	+	68
Ubiquitin-specific protease 7, USP7	1	+	128
NIMA-like kinase 9, Nek9	1	-	107

Tab. 3: Candidate substrates selected from the first and second screen. List of selected candidate Sumo substrates, for which antibodies were obtained. Listed are also the MS screens based on which the proteins were selected, the quality of the obtained antibodies tested by immunoblot analysis, and the theoretical molecular weight.

4.3. Testing selected candidate Sumo targets

As a first step to evaluate the selected candidate Sumo targets, their specific binding to and sumoylation by the mitotic RanGAP1-RanBP2-Ubc9 complex was analyzed. Control IgG and α RanGAP1 immunoprecipitates from mitotic cells were incubated in a sumoylation reaction with recombinant Sumo E1 and E2 enzymes and Sumo1 in the absence or presence of ATP. To distinguish between sumoylation and phosphorylation due to the presence of kinases identified in the first MS screen, an additional control was included omitting Sumo1 only. The samples were separated by SDS PAGE and immunoblotted with antibodies for all selected proteins. 2.5 % of the IP supernatants were analyzed in parallel on the same gel as an indication for the relative amount co-purifying with RanGAP1-RanBP2-Ubc9 compared to the entire protein pool present in the cell extracts. The respective western blots are compiled in Fig. 23.

As the α Sumo1 blot shows, sumoylated proteins migrating at 90 kD or higher (marked by RanGAP1*Sumo1) were detected only with α RanGAP1 immunoprecipitates in the presence of Sumo1 and ATP. The migration pattern of full-length RanBP2 and its

degradation fragments was equal in all immunopurified α RanGAP1 samples, however much less RanBP2 appeared to be present with Sumo1 and ATP. From *in vitro* studies with recombinant RanBP2 Δ FG it is known that the catalytic fragment can be conjugated with multiple Sumo moieties to such a high extent that it does not migrate into the resolving gel in SDS PAGE (Pichler et al. 2002). It is likely that this behavior also applies to the endogenous protein explaining the apparent disappearance of RanBP2 upon sumoylation in this experiment. RanGAP1 was already mostly sumoylated before the reaction (see –ATP control); the small fraction of unsumoylated RanGAP1 became modified in the presence of ATP and Sumo1 in addition to the appearance of a higher molecular weight band representing RanGAP1 conjugated to two Sumo1 molecules. No modifications were detected for Crm1, Ran, and Ubc9.

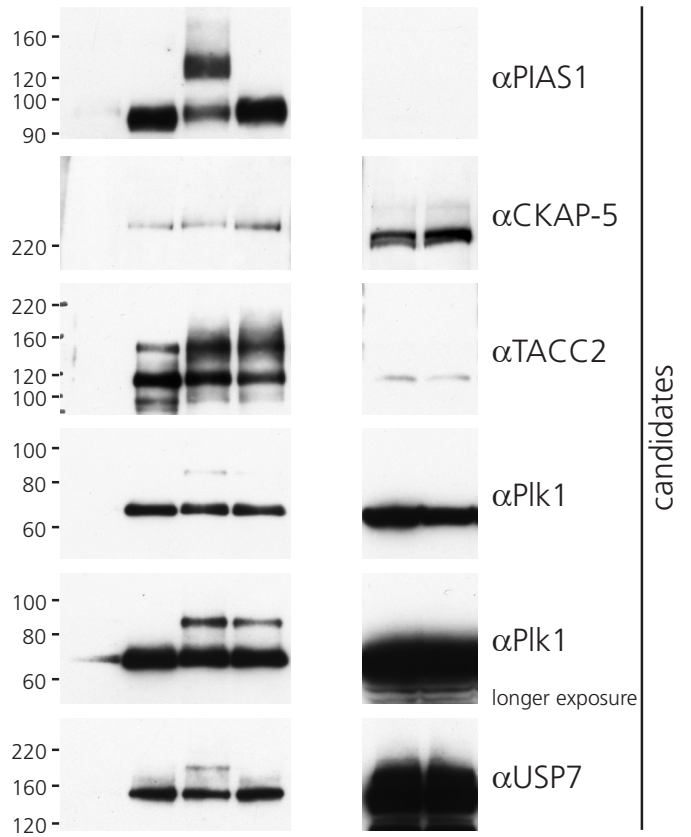
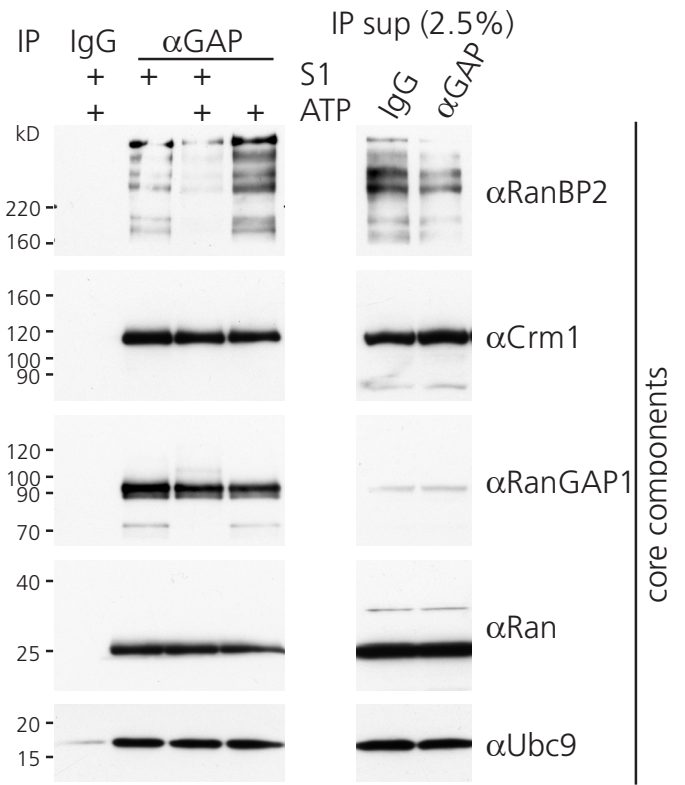
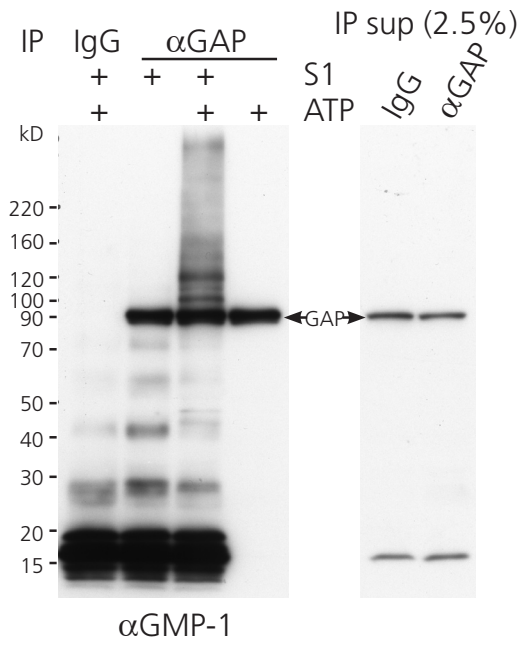


Fig. 23: Assay to test selected candidate Sumo targets. Control IgG or goat α RanGAP1 immunoprecipitates were incubated in a sumoylation reaction with 68 nM recombinant Aos1-Uba2 and 55 nM Ubc9 in the absence or presence of 23 μ M Sumo1 and/or 5 mM ATP. The samples and 2.5 % of the IP supernatants were separated by SDS PAGE and analyzed by western blotting with the indicated antibodies. The IP-sumoylation reactions and the corresponding IP supernatant samples were analyzed on the same gel and were spliced together from one western blot exposure. Note: a putative sumoylated form of Ubc9 would not be visible on the shown cut-out. However, it has been tested in other experiments that Ubc9 is not sumoylated in this case.

4.3.1. Topoisomerase II α , the only known in vivo substrate of RanBP2, binds to and is modified by the mitotic RanGAP1-RanBP2-Ubc9 complex

Topoisomerase II α was one of the putative candidates identified in the previously described screens. In mitosis it localizes to the inner centromere to decatenate chromosome bridges, a process essential to guarantee proper chromosome segregation in anaphase. In an earlier study, PIASy (also named PIAS4) had been shown to be specifically required for mitotic modification of Topoisomerase II α by Sumo2 in *Xenopus* egg extracts (Azuma et al. 2005). Furthermore, removal of PIASy interfered with sister chromatid separation. During the course of the here described studies, work by the van Deursen group identified RanBP2 as the Sumo E3 ligase modifying Topoisomerase II α in mouse embryonic fibroblasts; interfering with sumoylation by RanBP2 using a hypomorphic RanBP2 allele resulted in a strong decrease of Topoisomerase II α at the inner centromere, which could be rescued by overexpressing the catalytic RanBP2 Δ FG fragment (Dawlaty et al. 2008).

Fig. 24 shows that Topoisomerase II α specifically co-purified with mitotic RanGAP1-RanBP2-Ubc9 in the afore described binding and sumoylation assay. An additional slower migrating species of Topoisomerase II α representing a sumoylated form was detected in the presence of ATP, Sumo1 and recombinant Ubc9 (lane 4). It is likely that sumoylation occurred also in the absence of additional Ubc9 as the fastest migrating form representing unsumoylated Topoisomerase II α repeatedly vanished from detection in the presence of Sumo1 and ATP in such experiments (lane 3). It is possible that Topoisomerase II α becomes modified with multiple Sumo moieties diluting single species to amounts below the detection limit of the antibody. Our result is consistent with the published data describing Topoisomerase II α to be modified by Sumo. Considering the presence of PIAS proteins in the reaction (see following paragraph) it remains an open question whether RanBP2, a PIAS protein, or both promote sumoylation of this target

used for immunopurification of RanGAP1-RanBP2-Ubc9. To test whether interaction of RanGAP1 with PIAS1 was mutually exclusive with RanBP2 interaction, PIAS1 was immunoprecipitated from mitotic cells and analyzed for associating factors. Indeed RanGAP1 co-purified specifically with PIAS1; strikingly however, no RanBP2 and none of the other core components were detectable (Fig. 25B). These results strongly suggest that RanGAP1 can form at least two distinct complexes; either it associates with RanBP2 or with PIAS1 but not with the two E3 ligases in one complex.

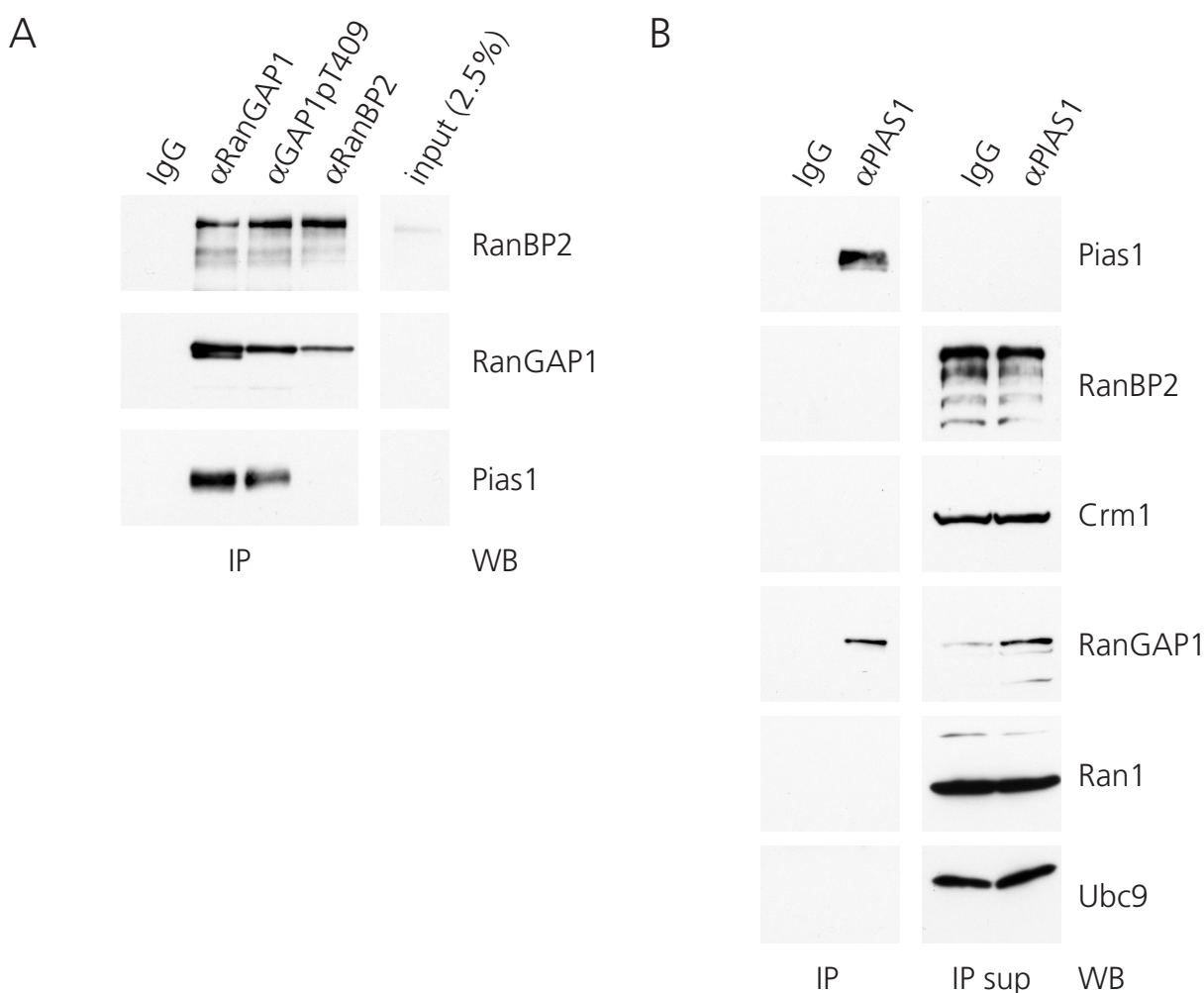


Fig. 25: PIAS1 associates in a complex with mitotic RanGAP1 distinct from the RanBP2 complex.

(A) PIAS1 is in stable association with mitotic RanGAP1. Control IgG, goat αRanGAP1, goat αRanGAP1 pT409 and goat αRanBP2 immunoprecipitates from nocodazole-arrested HeLa CSH cells and 2.5 % of the input were separated by SDS PAGE and analyzed by western blotting with the indicated antibodies. Note: this figure shows the same experiment as in Fig. 18.; the two top panels were already shown before, this figure adds the PIAS1 panel. (B) PIAS1 associates with RanGAP1 but not RanBP2. Control IgG and goat αPIAS1 immunoprecipitates from nocodazole-arrested HeLa CSH cells and 1.5 % of the corresponding IP supernatants were separated by SDS PAGE and analyzed by western blotting with the indicated antibodies. The IP and the input or corresponding IP supernatant samples were analyzed on the same gel and were spliced together from one western blot exposure. Note: unequal western blot signals for RanGAP1 in the IP supernatants result from a technical problem and have no further significance.

To be able to address which E3 ligase mediates modification of specific Sumo substrates identified in the binding and sumoylation assay, recombinant PIAS1 was produced. As PIAS proteins are prone to heavy degradation or premature termination during bacterial expression, full-length PIAS1 was cloned in fusion with a N-terminal GST and a C-terminal 8-fold His tag (of note, some PIAS1 constructs used in the Sumo field harbor a nonsense mutation resulting in truncation of approximately 100 amino acids of the C terminus; as described in Materials & Methods I repaired such a mutation prior to expression). Expression in bacteria was optimized to yield full-length protein and a purification procedure was established involving double affinity chromatography and removal of the GST tag. In short, GST-PIAS1-His was purified from bacterial lysates by a GST pull-down. Following elution with glutathione the GST tag was cleaved by Precission in an overnight dialysis to remove glutathione. Precission, uncleaved GST-PIAS1-His, and free GST were removed in a subsequent GST pull-down. The full-length protein was enriched on Ni²⁺ beads and eluted with imidazole. Fig. 26 shows a Coomassie stain of the purified fraction after SDS PAGE. A contaminating band possibly representing Hsp70 co-purified in equal stoichiometry to cleaved PIAS1-His. The protein was active in sumoylation towards the PIAS model substrate p53 (not shown).

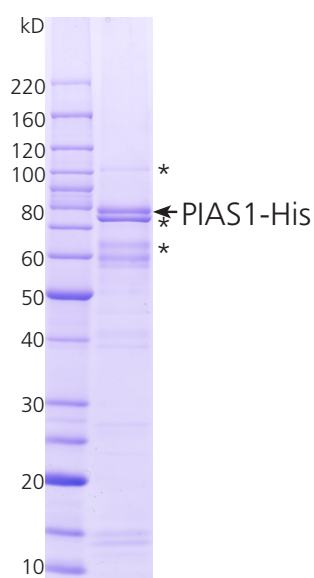


Fig. 26: Purification of recombinant PIAS1-His. GST-PIAS1-His was expressed in Rosetta bacteria by autoinduction. The protein was first purified by GST pull-down, subsequently the GST tag was cleaved by Precission in an overnight dialysis to remove GSH. Precission, uncleaved GST-PIAS1-His, and free GST were then removed by a second GST pull-down. The full-length protein was enriched by a Ni²⁺ pull-down. Shown is a Coomassie staining of the imidazole-eluted protein. The arrow indicates the full-length cleaved PIAS1-His, the asterisks mark (from top to bottom) uncleaved GST-PIAS1-His, co-purifying contaminants (potentially Hsp70 and others) and some shorter fragments of PIAS1-His.

4.3.3. The spindle/centrosome-associated proteins CKAP-5 and TACC2 bind to the RanGAP1-RanBP2 complex

CKAP-5 and TACC2 were selected as representatives of the spindle and centrosome-associated proteins. In the binding and sumoylation assay both proteins bound specifically, TACC2 being highly enriched in the α RanGAP1 immunoprecipitates compared to the protein pool present in the extracts (Fig. 23). Whereas CKAP-5 migrated at a higher molecular weight in the immunoprecipitated samples compared to the IP supernatants, no modification of CKAP-5 with Sumo1 was detected in this assay. Interestingly, TACC2 migrates as a 20 kD bigger species in SDS PAGE of mitotic cell extracts compared to interphase, a size difference expected upon sumoylation (Fig. 27). In the sumoylation assay TACC2 indeed underwent a shift from 100 to 120 kD and to higher molecular weight species, however these changes also occurred in the absence of Sumo suggesting that TACC2 became phosphorylated in the reaction (Fig. 23).

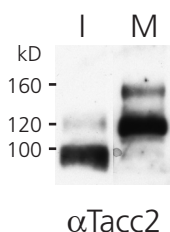


Fig. 27: Endogenous mitotic TACC2 migrates as a 20 kD bigger species in SDS PAGE compared to interphase TACC2. Cycling (I) or nocodazole-arrested (M) HeLa cells were lysed in 6M guanidine-HCl and solubilized protein was precipitated by methanol-chloroform precipitation. Precipitated protein was reconstituted in SDS sample buffer, separated by SDS PAGE and analyzed by western blot with rabbit α TACC2 antibodies. The two lanes shown in this figure were part of the same blot but not directly neighboring lanes.

To test whether the protein could be sumoylated *in vitro*, TACC2 was cloned and purified as bacterially expressed protein with a N-terminal His tag. So far, six isoforms of TACC2 have been described ranging between 60 to 300 kD and varying in their N-terminal sequence. To find out which isoform was present in the α RanGAP1 immunoprecipitates, TACC2 was amplified from HeLa cDNA with primer pairs representing the four isoforms of around 100 kD based on the migration of TACC2 in SDS PAGE. Indeed a TACC2 isoform was cloned with the primer pair for isoform 5; sequencing however identified this form as a so far unknown isoform closely related to isoform 5 (see supplementary information for the sequence). The corresponding protein migrated at a size around 200 kD in SDS PAGE when expressed in bacteria or in

HeLa cells (not shown). Based on this unusual migration behavior the shortest isoform 2 of approximately 60 kD was cloned and expressed in bacteria. This form migrated at around 90 kD closely matching the expected migration size. The bacterially expressed protein was purified by Ni²⁺ pull-down as described in Materials & Methods (p. 55). Next, recombinant His-TACC2 was tested for modification by Sumo1 and Sumo2 *in vitro* with recombinant Sumo E1 and E2 enzymes. TACC2 was efficiently conjugated to both Sumo paralogs in the presence of the catalytic RanBP2ΔFG fragment whereas PIAS1 supported modification only with Sumo2 (Fig. 28). Sumoylation of TACC2 depended strictly on an E3 ligase as the E1 and E2 enzymes alone were not sufficient. Thus, TACC2 is an E3-dependent Sumo target *in vitro*.

Initial experiments addressing sumoylation of TACC2 *in vivo* did not provide evidence that the protein is modified in cells (not shown), for this a more detailed analysis is needed.

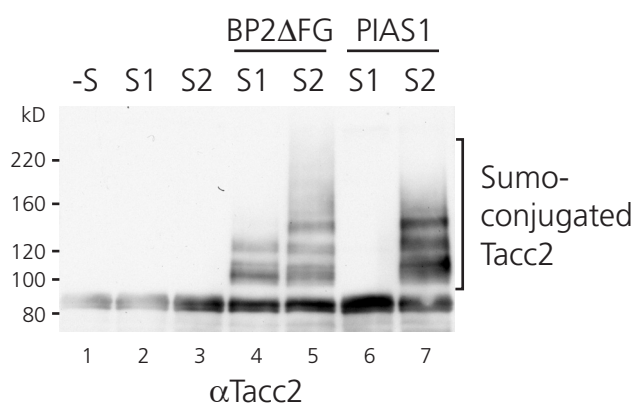


Fig. 28: Recombinant TACC2 can be sumoylated *in vitro*. Recombinant His-TACC2 (short isoform) was incubated in a sumoylation reaction with 68 nM Aos1-Uba2, 55 nM Ubc9 (lanes 1-7) in the presence of 16 nM RanBP2ΔFG (lanes 4-5) or of 17 nM PIAS1-His (lanes 6-7) with 13.5 μM Sumo1 (lanes 2, 4, 6) or Sumo2 (lanes 3, 5, 7). The reaction was started by adding 5 mM ATP. The samples were analyzed by western blotting with rabbit αTACC2 antibodies.

4.3.4. The mitotic kinase Plk1 is a Sumo target *in vitro* and the Polo box is important for PIAS1-mediated sumoylation

Polo-like kinase 1 is a cell cycle regulated kinase essential for various aspects of mitotic progression. It plays an important role throughout mitosis starting with centrosome maturation, spindle assembly, APC/C activation and removal of cohesin from sister chromatids at the meta- to anaphase transition, and ending with functions in cytokinesis and mitotic exit. The manifold involvement of Plk1 is also being reflected by its changing

localization (Golsteyn et al. 1994; Golsteyn et al. 1995; Arnaud et al. 1998): Plk1 can be found at kinetochores and centrosomes in prophase; it also localizes to the spindle and spindle poles in meta- and anaphase. From anaphase on it starts to enrich at the central spindle and can only be detected at the cleavage furrow in telophase and at the midbody towards the end of cytokinesis (see also Fig. 30A as example).

In the binding and sumoylation assay Plk1 was found to associate specifically with the RanGAP1-RanBP2-Ubc9 complex (Fig. 23). The protein was also detected as a 20 kD bigger species in the presence of Sumo1 and ATP; a comparable band however became also apparent after prolonged exposure of the western blot when Sumo was left out. This indicates that Plk1 can be phosphorylated in the reaction resulting in a 20 kD size shift in SDS PAGE. It is conceivable that Plk1 is also sumoylated in the experiment; the sumoylated species would not be distinguishable from the phosphorylated form in SDS PAGE.

To test whether Plk1 can be sumoylated *in vitro*, Flag-Plk1 was expressed in 293T cells and was immunopurified with α Flag agarose after mitotic arrest of the cells with nocodazole. In a sumoylation reaction with Aos1-Uba2, Ubc9 and Sumo1, a small fraction of Flag-Plk1 became sumoylated in the presence of RanBP2 Δ FG, and sumoylation worked more efficiently with a 3-fold molar excess of Pias1-His while E1 and E2 alone were not sufficient (Fig. 29). Thus, RanBP2 Δ FG and PIAS1 can promote modification of Plk1 with Sumo1.

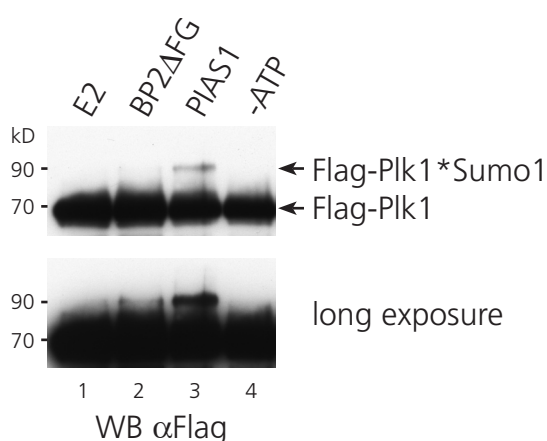


Fig. 29: Recombinant Flag-Plk1 can be sumoylated *in vitro*. 293T cells transiently transfected with pcDNA-Flag-Plk1 were arrested in mitosis with nocodazole. Flag-Plk1 immunoprecipitates were incubated in a sumoylation reaction with recombinant 68 nM Aos1-Uba2, 55 nM Ubc9 and 9 μ M Sumo1 (lanes 1-6) together with 16 nM RanBP2 Δ FG (lane 2), 68 nM PIAS1-His (lane 3) in the presence of 5 mM ATP except lane 4. The samples were eluted with SDS sample buffer, separated by SDS PAGE and analyzed by western blotting with rabbit α Plk1 antibodies.

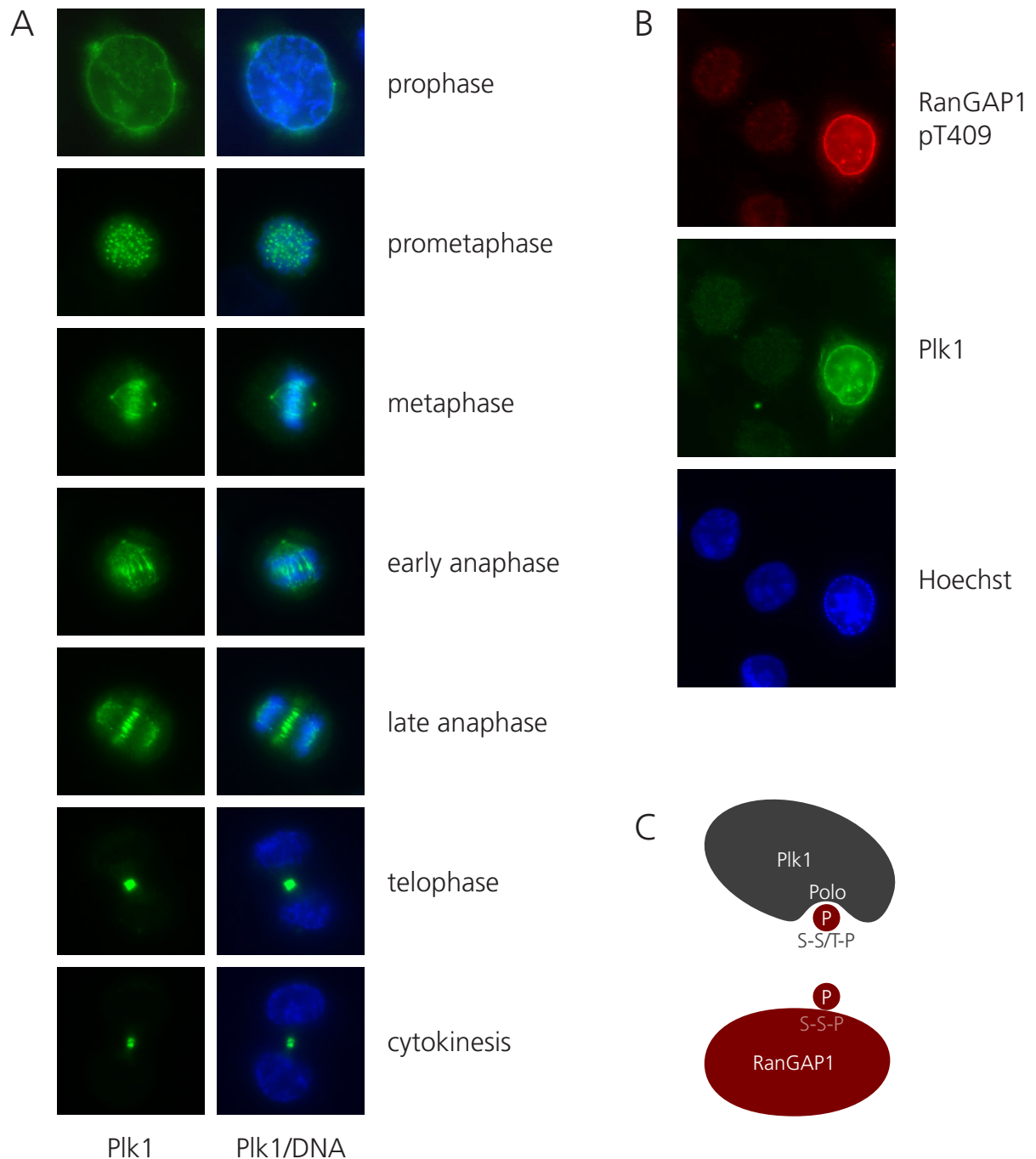


Fig. 30: Plk1 localizes to the nuclear envelope in early prophase, when RanGAP1 becomes phosphorylated. (A) HeLa cells were permeabilized prior to fixation. Immunostaining was performed with rabbit α Plk1/donkey α rabbit Alexa488 (green) and DNA was stained with Hoechst (blue). The samples were analyzed by fluorescence microscopy. (B) HeLa cells were permeabilized prior to fixation. Immunostaining was performed with rabbit α Plk1/donkey α rabbit Alexa488 (green) and goat α RanGAP1 pT409/donkey α goat Alexa594 (red), DNA was stained with Hoechst (blue). The samples were analyzed by fluorescence microscopy. (C) Model for Plk1 localization to the nuclear envelope in early prophase. The C terminus of Plk1 harbors two Polo boxes, which bind to specific phosphorylated motifs (consensus S-pS/pT-P/X) and are required for recruitment of Plk1 to its intracellular anchoring sites. The second mitotic phosphorylation site of RanGAP1, S428, represents such a motif.

Essential to proper localization of Plk1 in mitosis is a phospho-binding domain in the C terminus of the protein, the so-called Polo box. This domain binds to phosphorylated

serine or threonine in the sequence context S-pS/pT-P/X (Elia et al. 2003). Such a motif is provided by the second phosphorylation site in RanGAP1, serine 428 (Fig. 30C). Interestingly, Plk1 can be detected at the nuclear envelope in early prophase concomitant with RanGAP1 phosphorylation (Fig. 30A and B) raising the question whether Plk1 targeting to the nuclear envelope is linked to RanGAP1 phosphorylation. To address this issue endogenous Plk1 localization was monitored by immunofluorescence microscopy in cells in which the RanGAP1-RanBP2-Ubc9 complex had been removed from the nuclear pore by RNA interference towards RanBP2. In early prophase before completion of nuclear envelope breakdown (controlled by staining of various nucleoporins with the monoclonal m414 antibody recognizing FG repeats, not shown) the absence of RanBP2 did not abolish Plk1 targeting to the nuclear rim (Fig. 31). Thus, phosphorylated RanGAP1 is not essential for localization of Plk1 to the nuclear envelope in early prophase cells.

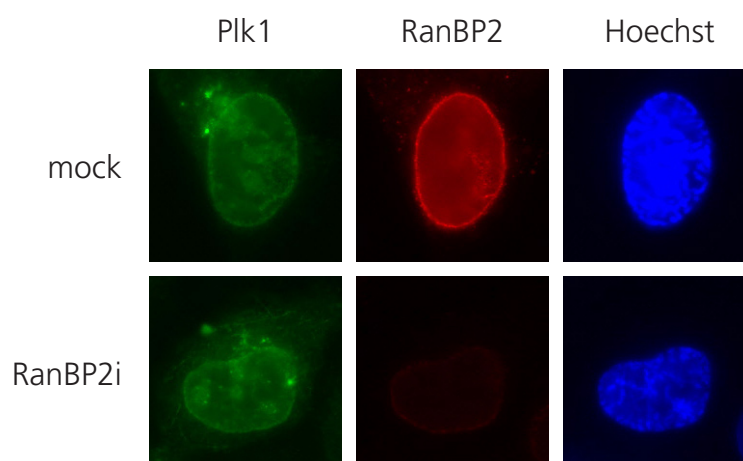


Fig. 31: Plk1 localizes to the nuclear envelope of early prophase cells independently of RanBP2. HeLa cells transfected with RanBP2 siRNA or with control siRNA oligonucleotides were pre-extracted with digitonin prior to fixation. Immunostaining was performed with rabbit α Plk1/donkey α rabbit Alexa488 and goat α RanBP2/donkey α goat Alexa594, and DNA was stained with Hoechst. The samples were analyzed by fluorescence microscopy.

Interestingly, analysis of the Plk1 sequence by SUMOsp 2.0 (Ren et al. submitted) identified four putative non-consensus sumoylation sites, one of which was situated within the second Polo box domain and a second one was neighboring closely at the very C terminus (Fig. 32A). To test whether Sumo may be involved in regulating the Polo box, the lysines within the putative Sumo target sequences (K556, K601) were exchanged for arginines. HA-Plk1 wild type and variants were expressed and

immunopurified from nocodazole-arrested HEK293T cells and tested for sumoylation by RanBP2 Δ FG and PIAS1-His as Sumo E3 ligases *in vitro*. As before, 16 nM RanBP2 Δ FG and 68 nM PIAS1-His were used. Again, PIAS1-His was more efficient in stimulating sumoylation of wild type HA-Plk1 than RanBP2 Δ FG (Fig. 32B, lanes 1 – 4). While RanBP2 Δ FG-dependent sumoylation was comparable for wild type and mutant HA-Plk1 (compare lanes 3, 7, 11), the K556R variant was strongly reduced in PIAS1-dependent sumoylation (compare lanes 4, 8, 12). This result suggests that the lysine within the second Polo box domain, K556, is important for PIAS1-dependent enhancement of Plk1 sumoylation *in vitro*. Since the sumoylation pattern of HA-Plk1 K556R with PIAS1 is indistinguishable from BP2 Δ FG-mediated Sumo species, it is unlikely that lysine 556 is targeted by Sumo1 directly. The result rather points towards the possibility that PIAS1 binds to Plk1 involving the lysine of the second Polo box domain.

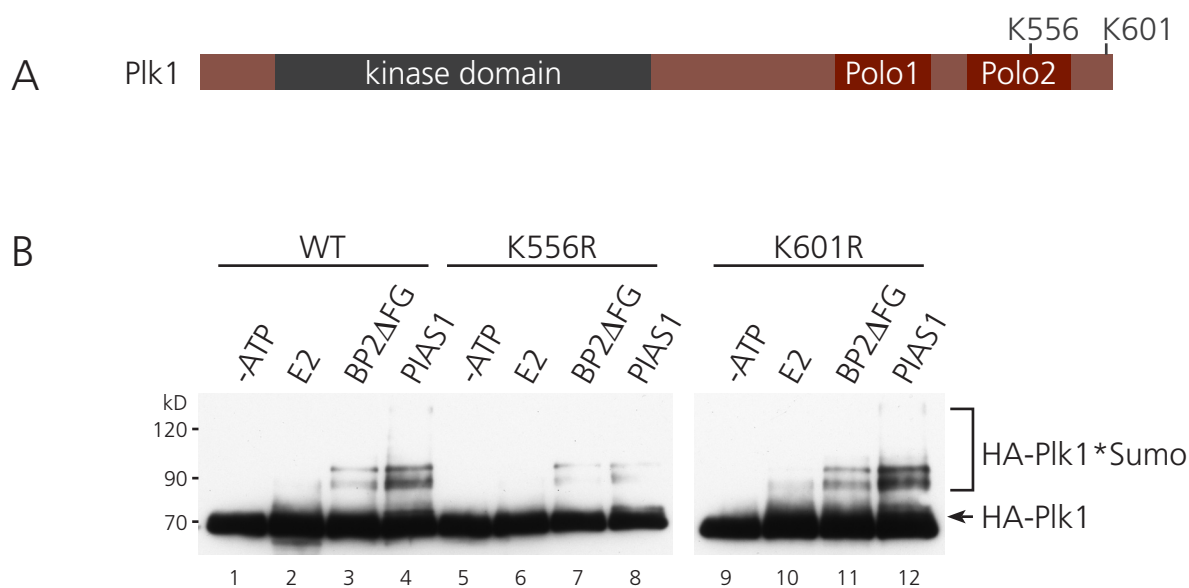


Fig. 32: Plk1 K556R is impaired in PIAS1-dependent sumoylation. (A) Schematic representation of Plk1. Indicated are the kinase domain, the Polo boxes (Polo) and the lysine residues 556 and 601. (B) 293T cells transiently transfected with pcDNA-HA-Plk1 wild type (lanes 1-4), a K556R and K601R variant (lanes 5-8 and 9-12, respectively) were arrested in mitosis with nocodazole. HA-Plk1 immunoprecipitates were incubated in a sumoylation reaction with recombinant factors: 68 nM Aos1-Uba2, 55 nM Ubc9 and 9 μ M Sumo1 together with 16 nM RanBP2 Δ FG (lanes 3, 7, 11), 68 nM PIAS1-His (lanes 4, 8, 12) in the presence of 5 mM ATP except lanes 1, 5, 9. The samples were eluted with SDS sample buffer, separated by SDS PAGE and analyzed by western blotting with mouse α HA antibodies.

4.3.5. The de-ubiquitinating enzyme USP7 binds to and is sumoylated by the mitotic RanGAP1-RanBP2-Ubc9 complex

In the binding and sumoylation assay a small fraction of USP7 co-purified specifically with mitotic RanGAP1-RanBP2-Ubc9 (Fig. 23). Strikingly, a significant fraction of the co-purifying protein was modified specifically in the presence of Sumo1 and ATP. Next to PIAS1 this result identified USP7 as the most promising Sumo target of the tested candidates.

The Ubiquitin-specific protease USP7, also known as HAUSP, is a de-ubiquitinating enzyme acting on p53, MDM2, MDMX and others. There is precedent for conjugation of a USP to Sumo in the literature: USP25 has been shown to be sumoylated preferentially with Sumo2/3 resulting in reduced hydrolysis of Ubiquitin chains (Meulmeester et al. 2008).

Furthermore USP7 contains several presumptive NES sequences, which may serve as a docking site for Crm1. Together this renders USP7 a preferred substrate to test whether some Sumo targets may be recruited to and sumoylated by RanGAP1-RanBP2-Ubc9 in dependence of Crm1 and Ran. Initial experiments with recombinant His-USP7 from insect cells suggest that USP7 can be sumoylated *in vitro*, however the efficiency of this reaction was very low suggesting that a factor or some other determinant such as a phosphorylation of the substrate was still missing.

In summary, the search for RanBP2-dependent Sumo targets resulted in about 90 potential candidates. 6 of these were selected for further analysis; all of these candidate substrates were specifically enriched in mitotic RanGAP1 complexes (PIAS1, Topo II α , TACC2, CKAP-5, Plk1, USP7). Several candidate targets could be confirmed to be sumoylated with recombinant factors (TACC2, Plk1) or as associated proteins of the mitotic RanGAP1-RanBP2 complex (Topo II α , Plk1, USP7). While the associated Sumo E3 ligase PIAS1 was also sumoylated in these reactions, the responsible mechanism remains to be determined.

As next step, *in vivo* evidence is needed to confirm these candidates as Sumo targets in cells and to gain insight into the responsible E3 ligase. Unraveling functional consequences of sumoylation for each of these targets is a long term goal and will likely involve identification of the modification site(s).

5. The mitotic RanGAP1-RanBP2-Ubc9 complex exhibits weak sumoylation activity towards Sp100

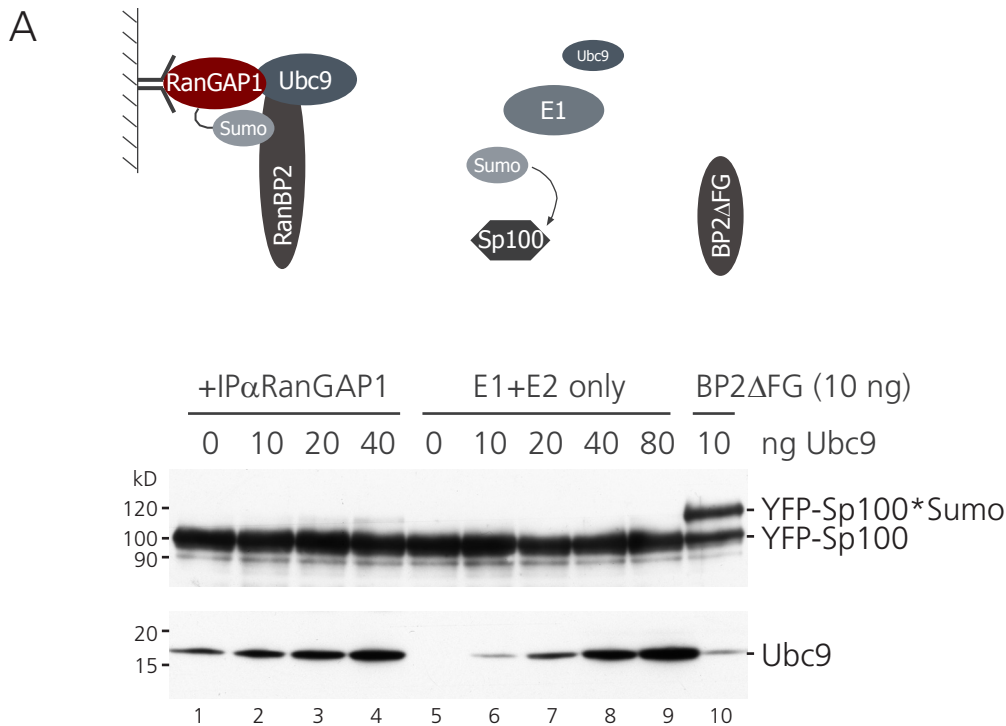
Substrate specificity in sumoylation is thought to reside within the E3 ligases. As an example, the minimal catalytic fragment of RanBP2 comprising only IR1 and M (see Fig. 33B) has the ability to enhance sumoylation of many proteins *in vitro*. By comparison, a fragment including the neighboring regions up to the FG repeats, RanBP2 Δ FG, displays increased selectivity towards modification of certain targets: p53 can be sumoylated by IR1+M but not BP2 Δ FG while the model substrate Sp100 is modified equally well with both catalytic fragments (Pichler et al. 2004).

RanBP2 Δ FG is a 30 kD fragment, approximately 1/10 of full-length RanBP2. To test whether the remaining areas of RanBP2 influence substrate selection, I took advantage of the fact that immunopurification of RanGAP1 from mitotic cells yields full-length RanBP2.

In an *in vitro* reaction I compared sumoylation of the E3 dependent Sumo model substrate Sp100 with RanGAP1-RanBP2-Ubc9 immunopurified from nocodazole-arrested HeLa cells as source of an E3 ligase to sumoylation with a recombinant catalytic fragment of RanBP2, BP2 Δ FG (see Fig. 33A for a cartoon of the experimental setup). By comparison to sumoylation reactions of Sp100 with recombinant Aos1-Uba2 and Ubc9 alone, approximately 20 ng of endogenous Ubc9 were present in the α RanGAP1 immunoprecipitates used per reaction (Fig. 33A, compare lane 1 to lanes 5-9). In the presence of 40 ng additional recombinant Ubc9, RanGAP1-RanBP2-Ubc9 stimulated sumoylation of Sp100 to a higher extent than 80 ng recombinant Ubc9 alone indicating that the complex is active as an E3 ligase (compare lanes 4 and 9). Based on current investigations in the lab (Andreas Werner, unpublished data) and on published data (Zhu et al. 2006), one to two molecules of Ubc9 (17 kD) are present in the complex per molecule of RanBP2 (360 kD); by extrapolation 20 ng of endogenous Ubc9 correspond to 200 to 400 ng of the 20-fold larger full-length RanBP2, which equals 20 to 40 ng of the recombinant RanBP2 Δ FG fragment (30kD). When compared to sumoylation with only 10 ng BP2 Δ FG, sumoylation of YFP-Sp100 with the RanGAP1-RanBP2-Ubc9 complex from cells was very inefficient (compare lane 10 to lanes 1-4).

There are multiple possibilities to account for this observation. In fact, it is not known whether Sp100 is indeed a substrate of RanBP2 *in vivo*. *In vitro*, several E3 ligases

promote sumoylation of Sp100, one of which is the BP2 Δ FG fragment. Potentially, full-length RanBP2 harbors additional substrate specificity not present in the smaller catalytic fragment resulting in decreased activity towards Sp100. Alternatively, putative associated regulatory factors may modify the activity or substrate specificity of the protein.



B



Fig. 33: Sp100 sumoylation by the mitotic RanGAP1-RanBP2-Ubc9 complex is weak compared to recombinant RanBP2. (A) Sumoylation of Sp100 by the mitotic RanGAP1-RanBP2-Ubc9 complex. 580 nM recombinant YFP-Sp100 were incubated in a sumoylation reaction for 45 minutes in the presence of 68 nM Aos1-Uba2, 9 μ M Sumo2, with the indicated amounts of Ubc9 (0 – 80 ng Ubc9 correspond to 0 – 220 nM in solution) and with either the mitotic RanGAP1-RanBP2-Ubc9 complex immunopurified α RanGAP1 from nocodazole-arrested HeLa CSH cells as source of a Sumo E3 ligase (lanes 1-4), with no E3 ligase added (lanes 5-9), or with 16 nM recombinant RanBP2 Δ FG in the presence of 5 mM ATP. The samples were analyzed by western blot with rabbit α YFP and goat α Ubc9 antibodies. (B) Schematic representation of full-length RanBP2, RanBP2 Δ FG and IR1+M. R - Ran binding domain, I - internal repeat, M - middle segment, CY - cyclophilin-like domain, dash - FG repeat.

To test whether association of additional factors such as Crm1 has an inhibitory effect towards sumoylation of Sp100 in this experiment or whether this is rather an intrinsic property of RanBP2 itself, detergents were used as a tool to hopefully remove associated proteins.

Again, recombinant Sp100 was incubated in a sumoylation reaction with recombinant Sumo E1 and E2 enzymes, Sumo2 and ATP in the presence of RanGAP1 immunoprecipitates from mitotic cells as source of an E3 ligase. To remove Crm1 and potentially other factors from the purified complexes, the immunoprecipitates were washed with RIPA buffer prior to the sumoylation reaction, which is sufficient to strip off Crm1 (Fig. 34, bottom panel) leaving the RanGAP1-RanBP2-Ubc9 core complex intact (it is known that the RanGAP1-RanBP2 interaction remains stable in RIPA buffer (Mahajan et al. 1997)). When the reactions were analyzed for Sp100 modification, removal of Crm1 from the mitotic RanGAP1-RanBP2-Ubc9 complex did not restore sumoylation compared to the transport buffer-treated control sample (top panel, compare lane 2 and 4) whereas Sp100 was efficiently sumoylated in the presence of the recombinant RanBP2 Δ FG catalytic fragment. Thus, Crm1 is not simply an inhibitory factor of full-length RanBP2; this finding rather supports the hypothesis that additional domains in RanBP2 influence substrate selection.

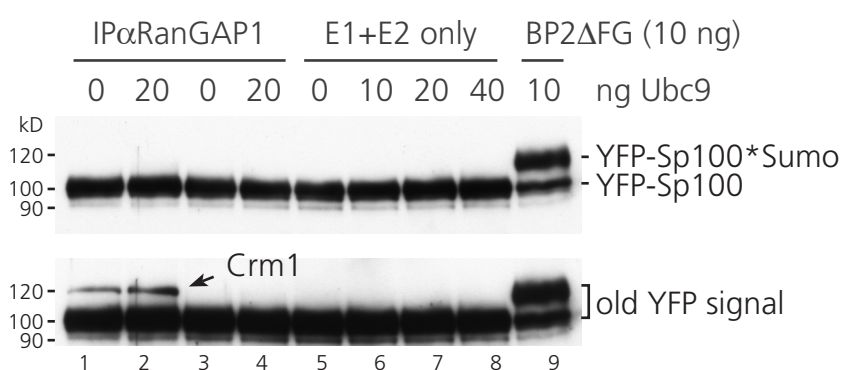


Fig. 34: Stripping off Crm1 does not reactivate sumoylation of Sp100 by the mitotic RanGAP1-RanBP2-Ubc9 complex. Mitotic goat α RanGAP1 immunoprecipitates purified from nocodazole-arrested HeLa CSH cells used as source of an E3 ligase were incubated with either transport buffer (lanes 1 and 2) or RIPA buffer (lanes 3 and 4) washing Crm1 out of the complexes prior to the sumoylation reaction. The Crm1 levels of the different preparations are shown in the lower panel. 580 nM recombinant YFP-Sp100 were incubated in a sumoylation reaction in the presence of 68 nM Aos1-Uba2, 9 μ M Sumo2, with the indicated amounts of Ubc9 and with either the immunopurified mitotic RanGAP1-RanBP2-Ubc9 complex (lanes 1-4), with no E3 ligase added (lanes 5-9), or with 16 nM recombinant RanBP2 Δ FG in the presence of 5 mM ATP. The samples were analyzed by western blotting with rabbit α YFP and rabbit α Crm1 antibodies.

Chapter II: An alternative mechanism of substrate specificity in sumoylation

According to prevalent concepts in sumoylation specificity for post-translational modification with Sumo is created at the level of the E3 ligases and/or the target itself. To date only few E3 ligases have been identified and even less regulatory modules at the substrate level have been described; compared to the rapidly growing number of Sumo targets and the manifold molecular pathways they are involved in, it seems unlikely that tight regulation in a spatial and timely manner can be guaranteed by these means only. The previous chapter raised the question whether the sumoylation machinery adopts a pre-existing system (Ran and export receptor) to extend substrate specificity of the Sumo E3 ligase RanBP2 by means of a substrate recruiting module. In this chapter a novel mechanism of substrate selectivity at the level of the Sumo E2 enzyme Ubc9 will be described. This work was performed in collaboration with Andrea Pichler, Puck Knipscheer, Helene Klug and others and was published in *Molecular Cell* (Knipscheer et al. 2008). A short summary of the biochemical analyses and the resulting molecular mechanism will be given in the following paragraph (6.1.). The experiments described therein were performed by others and are not part of this work. Own contributions will be presented subsequently (6.2./6.3.).

6. Ubc9 sumoylation regulates Sumo target discrimination

6.1. Conjugation of Sumo to lysine 14 in mammalian Ubc9 enhances its activity towards certain SIM-containing Sumo targets *in vitro*

Work by Puck Knipscheer and Andrea Pichler showed that Ubc9 can be sumoylated *in vitro*. MS analysis and mutagenesis identified lysine 14 as the major Sumo acceptor site of mammalian Ubc9 in contrast to yeast Ubc9, in which modification of lysine 153 prevailed. In striking opposition to what had been shown in a previous study for sumoylation of the Ubiquitin E2 enzyme E2-25K, which was severely impaired in activity upon modification (Pichler et al. 2005), conjugation of Sumo to the analogous lysine 14 in Ubc9 did not abolish thioester formation and activity.

Surprisingly, mammalian Ubc9*Sumo displayed an altered target preference compared

to the unmodified enzyme: Whereas modification of HDAC4, E2-25K, PML and TDG was equally efficient with both forms of Ubc9, sumoylation of Ubc9 strongly activated Sp100 modification. Enhanced sumoylation strictly depended on a Sumo interacting motif (SIM) in Sp100 increasing the affinity of Sp100 for covalently modified Ubc9*Sumo. When compared to other SIM containing Sumo targets sumoylation of some but not all was enhanced by sumoylation of Ubc9 suggesting that properties of the target determine the strength of activation.

A crystal structure of Ubc9 conjugated to Sumo on lysine 14 showed that a β hairpin specific to Ubc9 accounted for the different effect of sumoylation on E2 activity compared to E2-25K: Protrusion of the hairpin from the Ubc9 core domain positioned Sumo differently towards the core enzyme allowing for interaction of the E2 with the E1 enzyme and thereby for thioester bond formation of the E2 with Sumo.

In conclusion, covalent modification of Ubc9 by Sumo adds a second binding interface for SIM containing Sumo targets thereby promoting recruitment of these targets to Ubc9 (Fig. 35). It is likely that the positioning of the SIM in respect to the target lysine contributes to determining sumoylation efficiency.

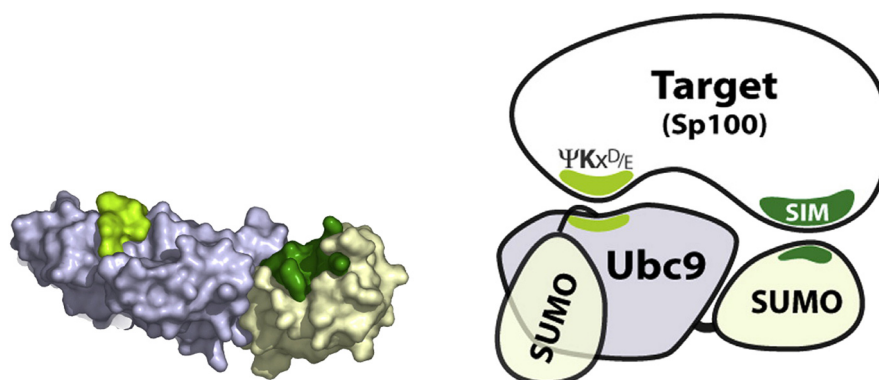


Fig. 35: Conjugation to Sumo adds a second binding interface for SIM containing Sumo targets. The model schematically represents binding of a SIM containing target (e.g. Sp100) to Ubc9 (grey) conjugated to Sumo (white) on lysine 14. The interaction site of the Ubc9 catalytic cleft with the Ubc9 consensus motif is highlighted in light green, the additional binding interface between Sumo and the SIM is marked in dark green. Figure adapted from Knipscheer et al. (Knipscheer et al. 2008).

6.2. Mammalian Ubc9 is sumoylated on lysine 14 *in vivo*

The afore presented mechanism for substrate selectivity of Ubc9 is based on biochemical analyses. It was my task to provide evidence that this mechanism also functions in cells to promote target discrimination. As first step towards this goal, it was essential to demonstrate that Ubc9 is sumoylated *in vivo*. Therefore HeLa cells co-transfected with Ubc9-StrepHis and HA-Sumo1 or an empty control vector were subjected to a two-step purification procedure. First, Ubc9-StrepHis species from guanidine lysates were enriched on Ni²⁺ beads and were eluted with 2 % SDS. Subsequent to diluting to RIPA buffer conditions, HA-Sumo1 conjugated species were purified by immunoprecipitation with α HA agarose. The samples were analyzed with α HA antibodies after SDS PAGE. A band of 40 kD representing a sumoylated species of Ubc9 was purified specifically in the presence of HA-Sumo1 indicating that Ubc9 can be sumoylated in mammalian cells (Fig. 36A).

To determine which lysine in Ubc9 is being targeted by Sumo, lysine 14 and lysine 153 were exchanged for arginine by site-directed mutagenesis. Co-expression of the Ubc9-His single and double mutants together with HA-Sumo1 in 293T cells showed that recovery of Ubc9-His by a Ni²⁺ pull-down was severely reduced in the absence of lysine 14 while at least equal amounts of wild type and the Ubc9-His K153R variant were detected (Fig. 36B). Thus, mammalian Ubc9 is preferentially sumoylated on lysine 14 in cells.

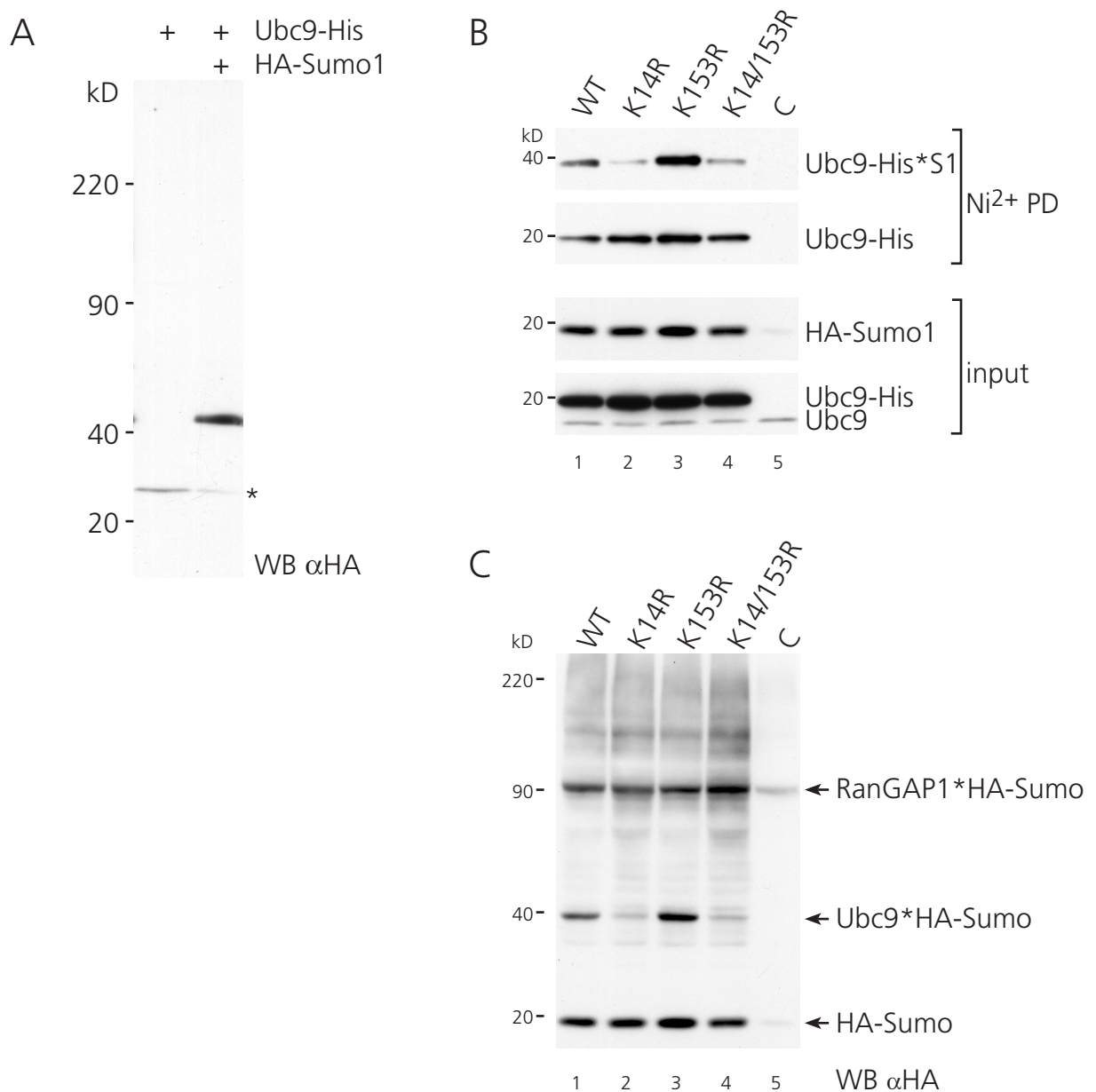


Fig. 36: Ubc9 is modified with Sumo on lysine 14 *in vivo*. (A) Two-step purification of sumoylated Ubc9 from cells. HeLa cells co-transfected with Ubc9-StrepHis and pcDNA or HA-Sumo1 in pcDNA were subjected to a two-step purification procedure involving a Ni²⁺ pull-down under denaturing conditions and subsequent enrichment on α HA sepharose under RIPA buffer conditions. Eluted samples and input were separated by SDS PAGE and analyzed by immunoblotting with mouse α HA (clone HA.7, Sigma). The asterisk indicates an unspecific band. (B) 293T cells co-transfected with HA-SUMO1 and Ubc9-His wt, the indicated K to R mutant variants or empty vector were subjected to a Ni²⁺ pull down under denaturing conditions. Input and purified samples were analyzed by western blot with mouse α HA (clone HA.7, Sigma; top panel of Ni²⁺ pull-down and input) and goat α Ubc9 antibodies (bottom panel of Ni²⁺ pull-down and input). The asterisk indicates endogenous Ubc9. Note that co-expression of Ubc9 significantly increased the expression of HA-Sumo1 (compare lanes 1-4 to lane 5). (C) A full view of the mouse α HA western blot on the input samples shows that under the chosen overexpression conditions, Ubc9 becomes a major Sumo target in cells.

6.3. Overexpression of a Sumo-deficient Ubc9 K14R variant does not alter the overall Sumoylation pattern in cells

To test whether sumoylation of Ubc9 influences target modification *in vivo*, Ubc9-His wild type and the K14R variant but no Sumo were overexpressed in 293T cells. However, no difference in the overall Sumo1 and Sumo2/3 patterns were detected in these cell lysates after SDS PAGE (Fig. 37). Likewise did co-expression with Sp100 not show apparent differences in Sp100 modification (not shown).

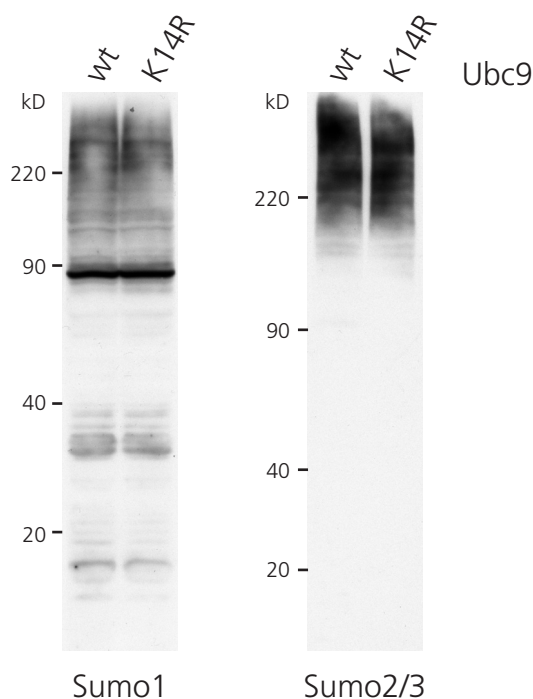


Fig. 37: The overall Sumoylation pattern remains unaffected upon overexpression of the Sumo-deficient Ubc9 K14R variant. 293T cells transiently overexpressing Ubc9-His wt or Ubc9-His K14R were lysed in 6M guanidine-HCl, 100 mM sodium phosphate, 10 mM Tris pH 8. Proteins were precipitated by methanol-chloroform extraction, resuspended in SDS sample buffer and separated by SDS PAGE. The immunoblot was performed with monoclonal mouse α Sumo1 ascites or goat α Sumo2/3 antibodies. Note that in contrast to the previous experiments, no Sumo was co-overexpressed, which explains the absence of a band corresponding to Ubc9*Sumo.

DISCUSSION

The RanGAP1-RanBP2-Ubc9 complex is a fascinating entity as it contains two distinct enzymatic activities, the RanGTP hydrolysis promoting function and sumoylation activity. The original aim of this work was to further characterize the RanGAP1-RanBP2 complex specifically in mitosis. The fact that RanGAP1 becomes quantitatively phosphorylated in mitotic cells promised to serve as a good starting point to gain further insight into its regulation. While I could demonstrate that phosphorylation does not contribute to RanGAP1 localization, further analysis was hampered by a number of technical hurdles such as low expression levels of stably transfected RanGAP1 variants. Therefore I focussed on the search for mitotic RanGAP1-RanBP2 interacting proteins, which led to the identification of the nuclear export receptor Crm1 and the GTPase Ran as stable components in complex with RanGAP1-RanBP2.

A study published by others during the course of this work established a functional link between Crm1 and RanGAP1-RanBP2 in mitosis: Crm1 is required for RanGAP1-RanBP2 localization and function at kintochores in mitosis (Arnaoutov et al. 2005). I therefore decided to focus my attention on the identification of RanGAP1-RanBP2 interacting proteins that may provide a novel link between Crm1 and RanBP2. Towards this goal I embarked on the identification of novel RanBP2 dependent Sumo targets associated with the mitotic RanGAP1-RanBP2-Ubc9 complex.

An additional project in collaboration with Andrea Pichler, a former postdoc in the Melchior laboratory, addressed the validation of a novel mechanism for substrate specificity in sumoylation.

In the following sections I will discuss a selection of important topics arising from the presented results in more detail.

1. Crm1 and Ran are stable interaction partners of the RanGAP1-RanBP2 complex

From previous work by several laboratories it is well established that RanGAP1 and RanBP2 fulfill important yet distinct functions in interphase and during the cell division cycle (see introduction). These are likely to be reflected in their cell cycle-specific interactions with other proteins.

In the study presented here, two known components of the Ran GTPase system, namely the nuclear export receptor Crm1 and the GTPase Ran itself, were identified as prominent and stable components of the mitotic RanGAP1-RanBP2-Ubc9 complex. This is based on co-immunoprecipitation experiments from mitotic HeLa cell extracts using four different antibodies, α RanGAP1, phospho-specific α RanGAP1 pT409, α RanBP2 and α Crm1 antibodies. The relative intensities of the RanGAP1 versus Crm1 representing Coomassie bands suggest that the majority of RanGAP1 is bound to a Crm1 molecule (Fig. 13A). Given that 50 – 80 % of all RanGAP1 in HeLa cells associates with RanBP2 (Mahajan et al. 1997; Hutten et al. 2008) and that this interaction remains stable throughout the cell cycle (Swaminathan et al. 2004), these findings make Crm1 a stoichiometric subunit of the RanGAP1-RanBP2 complex. The prominent presence of Crm1 is very interesting, especially in light of the absence of other transport receptors. While Crm1 is the major interacting protein in the size range from 90 to 350 kD, the size range from 20 to 60 kD was obscured by the antibody chains used for immunoprecipitation. Consequently, it can not be excluded that additional proteins are stoichiometric partners of this complex. To address this question I have started to explore several possibilities. Covalent linkage of the antibody to the matrix has proven unsuitable, however initial experiments to achieve specific elution of mitotic RanGAP1 and its binding partners using the phospho-specific α RanGAP1 pT409 peptide antibody in combination with peptide elution suggest that this may be a promising approach. An important question is to whom Crm1 binds. Alternatives include direct association to RanGAP1, association with the 358 kD protein RanBP2, with or without the help of Ran, or Ubc9 (see introduction p. 24, Fig. 6 for illustration). Considering the architecture of RanBP2, one likely possibility is that a cooperative interaction of Crm1 and Ran with the Ran binding sites and the FG repeats of RanBP2 confers stable binding. Based on my experiments, direct association of Crm1 with RanGAP1 is highly unlikely. From co-immunoprecipitation studies using a phospho-deficient RanGAP1 variant it becomes clear that Crm1 binding is independent of RanGAP1 phosphorylation. *In vitro* binding experiments with recombinant RanGAP1 and Crm1 suggest that the interaction with Crm1 is not mediated directly via RanGAP1. Technical pitfalls of this specific experiment however include the use of murine RanGAP1 in combination with human Crm1. While the homology of human and mouse RanGAP1 is rather high (88.6 % identity, 97.8 %

similarity, FASTA and SSEARCH - Protein Similarity Search, <http://www.ebi.ac.uk/Tools/fasta33>), it can not be excluded that the endogenous human proteins may interact with each other. Moreover, the experiment has been performed under conditions that would exclude low-affinity interactions due to the relatively low protein concentrations used; although the endogenous interaction with Crm1 is rather stable in co-immunoprecipitation experiments, it still may be that its formation would require higher protein concentrations. Based on published data, Crm1 has been reported to interact specifically with the N-terminal zinc finger domain of bovine RanBP2 independent of the NES binding site of Crm1 (Singh et al. 1999) in addition to the common concept that transport receptors interact transiently with the FG repeats of nucleoporins, of which several clusters are present throughout the RanBP2 protein. While full-length RanBP2 is currently technically inaccessible to recombinant expression and purification in bacteria due to its large size, it would be interesting to test various RanBP2 fragments for binding to Crm1 in the absence and presence of RanGTP, in particular fragments including the zinc finger domain or clusters of FG repeats in combination with neighboring Ran binding domains. Fragments of RanBP2 comprising both, potential Crm1-Ran binding site(s) and the RanGAP1-Ubc9 binding domain would allow to reconstitute the RanGAP1-RanBP2 complex *in vitro* and to dissect its functional inter-relationships. The presence of the GTPase Ran as stable interaction partner of RanGAP1-RanBP2 is rather surprising. Ran bound to GTP but not GDP displays high affinity for Ran binding domains (Coutavas et al. 1993; Bischoff et al. 1995b); in the course of the Ran GTPase cycle RanGTP in complex with Crm1 and a NES cargo binds to the Ran binding domains of RanBP2, which accelerates GTP hydrolysis thereby disassembling the export complex and relieving Crm1 and Ran from the nucleoporins (Kehlenbach et al. 1999). While previous work indicated that mitotic RanGAP1-RanBP2 stimulates GTP hydrolysis on Ran (Swaminathan et al. 2004), the finding that Crm1 and Ran are stable constituents of the mitotic RanGAP1-RanBP2 complex raises the question as to whether or not GTP hydrolysis can occur in this context. Currently it is unknown whether Crm1 and Ran bind RanGAP1-RanBP2 in a nucleotide dependent manner. It is interesting to note however, that the previously performed activity assays were performed with RanGAP1-RanBP2 immunoprecipitated from a detergent-containing buffer; similar conditions led to loss of Crm1 from the complex. It would therefore be worthwhile to revisit the GTPase

stimulating activity of mitotic RanGAP1-RanBP2 comparing conditions that allow or disallow for binding of Crm1.

A further question arising in this context is whether stable interaction with Crm1 is a feature specific to mitotic RanGAP1-RanBP2. In interphase the RanGAP1-RanBP2 complex is part of the NPC, which requires detergent-containing buffer conditions to solubilize this macromolecular assembly. From a technical point of view it is therefore impossible to isolate the RanGAP1-RanBP2 complex from interphase cells under conditions that would permit Crm1 binding. This issue will be interesting to reconsider in the context of putative functional aspects of Crm1 binding.

2. Functional aspects of Crm1 binding

While stable binding of Crm1 to the RanGAP1-RanBP2 complex is surprising, a functional link between these proteins specifically in mitosis has already been established. Similar to RanGAP1 and RanBP2, a pool of Crm1 can also be found at kinetochores from prometaphase until telophase (Arnaoutov et al. 2005). Interestingly, recruitment of RanGAP1-RanBP2 to kinetochores depends on ternary complex formation of Crm1 with RanGTP and a NES cargo. Here, kinetochore-localized Crm1 may for example serve to situate a specific adaptor NES cargo as receptor for RanGAP1-RanBP2 binding. In context of the here presented findings it seems likely that a complex of Crm1, Ran, a NES cargo, RanGAP1, RanBP2 and Ubc9 forms similar to the soluble one isolated biochemically in this work.

By immunoprecipitation from nocodazole-arrested cell extracts this complex behaves as a stable entity, in cells however, it appears to be more dynamic: upon leptomycin treatment, which interferes with NES binding to Crm1, RanGAP1 and RanBP2 mislocalize from kinetochores whereas a pool of Crm1 remains (Arnaoutov et al. 2005). Nocodazole treatment as used for biochemical studies in this work artificially and permanently activates the spindle checkpoint by depolymerizing the entire microtubule apparatus. As yet, it has not been tested what happens to the localization of RanGAP1, RanBP2 and Crm1 upon activation of the spindle checkpoint or to the GTPase promoting activity of RanGAP1-RanBP2 in cells; mutually exclusive localization of RanGAP1-RanBP2 and the checkpoint protein Mad1 to kinetochores (Joseph et al. 2004) suggests however that RanGAP1-RanBP2 are stably recruited to kinetochores only if these satisfy the spindle

checkpoint. An attractive model for GTP hydrolysis-regulated recruitment would be a checkpoint-responsive RanGAP1-RanBP2 regulator at the kinetochore that influences the GTP hydrolysis promoting function upon checkpoint satisfaction thereby allowing for stable recruitment of RanGAP1-RanBP2 to a localized Crm1-RanGTP-NES complex. Insights into the GAP activity in dependence of the spindle checkpoint however will mostly likely involve high resolution imaging of as yet undesignated FRET sensor probes. Interestingly, a direct link between Crm1 and checkpoint regulation has recently been discovered: recruitment of the chromosomal passenger complex (CPC) protein Survivin that mediates docking of the CPC onto kinetochores to correct aberrant microtubule attachments depends on Crm1 and a NES in Survivin (Knauer et al. 2006), raising the question whether Survivin may be a NES cargo within the RanGAP1-RanBP2-Crm1-Ran complex.

What may be the functional role of RanGAP1-RanBP2 in mitosis? Next to localized regulation of RanGTP levels as one potential aspect, the Sumo E3 ligase activity of RanBP2 offers fascinating options. While RanGAP1-RanBP2 function may not be restricted to kinetochores, it is interesting to note that increasing evidence supports an essential role for Sumo in kinetochore function. Not only has Sumo (also designated as Smt3) originally been identified as suppressor of a temperature-sensitive allele of mif two (Chen et al. 1998), the yeast homolog of the centromere protein Cenp-C, but also can Cenp-C be modified with Sumo *in vitro* (Chung et al. 2004). Moreover, many proteins involved in microtubule attachment and chromosome segregation have been identified as Sumo targets (Bachant et al. 2002; Hoegge et al. 2002; Stead et al. 2003; Panse et al. 2004; Wohlschlegel et al. 2004; Zhou et al. 2004; Denison et al. 2005; Hannich et al. 2005; Wykoff and O'Shea 2005; Dawlaty et al. 2008); these include the yeast homologs of Survivin and the kinetochore protein Hec1 (Montpetit et al. 2006), which is part of the Ndc80 complex essential for stable kinetochore-microtubule attachment (Tanaka and Desai 2008). Most recently, the microtubule motor Cenp-E has not only been shown to be a Sumo target *in vivo*, it also needs non-covalent interactions with Sumo2/3 chains to be recruited to kinetochores (Zhang et al. 2008).

3. RanGAP1 associates with two E3 ligases

Since its discovery as Sumo E3 ligase numerous proteins have been Sumo-modified with help of catalytic RanBP2 fragments *in vitro*; evidence for RanBP2's sumoylation activity *in vivo* as full-length protein has been scarce though. Sumoylation activity is associated with the nuclear envelope in permeabilized interphase cells (Pichler et al. 2002) and this activity largely depends on RanBP2 (data not shown) strongly suggesting that RanBP2 acts as an E3 ligase *in vivo*. Biochemical purification of mitotic RanGAP1 co-precipitates full-length RanBP2; these complexes display strong sumoylation activity towards associated proteins upon addition of recombinant Sumo E1 enzyme, Sumo and ATP. More than 90 Sumo candidates could be identified in mass spec analysis. Are these all targets for the RanBP2 E3 ligase? Unfortunately the answer is not that straight forward. To my surprise, α RanGAP1 immunoprecipitation led also to highly specific enrichment of PIAS E3 ligases. This makes it difficult to distinguish, which E3 ligase accounts for the activity. While it is likely that each E3 ligase adds to the overall sumoylation, immunoprecipitated full-length RanBP2 not yielding any detectable PIAS1 was also active in sumoylation. Additionally, the pattern of sumoylated species was similar when immunoprecipitated RanGAP1 or RanBP2 complexes were used for the experiment suggesting that RanBP2 contributes significantly to the sumoylation activity towards associated proteins. Interestingly, one major difference besides the overall efficiency was represented by a band just below 120 kD present in the α RanGAP1 but not α RanBP2 immunoprecipitates (p. 83, Fig. 21). Western blot analysis of comparable experiments allows to hypothesize that this band represents sumoylated PIAS1 and suggests that approximately 10 % of RanGAP1 may be associated with PIAS1 based on the intensities of the Sumo signals. Of note, it is currently unclear whether the α PIAS1 antibody recognizes only PIAS1 or also PIAS2/3.

Most direct evidence for RanBP2's activity as E3 ligase comes from the recent discovery of Topoisomerase II α as first *in vivo* substrate (Dawlaty et al. 2008). In context of previous studies reporting PIASy (PIAS4) to account for Topoisomerase II α modification (Azuma et al. 2005; Diaz-Martinez et al. 2006), it is striking that the here presented work confirms Topoisomerase II α as Sumo substrate in an IP that contains both types of E3 ligases. While a physical link is unlikely as the two E3 ligases appear to be part of distinct complexes, the question arises whether a so far unrecognized functional link

exists between the E3 ligases RanBP2 and PIAS1. In light of the conflicting published data it will be important to test whether Topoisomerase II α co-purification and sumoylation can also be found in association with RanBP2 immunoprecipitates.

4. *In vivo* targets of the Sumo E3 ligase RanBP2 – evaluation and alternative approaches

Identification of RanBP2 targets *in vivo* is hampered by its large size and its stable integration into one of the largest macromolecular machineries in the cell. While the here presented approach to search for novel *in vivo* Sumo targets of RanBP2 succeeded in confirming the only known substrate Topoisomerase II α , the list of candidates still awaiting further confirmation is long. The general screening strategy was to modify associated substrates of the mitotic RanGAP1-RanBP2 complex with His-tagged Sumo followed by purification of the sumoylated species. The first screen yielded about 90 putative candidates; certainly not all of these are sumoylated proteins, at least not considering the presence of the abundant but not Sumo-modified complex components Crm1, Ran and Ubc9. However, judging from the fact that the so far tested candidates identified only in the first screen (Topoisomerase II α , USP7, Plk1) can be modified with Sumo *in vitro*, it seems likely that this list comprises many more potential RanBP2 and PIAS-dependent Sumo substrates.

In comparison to the first screen that likely also identified many unmodified proteins associated with the mitotic RanGAP-RanBP2 complex, the setup of the second screen was geared at increased stringency towards the identification of sumoylated proteins specifically. Indeed, the second screen yielded a subset of proteins already identified in the original screen with a clear preference for two classes of proteins: PIAS E3 ligases and microtubule/centrosome-associated proteins. In agreement with published data (Schmidt and Muller 2002), PIAS1 and supposedly also other PIAS members are indeed efficiently sumoylated in this experiment; whether this is due to autosumoylation or may require RanBP2 remains to be determined. Currently, this analysis is not trivial as all known catalytic mutants of PIAS proteins destroy the SP-RING finger and concomitantly protein structure. The second class, the microtubule and centrosome-associated proteins, is rather difficult to assess in terms of sumoylation, and a draw-back opposing recombinant testing for many of these proteins is their relatively large molecular size.

The candidate TACC2 is an efficient Sumo substrate *in vitro* using recombinant E3 ligases; whether it also works with the endogenous RanGAP1-RanBP2 complex requires further investigation. An essential next step will be the verification of identified Sumo substrates *in vivo*; knock-down of RanBP2 or PIAS1 in cells will help to determine the E3 ligase responsible for modification of a certain substrate. This could be combined with localization analyses.

Intriguingly, the reported localization of the second class of proteins coincides with RanBP2 localization to the spindle and near centrosomes (Joseph et al. 2002); correspondingly, preliminary data suggest that the most prominent sumoylation activity in permeabilized mitotic cells is associated with centrosomes. It should be noted that under the experimental conditions used here and for substrate identification, the spindle apparatus and likely the kinetochores have been disassembled, which may account for the lack of kinetochore-associated sumoylation activity and substrates.

While originally designed to identify specifically mitotic Sumo substrates, the here chosen approach has the great advantage that it allows to purify full-length RanBP2 under physiological conditions rendering the use of mitotic cell extracts an excellent tool for the identification of associating proteins. Many of the potential Sumo candidates fit into the picture of mitotic regulation; however, none of these candidates have been confirmed to be Sumo targets in cells and it remains to be seen whether Sumo modification of substrates such as USP7 is a cell cycle regulated event.

In general, it is rather surprising that substrates of an enzymatic reaction bind to the catalyzing enzyme in such a stable fashion that would allow for co-purification. From this perspective, alternative approaches to search for Sumo targets could be designed to include more transient interactions. One closely related strategy would be to apply immunopurified endogenous RanBP2-RanGAP1-Ubc9 (preferentially using RanBP2 antibodies not directed against the catalytic domain) or recombinant E2 as control in a sumoylation reaction with recombinant Sumo E1, a double affinity-tagged form of Sumo and a sumoylation-inhibited (e.g. NEM treated) cell extract from interphase or mitotic cells as source of Sumo substrates. Sumoylated proteins may then be enriched, preferentially including a denaturing step to avoid non-covalent Sumo interactions, followed by MS identification. Alternatively, the pool of sumoylated proteins in RanBP2-depleted (siRNA treated) cells compared to untreated cells could be analyzed choosing

a SILAC (stable isotope labeling with amino acids in cell culture) approach. This method could be combined with the enrichment of sumoylated proteins by immunoprecipitating Sumo to decrease the complexity of the sample. A SILAC approach may however not be suited for the identification of mitosis-specific Sumo substrates given that RanBP2-depleted cells show cell cycle defects and will therefore be hard to compare to untreated cells.

5. Crm1 and Ran as a specificity module for the Sumo E3 ligase RanBP2?

Based on the intriguing connection of the Sumo E3 ligase RanBP2 to the nuclear transport system, a mechanism to guarantee proper target selection has been proposed in this work: the adoption of the export receptor Crm1 as adaptor to recruit NES containing Sumo targets to RanBP2. Given that a set of transport receptors has evolved to guarantee tightly regulated transport of many proteins across the nuclear envelope, this system seems well suited to confer substrate selectivity to a large array of proteins. In combination with the presence of RanGAP1 in the same complex it is tempting to speculate that the two enzymatic activities of the RanGAP1-RanBP2 complex may act in concert: GTP hydrolysis by RanGAP1-RanBP2 as a regulated substrate release mechanism from Crm1 after sumoylation by RanBP2-Ubc9. Intriguingly, the same mechanism could also act to couple sumoylation to nuclear transport in interphase cells.

While experimental evidence for this model is still missing, the tools are now available. For example, the here identified Sumo substrate USP7 comprises several putative NES sequences and to test binding of USP7 to Crm1 in dependence of Ran-GTP would be a first step in this direction. Larger catalytic fragments of RanBP2 including transport receptor and Ran binding sites could then be used to analyze Crm1 and Ran-GTP dependent sumoylation of USP7.

As an alternative approach to test or eventually identify Crm1 dependent Sumo substrates at an endogenous level, one could take advantage of the Crm1 inhibitor LMB. In this case, the here developed α RanGAP1 immunoprecipitation and sumoylation assay could be modified such that a pool of nocodazole-arrested cells would be treated with LMB for 15 to 30 minutes just before cell harvest in comparison to untreated cells; Crm1 dependent Sumo targets would be expected to be absent in the LMB treated

sample. This approach however relies on dynamic association of targets with Crm1 as LMB can only modify the free NES binding site.

6. Ubc9 sumoylation as means for Sumo substrate selection

In addition to my work on target recruitment to RanBP2, I was also involved in dissecting an E3 ligase independent mechanism of Sumo target recognition. Until recently, substrate specificity in sumoylation has been thought to be contained exclusively within the Sumo E3 ligases. Considering the multitude of targets compared to the limited number of identified Sumo E3 ligases, further mechanisms are required to ensure specificity. Sumo interacting motifs in several targets have been shown to be crucial for their efficient modification. Work by Knipscheer et al. identifies a novel mechanism, namely sumoylation of the E2 enzyme Ubc9 itself, that enhances sumoylation of selected SIM containing Sumo targets (Knipscheer et al. 2008). Biochemical and structural characterization of Ubc9 modified on K14 shows that *in vitro* Sumo adds a second binding interface that allows for efficient binding of Ubc9 to the target, a mechanism similar to the function of Sumo E3 ligases or the second binding interface shared between Ubc9 and RanGAP1 (p. 110, Fig. 33). Comparable mechanisms have also been suggested for a Ubiquitin E2~ubiquitin thioester (Hoeller et al. 2007) and most recently for the Ubc9~Sumo thioester (Zhu et al. 2008). While essential, the presence of a SIM is not sufficient for enhanced sumoylation by Ubc9*Sumo1 suggesting that structural constraints such as the positioning of the SIM in respect to the sumoylated lysine determines the efficiency of target modification. While sumoylated Ubc9 works as efficiently as an E3 ligase on Sp100, efficient modification of other targets such as Daxx or TDG may require the action of an additional E3 ligase. In this case, the combination of several specificity modules offers an option to significantly expand substrate specificity with a limited set of players. Whether this mechanism contributes to substrate specificity *in vivo* requires further work; the here presented data show that Ubc9 becomes sumoylated on lysine 14 *in vivo*, sumoylation of endogenous Ubc9 however is difficult to detect and may be a regulated event. While Sp100 is a great model substrate *in vitro*, various E3 ligases are able to modify Sp100 *in vitro* and most likely also *in vivo*; combined with low levels of sumoylated Ubc9, this renders Sp100 unsuitable for *in vivo* analysis of the suggested mechanism. Ongoing work in Andrea Pichler's laboratory aims

at identifying *in vivo* substrates of sumoylated Ubc9.

7. The role of mitotic RanGAP1 phosphorylation

RanGAP1 phosphorylation in mitosis has been well characterized; based on quantitative phosphorylation of defined residues it is likely to be important for RanGAP1 regulation, its role however still remains elusive. Since RanGAP1 phosphorylation does not affect the most obvious aspects of RanGAP1 function, that is GAP activity, complex formation with RanBP2 and Ubc9 and protein localization, an unbiased search for potential defects of a phosphorylation-deficient or phosphorylation-mimicking RanGAP1 variant are required to gain further insights. While the here presented experimental design aimed at replacing endogenous RanGAP1 with adequate variants at levels that allow for physiological protein function essential to cell viability, the implementation was obstructed by low expression levels and the inability of the engineered RanGAP1 variants to replace the endogenous protein. It is well established that the interaction of RanGAP1*Sumo1 with RanBP2 and Ubc9 involves the C-terminal domain of RanGAP1 including the sumoylation site, ongoing work by Andreas Werner in the Melchior lab however recently raised the question whether complex formation involves additional interaction sites in the N-terminal catalytic domain of RanGAP1. Interestingly, a RanGAP1 variant N-terminally tagged with GFP constructed by Daniël Splinter et al. efficiently replaced endogenous sumoylated RanGAP1 with the GFP-tagged version and localized to the nuclear envelope in interphase when stably expressed in cells (Splinter et al. manuscript submitted) suggesting that in principal endogenous RanGAP1 can be replaced. In light of these preliminary findings it is interesting to note that the construct by Splinter et al. includes 14 additional amino acids at the N terminus as linker between the protein and the GFP moiety whereas the HA tag used in this study was fused to RanGAP1 with a minimal linker of two amino acids, which may sterically interfere with interactions required for efficient complex formation. It seems worthwhile to start a new attempt to replace endogenous RanGAP1 with phospho-variants using the construct by Splinter et al..

In addition to the replacement strategy, the search for phospho-specific RanGAP1 interacting proteins is still an aspect to pursue. Corresponding to the fact that endogenous RanGAP1 is part of stable protein complexes in mitosis, the here and

elsewhere presented pull-down strategies with peptides or recombinant proteins are not very promising. An alternative approach to address phospho-specific interaction partners at an endogenous level would be to purify endogenous RanGAP1 from mitotic cells by immunoprecipitation and to compete with binding to RanGAP1 using phosphorylated RanGAP1 peptides to elute potential phospho-specific interaction partners.

Finally, the here presented experiments suggest that PIAS1 can stably interact with RanGAP1 independent of RanBP2. Further work is needed to test whether this interaction is a direct one and whether it is mitosis-specific. If this were the case then PIAS1 is certainly an interesting candidate to test in respect to phospho-specific binding to RanGAP1.

8. Plk1 as putative mitotic Sumo substrate

One of the very interesting mitotic Sumo candidates identified in this work is the mitosis-specific kinase Plk1. While the presented data strongly suggest that Plk1 is a Sumo substrate *in vitro*, it is currently not clear whether sumoylation depends on RanBP2, PIAS1 or both. In sumoylation reactions with recombinant enzymes, both RanBP2 and PIAS1 are able to promote conjugation of Sumo1 to the kinase.

The characteristic feature of Polo-like kinases is a phospho-binding domain in the C terminus, the Polo box. This domain mediates localization of Plk1 to many of its described sites such as centrosomes and kinetochores by interaction with specific phospho-epitopes of selected proteins. While proper localization is not always essential for the function, it is a highly regulated aspect. Some of these phospho-epitopes can be created by other proline-directed kinases such as Cdk1, others result from Plk1 action directly, providing a positive feed-back mechanism and suggesting that temporally and spatially regulated creation of binding sites guides the kinase through the cell (Lee et al. 2008; Petronczki et al. 2008). While not yet reported, it is well conceivable that other modifications of the Polo box may contribute to the orchestration. Interestingly, mutation of lysine 556 in the second Polo box interferes with PIAS1-mediated *in vitro* sumoylation. Based on a structure of the Polo box (Cheng et al. 2003) this lysine is situated in the loop region of a β sheet hairpin reminiscent of lysine 164 in PCNA and facing the phospho peptide binding pocket. Sumo modification of this residue would likely influence the binding properties of Plk1 to phosphorylated proteins in a

negative or positive manner. While the data do not allow to conclude that lysine 556 of Plk1 becomes sumoylated, it is interesting to note that PCNA has been shown to be sumoylated by a PIAS-type E3 ligase (Reindle et al. 2006).

9. Outlook

The mitotic RanGAP1-RanBP2 complex is embedded in an intricate regulatory network involving the Ran system and the sumoylation machinery to affect pathways important for mitotic progression. New tools and a lot of work will be required to dissect the different aspects at a functional, temporal and spatial level.

The here presented work is far from providing a final picture of the RanGAP1-RanBP2 complex in mitosis, however it offers a variety of novel findings to further pursue, in particular in respect to sumoylation. A long list of candidate Sumo targets awaits confirmation, and especially the microtubule and centrosome-associated proteins promise to provide further insight into RanGAP1-RanBP2 regulation and function. Stable complex formation of RanGAP1-RanBP2 with the nuclear export receptor Crm1 raises the question whether the Ran system has been adopted to provide a substrate specificity module for RanBP2, a model that will be tested with tools now available in our laboratory. Finally, in light of the tight link of RanGAP1 to RanBP2 that has always provoked the question about its functional significance, it is very interesting that RanGAP1 may also form a complex with another Sumo E3 ligase, PIAS1, extending the potential interplay between the Ran system and the sumoylation machinery.

REFERENCES

- Arnaoutov A, Dasso M (2003) The Ran GTPase regulates kinetochore function. *Dev Cell* 5(1): 99-111.
- Arnaoutov A, Azuma Y, Ribbeck K, Joseph J, Boyarchuk Y, Karpova T, McNally J, Dasso M (2005) Crm1 is a mitotic effector of Ran-GTP in somatic cells. *Nat Cell Biol* 7(6): 626-632.
- Arnaud L, Pines J, Nigg EA (1998) GFP tagging reveals human Polo-like kinase 1 at the kinetochore/centromere region of mitotic chromosomes. *Chromosoma* 107(6-7): 424-429.
- Azuma Y, Arnaoutov A, Anan T, Dasso M (2005) PIASy mediates SUMO-2 conjugation of Topoisomerase-II on mitotic chromosomes. *Embo J* 24(12): 2172-2182.
- Bachant J, Alcasabas A, Blat Y, Kleckner N, Elledge SJ (2002) The SUMO-1 isopeptidase Smt4 is linked to centromeric cohesion through SUMO-1 modification of DNA topoisomerase II. *Mol Cell* 9(6): 1169-1182.
- Bayer P, Arndt A, Metzger S, Mahajan R, Melchior F, Jaenicke R, Becker J (1998) Structure determination of the small ubiquitin-related modifier SUMO-1. *J Mol Biol* 280(2): 275-286.
- Beausoleil SA, Villen J, Gerber SA, Rush J, Gygi SP (2006) A probability-based approach for high-throughput protein phosphorylation analysis and site localization. *Nat Biotechnol* 24(10): 1285-1292.
- Beausoleil SA, Jedrychowski M, Schwartz D, Elias JE, Villen J, Li J, Cohn MA, Cantley LC, Gygi SP (2004) Large-scale characterization of HeLa cell nuclear phosphoproteins. *Proc Natl Acad Sci U S A* 101(33): 12130-12135.
- Becker J, Melchior F, Gerke V, Bischoff FR, Ponstingl H, Wittinghofer A (1995) RNA1 encodes a GTPase-activating protein specific for Gsp1p, the Ran/TC4 homologue of *Saccharomyces cerevisiae*. *J Biol Chem* 270(20): 11860-11865.
- Bernier-Villamor V, Sampson DA, Matunis MJ, Lima CD (2002) Structural basis for E2-mediated SUMO conjugation revealed by a complex between ubiquitin-conjugating enzyme Ubc9 and RanGAP1. *Cell* 108(3): 345-356.
- Birnboim HC, Doly J (1979) A rapid alkaline extraction procedure for screening recombinant plasmid DNA. *Nucleic Acids Res* 7(6): 1513-1523.
-

- Bischoff FR, Krebber H, Kempf T, Hermes I, Ponstingl H (1995a) Human RanGTPase-activating protein RanGAP1 is a homologue of yeast Rna1p involved in mRNA processing and transport. *Proc Natl Acad Sci U S A* 92(5): 1749-1753.
- Bischoff FR, Krebber H, Smirnova E, Dong W, Ponstingl H (1995b) Co-activation of RanGTPase and inhibition of GTP dissociation by Ran-GTP binding protein RanBP1. *Embo J* 14(4): 705-715.
- Bogerd HP, Fridell RA, Benson RE, Hua J, Cullen BR (1996) Protein sequence requirements for function of the human T-cell leukemia virus type 1 Rex nuclear export signal delineated by a novel in vivo randomization-selection assay. *Mol Cell Biol* 16(8): 4207-4214.
- Bosu DR, Kipreos ET (2008) Cullin-RING ubiquitin ligases: global regulation and activation cycles. *Cell Div* 3: 7.
- Carazo-Salas RE, Gruss OJ, Mattaj JW, Karsenti E (2001) Ran-GTP coordinates regulation of microtubule nucleation and dynamics during mitotic-spindle assembly. *Nat Cell Biol* 3(3): 228-234.
- Caudron M, Bunt G, Bastiaens P, Karsenti E (2005) Spatial coordination of spindle assembly by chromosome-mediated signaling gradients. *Science* 309(5739): 1373-1376.
- Chen A, Mannen H, Li SS (1998) Characterization of mouse ubiquitin-like SMT3A and SMT3B cDNAs and gene/pseudogenes. *Biochem Mol Biol Int* 46(6): 1161-1174.
- Cheng KY, Lowe ED, Sinclair J, Nigg EA, Johnson LN (2003) The crystal structure of the human polo-like kinase-1 polo box domain and its phospho-peptide complex. *Embo J* 22(21): 5757-5768.
- Chung TL, Hsiao HH, Yeh YY, Shia HL, Chen YL, Liang PH, Wang AH, Khoo KH, Shoei-Lung Li S (2004) In vitro modification of human centromere protein CENP-C fragments by small ubiquitin-like modifier (SUMO) protein: definitive identification of the modification sites by tandem mass spectrometry analysis of the isopeptides. *J Biol Chem* 279(38): 39653-39662.
- Clarke PR, Zhang C (2008) Spatial and temporal coordination of mitosis by Ran GTPase. *Nat Rev Mol Cell Biol* 9(6): 464-477.
- Conti E, Muller CW, Stewart M (2006) Karyopherin flexibility in nucleocytoplasmic transport. *Curr Opin Struct Biol* 16(2): 237-244.
-

- Coutavas E, Ren M, Oppenheim JD, D'Eustachio P, Rush MG (1993) Characterization of proteins that interact with the cell-cycle regulatory protein Ran/TC4. *Nature* 366(6455): 585-587.
- Dawlaty MM, Malureanu L, Jeganathan KB, Kao E, Sustmann C, Tahk S, Shuai K, Grosschedl R, van Deursen JM (2008) Resolution of sister centromeres requires RanBP2-mediated SUMOylation of topoisomerase IIalpha. *Cell* 133(1): 103-115.
- Denison C, Rudner AD, Gerber SA, Bakalarski CE, Moazed D, Gygi SP (2005) A proteomic strategy for gaining insights into protein sumoylation in yeast. *Mol Cell Proteomics* 4(3): 246-254.
- Diaz-Martinez LA, Gimenez-Abian JF, Azuma Y, Guacci V, Gimenez-Martin G, Lanier LM, Clarke DJ (2006) PIASgamma is required for faithful chromosome segregation in human cells. *PLoS ONE* 1: e53.
- Elia AE, Rellos P, Haire LF, Chao JW, Ivins FJ, Hoepker K, Mohammad D, Cantley LC, Smerdon SJ, Yaffe MB (2003) The molecular basis for phosphodependent substrate targeting and regulation of Plks by the Polo-box domain. *Cell* 115(1): 83-95.
- Favreau C, Worman HJ, Wozniak RW, Frappier T, Courvalin JC (1996) Cell cycle-dependent phosphorylation of nucleoporins and nuclear pore membrane protein Gp210. *Biochemistry* 35(24): 8035-8044.
- Fried H, Kutay U (2003) Nucleocytoplasmic transport: taking an inventory. *Cell Mol Life Sci* 60(8): 1659-1688.
- Geiss-Friedlander R, Melchior F (2007) Concepts in sumoylation: a decade on. *Nat Rev Mol Cell Biol* 8(12): 947-956.
- Golsteyn RM, Mundt KE, Fry AM, Nigg EA (1995) Cell cycle regulation of the activity and subcellular localization of Plk1, a human protein kinase implicated in mitotic spindle function. *J Cell Biol* 129(6): 1617-1628.
- Golsteyn RM, Schultz SJ, Bartek J, Ziemiecki A, Ried T, Nigg EA (1994) Cell cycle analysis and chromosomal localization of human Plk1, a putative homologue of the mitotic kinases *Drosophila polo* and *Saccharomyces cerevisiae Cdc5*. *J Cell Sci* 107 (Pt 6): 1509-1517.
- Gorlich D, Kutay U (1999) Transport between the cell nucleus and the cytoplasm. *Annu Rev Cell Dev Biol* 15: 607-660.
-

- Gorlich D, Seewald MJ, Ribbeck K (2003) Characterization of Ran-driven cargo transport and the RanGTPase system by kinetic measurements and computer simulation. *Embo J* 22(5): 1088-1100.
- Gruss OJ, Carazo-Salas RE, Schatz CA, Guarguaglini G, Kast J, Wilm M, Le Bot N, Vernos I, Karsenti E, Mattaj JW (2001) Ran induces spindle assembly by reversing the inhibitory effect of importin alpha on TPX2 activity. *Cell* 104(1): 83-93.
- Hall TA (1999) BioEdit: a user-friendly biological sequence alignment editor and analysis program for Windows 95/98/NT. *Nucl Acids Symp Ser* 41: 95-98.
- Hannich JT, Lewis A, Kroetz MB, Li SJ, Heide H, Emili A, Hochstrasser M (2005) Defining the SUMO-modified proteome by multiple approaches in *Saccharomyces cerevisiae*. *J Biol Chem* 280(6): 4102-4110.
- Harel A, Chan RC, Lachish-Zalait A, Zimmerman E, Elbaum M, Forbes DJ (2003) Importin beta negatively regulates nuclear membrane fusion and nuclear pore complex assembly. *Mol Biol Cell* 14(11): 4387-4396.
- Hay RT (2005) SUMO: a history of modification. *Mol Cell* 18(1): 1-12.
- Hay RT (2007) SUMO-specific proteases: a twist in the tail. *Trends Cell Biol* 17(8): 370-376.
- Hecker CM, Rabiller M, Haglund K, Bayer P, Dikic I (2006) Specification of SUMO1- and SUMO2-interacting motifs. *J Biol Chem* 281(23): 16117-16127.
- Hillig RC, Renault L, Vetter IR, Drell Tt, Wittinghofer A, Becker J (1999) The crystal structure of rna1p: a new fold for a GTPase-activating protein. *Mol Cell* 3(6): 781-791.
- Ho MS, Tsai PI, Chien CT (2006) F-box proteins: the key to protein degradation. *J Biomed Sci* 13(2): 181-191.
- Hochstrasser M (2001) SP-RING for SUMO: new functions bloom for a ubiquitin-like protein. *Cell* 107(1): 5-8.
- Hochstrasser M (2007) Ubiquitin ligation without a ligase. *Dev Cell* 13(1): 4-6.
- Hoege C, Pfander B, Moldovan GL, Pyrowolakis G, Jentsch S (2002) RAD6-dependent DNA repair is linked to modification of PCNA by ubiquitin and SUMO. *Nature* 419(6903): 135-141.
- Hoeller D, Hecker CM, Wagner S, Rogov V, Dotsch V, Dikic I (2007) E3-independent monoubiquitination of ubiquitin-binding proteins. *Mol Cell* 26(6): 891-898.
-

- Hopper AK, Traglia HM, Dunst RW (1990) The yeast RNA1 gene product necessary for RNA processing is located in the cytosol and apparently excluded from the nucleus. *J Cell Biol* 111(2): 309-321.
- Hutchins JR, Moore WJ, Hood FE, Wilson JS, Andrews PD, Swedlow JR, Clarke PR (2004) Phosphorylation regulates the dynamic interaction of RCC1 with chromosomes during mitosis. *Curr Biol* 14(12): 1099-1104.
- Hutten S, Kehlenbach RH (2006) Nup214 is required for CRM1-dependent nuclear protein export in vivo. *Mol Cell Biol* 26(18): 6772-6785.
- Hutten S, Flotho A, Melchior F, Kehlenbach RH (2008) The Nup358-RanGAP Complex Is Required for Efficient Importin α/β -dependent Nuclear Import. *Mol Biol Cell* 19(5): 2300-2310.
- Jeong SY, Rose A, Joseph J, Dasso M, Meier I (2005) Plant-specific mitotic targeting of RanGAP requires a functional WPP domain. *Plant J* 42(2): 270-282.
- Johnson ES (2004) Protein modification by SUMO. *Annu Rev Biochem* 73: 355-382.
- Joseph J, Tan SH, Karpova TS, McNally JG, Dasso M (2002) SUMO-1 targets RanGAP1 to kinetochores and mitotic spindles. *J Cell Biol* 156(4): 595-602.
- Joseph J, Liu ST, Jablonski SA, Yen TJ, Dasso M (2004) The RanGAP1-RanBP2 complex is essential for microtubule-kinetochore interactions in vivo. *Curr Biol* 14(7): 611-617.
- Kalab P, Heald R (2008) The RanGTP gradient - a GPS for the mitotic spindle. *J Cell Sci* 121(Pt 10): 1577-1586.
- Kalab P, Pu RT, Dasso M (1999) The ran GTPase regulates mitotic spindle assembly. *Curr Biol* 9(9): 481-484.
- Kalab P, Weis K, Heald R (2002) Visualization of a Ran-GTP gradient in interphase and mitotic *Xenopus* egg extracts. *Science* 295(5564): 2452-2456.
- Kalab P, Pralle A, Isacoff EY, Heald R, Weis K (2006) Analysis of a RanGTP-regulated gradient in mitotic somatic cells. *Nature* 440(7084): 697-701.
- Kehlenbach RH, Dickmanns A, Kehlenbach A, Guan T, Gerace L (1999) A role for RanBP1 in the release of CRM1 from the nuclear pore complex in a terminal step of nuclear export. *J Cell Biol* 145(4): 645-657.
- Kerscher O, Felberbaum R, Hochstrasser M (2006) Modification of proteins by ubiquitin and ubiquitin-like proteins. *Annu Rev Cell Dev Biol* 22: 159-180.
-

- Knauer SK, Bier C, Habtemichael N, Stauber RH (2006) The Survivin-Crm1 interaction is essential for chromosomal passenger complex localization and function. *EMBO Rep* 7(12): 1259-1265.
- Knipscheer P, Flotho A, Klug H, Olsen JV, van Dijk WJ, Fish A, Johnson ES, Mann M, Sixma TK, Pichler A (2008) Ubc9 sumoylation regulates SUMO target discrimination. *Mol Cell* 31(3): 371-382.
- Kuersten S, Ohno M, Mattaj JW (2001) Nucleocytoplasmic transport: Ran, beta and beyond. *Trends Cell Biol* 11(12): 497-503.
- Kusano A, Staber C, Ganetzky B (2001) Nuclear mislocalization of enzymatically active RanGAP causes segregation distortion in *Drosophila*. *Dev Cell* 1(3): 351-361.
- Laemmli UK (1970) Cleavage of structural proteins during the assembly of the head of bacteriophage T4. *Nature* 227(5259): 680-685.
- Lee KS, Park JE, Kang YH, Zimmerman W, Soung NK, Seong YS, Kwak SJ, Erikson RL (2008) Mechanisms of mammalian polo-like kinase 1 (Plk1) localization: self-versus non-self-priming. *Cell Cycle* 7(2): 141-145.
- Li HY, Zheng Y (2004) Phosphorylation of RCC1 in mitosis is essential for producing a high RanGTP concentration on chromosomes and for spindle assembly in mammalian cells. *Genes Dev* 18(5): 512-527.
- Lin DY, Huang YS, Jeng JC, Kuo HY, Chang CC, Chao TT, Ho CC, Chen YC, Lin TP, Fang HI, Hung CC, Suen CS, Hwang MJ, Chang KS, Maul GG, Shih HM (2006) Role of SUMO-interacting motif in Daxx SUMO modification, subnuclear localization, and repression of sumoylated transcription factors. *Mol Cell* 24(3): 341-354.
- Macaulay C, Meier E, Forbes DJ (1995) Differential mitotic phosphorylation of proteins of the nuclear pore complex. *J Biol Chem* 270(1): 254-262.
- Mahajan R, Gerace L, Melchior F (1998) Molecular characterization of the SUMO-1 modification of RanGAP1 and its role in nuclear envelope association. *J Cell Biol* 140(2): 259-270.
- Mahajan R, Delphin C, Guan T, Gerace L, Melchior F (1997) A small ubiquitin-related polypeptide involved in targeting RanGAP1 to nuclear pore complex protein RanBP2. *Cell* 88(1): 97-107.
- Matunis MJ, Coutavas E, Blobel G (1996) A novel ubiquitin-like modification modulates the partitioning of the Ran-GTPase-activating protein RanGAP1 between the
-

- cytosol and the nuclear pore complex. *J Cell Biol* 135(6 Pt 1): 1457-1470.
- Matunis MJ, Wu J, Blobel G (1998) SUMO-1 modification and its role in targeting the Ran GTPase-activating protein, RanGAP1, to the nuclear pore complex. *J Cell Biol* 140(3): 499-509.
- Melchior F, Guan T, Yokoyama N, Nishimoto T, Gerace L (1995) GTP hydrolysis by Ran occurs at the nuclear pore complex in an early step of protein import. *J Cell Biol* 131(3): 571-581.
- Meulmeester E, Kunze M, Hsiao HH, Urlaub H, Melchior F (2008) Mechanism and consequences for paralog-specific sumoylation of ubiquitin-specific protease 25. *Mol Cell* 30(5): 610-619.
- Minty A, Dumont X, Kaghad M, Caput D (2000) Covalent modification of p73alpha by SUMO-1. Two-hybrid screening with p73 identifies novel SUMO-1-interacting proteins and a SUMO-1 interaction motif. *J Biol Chem* 275(46): 36316-36323.
- Mitchison TJ, Maddox P, Groen A, Cameron L, Perlman Z, Ohi R, Desai A, Salmon ED, Kapoor TM (2004) Bipolarization and poleward flux correlate during *Xenopus* extract spindle assembly. *Mol Biol Cell* 15(12): 5603-5615.
- Montpetit B, Hazbun TR, Fields S, Hieter P (2006) Sumoylation of the budding yeast kinetochore protein Ndc10 is required for Ndc10 spindle localization and regulation of anaphase spindle elongation. *J Cell Biol* 174(5): 653-663.
- Moore W, Zhang C, Clarke PR (2002) Targeting of RCC1 to chromosomes is required for proper mitotic spindle assembly in human cells. *Curr Biol* 12(16): 1442-1447.
- Mosammamarast N, Pemberton LF (2004) Karyopherins: from nuclear-transport mediators to nuclear-function regulators. *Trends Cell Biol* 14(10): 547-556.
- Mukhopadhyay D, Dasso M (2007) Modification in reverse: the SUMO proteases. *Trends Biochem Sci* 32(6): 286-295.
- Nachury MV, Maresca TJ, Salmon WC, Waterman-Storer CM, Heald R, Weis K (2001) Importin beta is a mitotic target of the small GTPase Ran in spindle assembly. *Cell* 104(1): 95-106.
- Nemergut ME, Mizzen CA, Stukenberg T, Allis CD, Macara IG (2001) Chromatin docking and exchange activity enhancement of RCC1 by histones H2A and H2B. *Science* 292(5521): 1540-1543.
- Nousiainen M, Sillje HH, Sauer G, Nigg EA, Korner R (2006) Phosphoproteome analysis
-

- of the human mitotic spindle. *Proc Natl Acad Sci U S A* 103(14): 5391-5396.
- Ohba T, Nakamura M, Nishitani H, Nishimoto T (1999) Self-organization of microtubule asters induced in *Xenopus* egg extracts by GTP-bound Ran. *Science* 284(5418): 1356-1358.
- Ohtsubo M, Okazaki H, Nishimoto T (1989) The RCC1 protein, a regulator for the onset of chromosome condensation locates in the nucleus and binds to DNA. *J Cell Biol* 109(4 Pt 1): 1389-1397.
- Panse VG, Hardeland U, Werner T, Kuster B, Hurt E (2004) A proteome-wide approach identifies sumoylated substrate proteins in yeast. *J Biol Chem* 279(40): 41346-41351.
- Pay A, Resch K, Frohnmeyer H, Fejes E, Nagy F, Nick P (2002) Plant RanGAPs are localized at the nuclear envelope in interphase and associated with microtubules in mitotic cells. *Plant J* 30(6): 699-709.
- Petronczki M, Lenart P, Peters JM (2008) Polo on the Rise-from Mitotic Entry to Cytokinesis with Plk1. *Dev Cell* 14(5): 646-659.
- Pichler A, Gast A, Seeler JS, Dejean A, Melchior F (2002) The nucleoporin RanBP2 has SUMO1 E3 ligase activity. *Cell* 108(1): 109-120.
- Pichler A, Knipscheer P, Saitoh H, Sixma TK, Melchior F (2004) The RanBP2 SUMO E3 ligase is neither HECT- nor RING-type. *Nat Struct Mol Biol* 11(10): 984-991.
- Pichler A, Knipscheer P, Oberhofer E, van Dijk WJ, Korner R, Olsen JV, Jentsch S, Melchior F, Sixma TK (2005) SUMO modification of the ubiquitin-conjugating enzyme E2-25K. *Nat Struct Mol Biol* 12(3): 264-269.
- Reindle A, Belichenko I, Bylebyl GR, Chen XL, Gandhi N, Johnson ES (2006) Multiple domains in Siz SUMO ligases contribute to substrate selectivity. *J Cell Sci* 119(Pt 22): 4749-4757.
- Ren J, Wen L, Gao X, Jin C, Xue Y, Yao X (submitted) SUMOsp 2.0: an updated WWW service for sumoylation sites prediction.
- Ren M, Drivas G, D'Eustachio P, Rush MG (1993) Ran/TC4: a small nuclear GTP-binding protein that regulates DNA synthesis. *J Cell Biol* 120(2): 313-323.
- Reverter D, Lima CD (2005) Insights into E3 ligase activity revealed by a SUMO-RanGAP1-Ubc9-Nup358 complex. *Nature* 435(7042): 687-692.
- Richards SA, Lounsbury KM, Carey KL, Macara IG (1996) A nuclear export signal is
-

- essential for the cytosolic localization of the Ran binding protein, RanBP1. *J Cell Biol* 134(5): 1157-1168.
- Rose A, Meier I (2001) A domain unique to plant RanGAP is responsible for its targeting to the plant nuclear rim. *Proc Natl Acad Sci U S A* 98(26): 15377-15382.
- Ryan KJ, McCaffery JM, Wentz SR (2003) The Ran GTPase cycle is required for yeast nuclear pore complex assembly. *J Cell Biol* 160(7): 1041-1053.
- Ryan KJ, Zhou Y, Wentz SR (2007) The karyopherin Kap95 regulates nuclear pore complex assembly into intact nuclear envelopes in vivo. *Mol Biol Cell* 18(3): 886-898.
- Saitoh H, Pizzi MD, Wang J (2002) Perturbation of SUMOylation enzyme Ubc9 by distinct domain within nucleoporin RanBP2/Nup358. *J Biol Chem* 277(7): 4755-4763.
- Saitoh H, Pu R, Cavenagh M, Dasso M (1997) RanBP2 associates with Ubc9p and a modified form of RanGAP1. *Proc Natl Acad Sci U S A* 94(8): 3736-3741.
- Salina D, Enarson P, Rattner JB, Burke B (2003) Nup358 integrates nuclear envelope breakdown with kinetochore assembly. *J Cell Biol* 162(6): 991-1001.
- Schmidt D (2005) Charakterisierung von PIAS-Proteinen als E3-ähnliche Faktoren im SUMO-System [PhD thesis]. München: Ludwig-Maximilians-Universität.
- Schmidt D, Muller S (2002) Members of the PIAS family act as SUMO ligases for c-Jun and p53 and repress p53 activity. *Proc Natl Acad Sci U S A* 99(5): 2872-2877.
- Shevchenko A, Wilm M, Vorm O, Mann M (1996) Mass spectrometric sequencing of proteins silver-stained polyacrylamide gels. *Anal Chem* 68(5): 850-858.
- Singh BB, Patel HH, Roepman R, Schick D, Ferreira PA (1999) The zinc finger cluster domain of RanBP2 is a specific docking site for the nuclear export factor, exportin-1. *J Biol Chem* 274(52): 37370-37378.
- Song J, Zhang Z, Hu W, Chen Y (2005) Small ubiquitin-like modifier (SUMO) recognition of a SUMO binding motif: a reversal of the bound orientation. *J Biol Chem* 280(48): 40122-40129.
- Song J, Durrin LK, Wilkinson TA, Krontiris TG, Chen Y (2004) Identification of a SUMO-binding motif that recognizes SUMO-modified proteins. *Proc Natl Acad Sci U S A* 101(40): 14373-14378.
- Splinter D, Tanenbaum ME, Flotho A, Grigoriev I, Dieuwke, Engelsma, Keijzer N, Demmers J, Yu KL, Fornerod M, Melchior F, Hoogenraad C, Medema RH,
-

- Akhmanova A (manuscript submitted) Bicaudal D2, dynein and kinesin-1 associate with nuclear pore complexes and regulate centrosome positioning during mitotic entry.
- Stead K, Aguilar C, Hartman T, Drexel M, Meluh P, Guacci V (2003) Pds5p regulates the maintenance of sister chromatid cohesion and is sumoylated to promote the dissolution of cohesion. *J Cell Biol* 163(4): 729-741.
- Stewart M (2006) Structural basis for the nuclear protein import cycle. *Biochem Soc Trans* 34(Pt 5): 701-704.
- Stewart M (2007) Molecular mechanism of the nuclear protein import cycle. *Nat Rev Mol Cell Biol* 8(3): 195-208.
- Strom AC, Weis K (2001) Importin-beta-like nuclear transport receptors. *Genome Biol* 2(6): REVIEWS3008.
- Stucke VM, Sillje HH, Arnaud L, Nigg EA (2002) Human Mps1 kinase is required for the spindle assembly checkpoint but not for centrosome duplication. *Embo J* 21(7): 1723-1732.
- Swaminathan S, Kiendl F, Korner R, Lupetti R, Hengst L, Melchior F (2004) RanGAP1*SUMO1 is phosphorylated at the onset of mitosis and remains associated with RanBP2 upon NPC disassembly. *J Cell Biol* 164(7): 965-971.
- Takahashi H, Hatakeyama S, Saitoh H, Nakayama KI (2005) Noncovalent SUMO-1 binding activity of thymine DNA glycosylase (TDG) is required for its SUMO-1 modification and colocalization with the promyelocytic leukemia protein. *J Biol Chem* 280(7): 5611-5621.
- Takeda E, Hieda M, Katahira J, Yoneda Y (2005) Phosphorylation of RanGAP1 stabilizes its interaction with Ran and RanBP1. *Cell Struct Funct* 30(2): 69-80.
- Tanaka TU, Desai A (2008) Kinetochores-microtubule interactions: the means to the end. *Curr Opin Cell Biol* 20(1): 53-63.
- Trieselmann N, Wilde A (2002) Ran localizes around the microtubule spindle in vivo during mitosis in *Drosophila* embryos. *Curr Biol* 12(13): 1124-1129.
- Trieselmann N, Armstrong S, Rauw J, Wilde A (2003) Ran modulates spindle assembly by regulating a subset of TPX2 and Kid activities including Aurora A activation. *J Cell Sci* 116(Pt 23): 4791-4798.
- Villa Braslavsky CI, Nowak C, Gorlich D, Wittinghofer A, Kuhlmann J (2000) Different
-

- structural and kinetic requirements for the interaction of Ran with the Ran-binding domains from RanBP2 and importin-beta. *Biochemistry* 39(38): 11629-11639.
- Vörsmann H (2007) Untersuchungen zur mitotischen Phosphorylierung von RanGAP1 [Diplomarbeit]. Göttingen: Georg-August-Universität Göttingen.
- Walther TC, Pickersgill HS, Cordes VC, Goldberg MW, Allen TD, Mattaj IW, Fornerod M (2002) The cytoplasmic filaments of the nuclear pore complex are dispensable for selective nuclear protein import. *J Cell Biol* 158(1): 63-77.
- Walther TC, Askjaer P, Gentzel M, Habermann A, Griffiths G, Wilm M, Mattaj IW, Hetzer M (2003) RanGTP mediates nuclear pore complex assembly. *Nature* 424(6949): 689-694.
- Wang W, Budhu A, Forgues M, Wang XW (2005) Temporal and spatial control of nucleophosmin by the Ran-Crm1 complex in centrosome duplication. *Nat Cell Biol* 7(8): 823-830.
- Weis K (2003) Regulating access to the genome: nucleocytoplasmic transport throughout the cell cycle. *Cell* 112(4): 441-451.
- Weis K (2007) The nuclear pore complex: oily spaghetti or gummy bear? *Cell* 130(3): 405-407.
- Wiese C, Wilde A, Moore MS, Adam SA, Merdes A, Zheng Y (2001) Role of importin-beta in coupling Ran to downstream targets in microtubule assembly. *Science* 291(5504): 653-656.
- Wilde A, Zheng Y (1999) Stimulation of microtubule aster formation and spindle assembly by the small GTPase Ran. *Science* 284(5418): 1359-1362.
- Wilde A, Lizarraga SB, Zhang L, Wiese C, Gliksman NR, Walczak CE, Zheng Y (2001) Ran stimulates spindle assembly by altering microtubule dynamics and the balance of motor activities. *Nat Cell Biol* 3(3): 221-227.
- Wohlschlegel JA, Johnson ES, Reed SI, Yates JR, 3rd (2004) Global analysis of protein sumoylation in *Saccharomyces cerevisiae*. *J Biol Chem* 279(44): 45662-45668.
- Wu J, Matunis MJ, Kraemer D, Blobel G, Coutavas E (1995) Nup358, a cytoplasmically exposed nucleoporin with peptide repeats, Ran-GTP binding sites, zinc fingers, a cyclophilin A homologous domain, and a leucine-rich region. *J Biol Chem* 270(23): 14209-14213.
-

- Wykoff DD, O'Shea EK (2005) Identification of sumoylated proteins by systematic immunoprecipitation of the budding yeast proteome. *Mol Cell Proteomics* 4(1): 73-83.
- Yokoyama N, Hayashi N, Seki T, Pante N, Ohba T, Nishii K, Kuma K, Hayashida T, Miyata T, Aebi U, et al. (1995) A giant nucleopore protein that binds Ran/TC4. *Nature* 376(6536): 184-188.
- Zhang C, Goldberg MW, Moore WJ, Allen TD, Clarke PR (2002a) Concentration of Ran on chromatin induces decondensation, nuclear envelope formation and nuclear pore complex assembly. *Eur J Cell Biol* 81(11): 623-633.
- Zhang H, Saitoh H, Matunis MJ (2002b) Enzymes of the SUMO modification pathway localize to filaments of the nuclear pore complex. *Mol Cell Biol* 22(18): 6498-6508.
- Zhang HL, Singer RH, Bassell GJ (1999) Neurotrophin regulation of beta-actin mRNA and protein localization within growth cones. *J Cell Biol* 147(1): 59-70.
- Zhang XD, Goeres J, Zhang H, Yen TJ, Porter AC, Matunis MJ (2008) SUMO-2/3 modification and binding regulate the association of CENP-E with kinetochores and progression through mitosis. *Mol Cell* 29(6): 729-741.
- Zhao Q, Brkljacic J, Meier I (2008) Two Distinct Interacting Classes of Nuclear Envelope-Associated Coiled-Coil Proteins Are Required for the Tissue-Specific Nuclear Envelope Targeting of Arabidopsis RanGAP. *Plant Cell* 20(6): 1639-1651.
- Zhou W, Ryan JJ, Zhou H (2004) Global analyses of sumoylated proteins in *Saccharomyces cerevisiae*. Induction of protein sumoylation by cellular stresses. *J Biol Chem* 279(31): 32262-32268.
- Zhu J, Zhu S, Guzzo CM, Ellis NA, Sung KS, Choi CY, Matunis MJ (2008) Sumo binding determines substrate recognition and paralog-selective sumo modification. *J Biol Chem*.
- Zhu S, Zhang H, Matunis MJ (2006) SUMO modification through rapamycin-mediated heterodimerization reveals a dual role for Ubc9 in targeting RanGAP1 to nuclear pore complexes. *Exp Cell Res* 312(7): 1042-1049.
-

SUPPLEMENTARY INFORMATION

1. Sequence of TACC2 ("isoform 7")

ATGGGCAATGAGAACAGCACCTCGGACAACCAGAGGACTTTATCAGCTCAGACTCCA
AGGTCCGCGCAGCCACCCGGGAACAGTCAGAATATAAAAAGGAAGCAGCAGGACAC
GCCCCGAAGCCCTGACCACAGAGACGCGTCCAGCATCTCCCCAGCTGCTGCCCATGC
GGGTCTTCCCTCGGCTGCAGAACACATAGTTTCGCCATCTGCCCCAGCTGGTGACA
GAGTAGAAGCTTCCACTCCCTCCTGCCAGATCCGGCCAAAGACCTCAGCAGGAGTTC
CGATTCTGAAGAGGCATTTGAGACCCCCGGAGTCAACGACCCCTGTCAAAGCTCCGCCA
GCTCCACCCCCACCACCCCCGAAGTCATCCAGAACCCGAGGTCAGCACACAGCC
ACCCCCGGAAGAACCAGGATGTGGTTCTGAGACAGTCCCTGTCCCTGATGGCCCACG
GAGCGACTCGGTGGAAGGAAGTCCCTTTCGTCCCCCGTCACACTCCTTCTCTGCCGTCT
TCGATGAAGACAAGCCGATAGCCAGCAGTGGGACTTACAACCTTGACTTTGACAACAT
TGAGCTTGTGGATACCTTTCAGACCTTGGAGCCTCGTGCCTCAGACGCTAAGAATCAGG
AGGGCAAAGTGAACACACGGAGGAAGTCCACGGATTCCGTCCCCATCTCTAAGTCTAC
ACTGTCCCGGTCGCTCAGCCTGCAAGCCAGTGACTTTGATGGTGCTTCTTCCCTCAGGCA
ATCCCGAGGCCGTGGCCCTTGCCCCAGATGCATATAGCACGGGTTCCAGCAGTGCTTC
TAGTACCCTTAAGCGAACTAAAAAACCGAGGCCGCCTTCCTTAAAAAAGAAACAGACC
ACCAAGAAACCCACAGAGACCCCCCAGTGAAGGAGACGCAACAGGAGCCAGATGA
AGAGAGCCTTGTCCCCAGTGGGGAGAATCTAGCATCTGAGACGAAAACGGAATCTGC
CAAGACGGAAGGTCCTAGCCCAGCCTTATTGGAGGAGACGCCCCCTTGAGCCCGCTGT
GGGGCCCAAAGCTGCCTGCCCTCTGGACTCAGAGAGTGCAGAAGGGGTTGTCCCCC
GGCTTCTGGAGGTGGCAGAGTGCAGAACTACCCCCTGTCGGGAGGAAAACGCTGCC
TCTTACCACGGCCCCGGAGGCAGGGGAGGTAACCCCATCGGATAGCGGGGGGCAAG
AGGACTCTCCAGCCAAAGGGCTCTCCGTAAGGCTGGAGTTTACTATTCTGAGGACaA
GAGTAGTTGGGACAACCAGCAGGAAAACCCCCCTCCTACCAAAAAGATAGGCAAAAA
GCCAGTTGCCAAAATGCCCTGAGGAGGCCAAAGATGAAAAAGACACCCGAGAACT
TGACAACACTCCTGCCTCACCTCCAGATCCCCTGCTGAACCCAATGACATCCCCATTG
CTAAAGGTACTTACACCTTTGATATTGACAAGTGGGATGACCCCAATTTTAACCTTTTTTC
TTCCAnGCCCCGCAAGAAGAAGAAGACGCCCTAAAGACTGACACATTTAGGGTGAA
AAAGTCGCCAAAACGGTCTCCTCTCTGATCCACCTTCCAGGACCCACCCAGCT

GCTACACCAGAAACACCACCAGTGATCTCTGCGGTGGTCCACGCCACAGATGAGGAA
AAGCTGGCGGTCACCAACCAGAAGTGGACGTGCATGACAGTGGACCTAGAGGCTGAC
AAACAGGACTACCCGCAGCCCTCGGACCTGTCCACCTTTGTAAACGAGACCAAATTCA
GTTACCCACTGAGGAGTTGGATTACAGAACTCCTATGAAATTGAATATATGGAGAAA
ATTGGCTCCTCCTTACCTCAGGACGACGATGCCCCGAAGAAGCAGGCCTTGTACCTTAT
GTTTGACACTTCTCAGGAGAGCCCTGTCAAGTCATCTCCCGTCCGCATGTCAGAGTCCC
CGACGCCGTGTTCAGGGTCAAGTTTTGAAGAGACTGAAGCCCTTGTGAACACTGCTGC
GAAAAAACAGCATCCTGTCCCACGAGGACTGGCCCCTAACCAAGAGTCACACTTGCA
GGTGCCAGAGAAATCCTCCCAGAAGGAGCTGGAGGCCATGGGCTTGGGCACCCCTTC
AGAAGCGATTGAAATTAGAGAGGCTGCTACCCAACAGACGTCTCCATCTCCAAAACA
GCCTTGTA CTCCCGCATCGGGACCGCTGAGGTGGAGAAACCTGCAGGCCTTCTGTTCC
AGCAGCCCGACCTGGACTCTGCCCTCAGATCGCCAGAGCAGAGATCATAACCAAGG
AGAGAGAGGTCTCAGAATGGAAAGATAAATATGAAGAAAGCAGGCGGGAAGTGATG
GAAATGAGGAAAATAGTGGCCGAGTATGAGAAGACCATCGCTCAGATGATAGAGGAC
GAACAGAGAGAGAAGTCAGTCTCCCACCAGACGGTGCAGCAGCTGGTTCTGGAGAAG
GAGCAAGCCCTGGCCGACCTGAACTCCGTGGAGAAGTCTCTGGCCGACCTCTTCAGA
AGATATGAGAAGATGAAGGAGGTCCTAGAAGGCTTCCGCAAGAATGAAGAGGTGTTG
AAGAGATGTGCGCAGGAGTACCTGTCCCGGGTGAAGAAGGAGGAGCAGAGGTACCA
GGCCCTGAAGGTGCACGCGGAGGAGAACTGGACAGGGCCAATGCTGAGATTGCTC
AGGTTTCGAGGCAAGGCCAGCAGGAGCAAGCCGCCACCACGCCAGCCTGCGGAA
GGAGCAGCTGCGAGTGGACGCCCTGGAAAGGACGCTGGAGCAGAAGAATAAAGAAA
TAGAAGA ACTCACCAAGATTTGTGACGAACTGATTGCCAAAATGGGGAAAAGCTAA

ABBREVIATIONS

General abbreviations

*	covalently conjugated, in context of sumoylation
Δ Cx	deletion of x C-terminal amino acids, in context of Sumo
Δ FG	deletion of the phenyl glycine repeats
A	adenine, in context of DNA and RNA
aa	amino acids
ADP	adenosine-5'-diphosphate
APS	ammonium persulfate
ATP	adenosine-5'-triphosphate
BP	binding protein
BSA	bovine serum albumine
C	cytosine, in context of DNA and RNA
C / c-	carboxyl-, in context of proteins
cDNA	complementary DNA
CMVp	cytomegalovirus promoter
CPC	chromosomal passenger complex
DEAE	diethylaminoethyl-
DMEM	Dulbecco' s modified Eagles medium
DMP	dimethyl pimelimidate
DMS	dimethyl suberimidate
DMSO	dimethyl sulfoxide
DNA	desoxyribonucleic acid
dNTP	2'-desoxynucleoside-5'-triphosphate
DTT	dithiothreitol
E1	Ubiquitin / Sumo activating enzyme
E2	Ubiquitin / Sumo conjugating enzyme
E3	Ubiquitin / Sumo ligase
EDTA	ethylenediaminetetraacetic acid
EGS	ethylene glycol bis[succinimidylsuccinate]
EGTA	ethylene glycol tetraacetic acid

FCS	fetal calf serum
FRET	fluorescence resonance energy transfer
G	guanine, in context of DNA and RNA
GAP	GTPase activating protein
GDP	guanosine-5'-diphosphate
GEF	guanine nucleotide exchange factor
GFP	green fluorescent protein
GSH	glutathione
GST	glutathione-S-transferase
GTP	guanosine-5'-triphosphate
HA	hemagglutinin
HCl	hydrochloric acid
HEPES	[4-(2-hydroxyethyl)-1-piperazine]ethanesulfonic acid
His-	hexa- to octahistidine, in context of fusion proteins
I	interphase, in context of cell/immunoprecipitation samples
IF	immunofluorescence
IgG	immunoglobuline G
IP	immunoprecipitation
IPTG	isopropyl-beta-D-thiogalactopyranoside
kD	kilodalton
LB	Luria-Bertani
LMB	leptomycin B (Crm1 inhibitor)
M	mitotic, in context of cell/immunoprecipitation samples
M	molar (Mol /l), in context of concentration
MCS	multiple cloning site
mmu	millimass unit
MS	mass spectrometry
N/ n-	amino-, in context of proteins
NCS	newborn calf serum
n.d.	not determined
NEM	N-ethylmaleimide
NES	nuclear export signal

NLS	nuclear localization signal
NP-40	octyl phenoxy polyethoxy ethanol
OH	hydroxyl
P / p	phosphate, phospho-
PAGE	polyacrylamide gel electrophoresis
PBS	phosphate buffered saline
PCR	polymerase chain reaction
PEFA bloc	4-(2-aminoethyl)benzenesulfonyl fluoride hydrochloride
pH	negative common logarithm of the proton concentration
PMSF	phenylmethylsulphonyl fluoride
RIPA	radio immunoprecipitation assay
RNA	ribonucleic acid
RNAi	RNA interference
RNase	ribonuclease
rpm	rotations per minute
SBM	Sumo binding motif
SDS	sodium dodecyl sulfate
SILAC	stable isotope labeling in cell culture
SIM	Sumo interacting motif
siRNA	small interfering RNA
T	thymine, in context of DNA and RNA
TAE	Tris / acetate / EDTA
TE	Tris / EDTA
TEMED	tetramethylethylenediamine
Tris	tris(hydroxymethyl)aminomethane
Triton-X100	4-octylphenol polyethoxylate
Tween-20	polyoxyethylene (20) sorbitan monolaurate
U	uracil, in context of RNA
USP	Ubiquitin specific protease
UV	ultraviolet
Vme	vinylmethylester
v/v	volume per volume

w/v	weight per volume
WB	western blot
WT/wt	wild type
YFP	yellow fluorescent protein

Physical units

A	ampere
°C	degree Celsius
g	acceleration of gravity on Earth
g	gram
h	hour
l	liter
m	meter
min	minute
OD	optical density
s	second
V	volt

Prefixes

c-	centi-
k-	kilo-
m-	milli-
μ-	micro-
n-	nano-
p-	pico-

One and three letter code for amino acids

A	Ala	alanine
D	Asp	aspartate
E	Glu	glutamate
F	Phe	phenylalanine
G	Gly	glycine
H	His	histidine
I	Ile	isoleucine
K	Lys	lysine
L	Leu	leucine
M	Met	methionine
P	Pro	proline
Q	Gln	glutamine
R	Arg	arginine
S	Ser	serine
T	Thr	threonine
V	Val	valine
x	-	any
Ψ	-	aliphatic

ACKNOWLEDGEMENTS

Ganz herzlich bedanken möchte ich mich bei Prof. Dr. Frauke Melchior, für ein spannendes und zudem auch häufig herausforderndes Projekt, für ihre Unterstützung und vor allem auch für ihren Optimismus, der manchmal für zwei reichen musste.

Bedanken möchte ich mich ebenfalls bei Prof. Dr. R. Ficner für die Übernahme des Korreferates. Gleichfalls danke ich Prof. Dr. G. Braus und PD Dr. M. Hoppert, sich als Mitglieder des Prüfungskomitees zur Verfügung gestellt zu haben und auch für das Entgegenkommen, einen Prüfungstermin zu finden.

I also would like to thank my collaborators: This work would not exist without my mass spec collaborators Dr. Guido Sauer, Dr. Henning Urlaub and Monika Raabe. My - ultimately successful - excursion into the abyss of Ubc9 regulation I owe especially Dr. Andrea Pichler and Dr. Puck Knipscheer. For a very pleasant and fruitful collaboration I would like to thank Dr. Anna Akhmanova and Daniel Splinter. I am also indebted to Dr. Saskia Hutten and Dr. Ralph Kehlenbach. Finally, I would like to thank Dr. Duane Compton, Dr. Giulia Guarguaglini and Dr. Madelon Maurice for kind gifts of antibodies.

I am especially grateful to my past and present colleagues for a very pleasant and stimulating environment, for many scientific discussions and for also not so scientific ones... My very personal and special thanks go to Florian, Andrea, Guido and Tanja, Marie-Christine and Erik.

Nicht zuletzt danke ich auch meiner Schwester Laura für ihre unermüdliche und tatkräftige Unterstützung, die letzte Woche wäre sonst noch um einiges nervenaufreibender geworden.

CURRICULUM VITAE

Personal Data

Name: Annette Flotho
Born: March 4, 1974 in Aachen, Germany

School Education

Dietrich Bonhoeffer Gymnasium, Bergisch Gladbach 1984-1993
graduation: Abitur (qualification for admission to the university) 1993

Academic Studies and Degrees

PhD student in the laboratory of Dr. Frauke Melchior, initially at the Max-Planck-Institute of Biochemistry, Martinsried, then at the University of Göttingen since 2003
Diploma in Biology 10 / 2001
University of Konstanz, Diploma Program in Biology 1996-2001
University of Freiburg, studies in Romanistics 1995-1996
University of Dortmund, studies in Architecture 1995-1996
University of Cologne, studies in Musicology 1993-1995

Research Experience

Ph.D. student in the laboratory of Prof. Dr. Frauke Melchior, initially Max-Planck-Institute of Biochemistry, Martinsried, then University of Göttingen since 2003
Research fellow in the laboratory of Dr. Elaine Elion, Department of Biological Chemistry and Molecular Pharmacology, Harvard Medical School, Boston, MA, U.S.A. 2000-2003
Research student in the group of Dr. Verena Weiss (laboratory of Prof. Dr. W. Boos), Department of Biology, University of Konstanz, 10 months 1999-2000
Research Internship at the Department of Cellular Physiology, Max-Planck Institute for Medical Research, Heidelberg - Germany, 2 months 1998

Selected Presentations

- 'Nuclear transport and mitosis, the evolving relationship', Fondation Les Treilles, France, talk 2007
- EMBO Workshop 'Signal-Transduction-Mediated Regulation of Nuclear Transport', Strasbourg, France, talk 2001

Publications and Thesis

Flotho A (2001) Characterizing Ste5 Modifications and cis-Elements Required for Recruitment to G β at the Plasma Membrane [Diploma thesis]. Konstanz: Universität Konstanz.

Weiss V, Kramer G, Dunnebier T, **Flotho A** (2002) Mechanism of regulation of the bifunctional histidine kinase NtrB in *Escherichia coli*. *J Mol Microbiol Biotechnol* 4(3): 229-233.

Flotho A, Simpson DM, Qi M, Elion EA (2004) Localized feedback phosphorylation of Ste5p scaffold by associated MAPK cascade. *J Biol Chem* 279(45): 47391-47401.

Hutten S, **Flotho A**, Melchior F, Kehlenbach RH (2008) The Nup358-RanGAP Complex Is Required for Efficient Importin α/β -dependent Nuclear Import. *Mol Biol Cell* 19(5): 2300-2310.

Knipscheer P*, **Flotho A***, Klug H*, Olsen JV, van Dijk WJ, Fish A, Johnson ES, Mann M, Sixma TK, Pichler A (2008) Ubc9 sumoylation regulates SUMO target discrimination. *Mol Cell* 31(3): 371-382.

Splinter D*, Tanenbaum ME*, **Flotho A**, Grigoriev I, Dieuwke, Engelsma, Keijzer N, Demmers J, Yu KL, Fornerod M, Melchior F, Hoogenraad C, Medema RH, Akhmanova A (manuscript submitted) Bicaudal D2, dynein and kinesin-1 associate with nuclear pore complexes and regulate centrosome positioning during mitotic entry.

* These authors contributed equally to the respective work.
